

AD-A269 846



4

Technical Report 1194
December 1992

Survey of Collision Avoidance and Ranging Sensors for Mobile Robots

Revision 1

H. R. Everett
D. E. DeMuth
E. H. Stitz

DTIC
ELECTE
SEP 29 1993
S E D

Approved for public release; distribution is unlimited.

93-22538



Technical Report 1194

December 1992

Survey of Collision Avoidance and Ranging Sensors for Mobile Robots

Revision 1

H. R. Everett
D. E. DeMuth
E. H. Stitz

Accession For	
NTIS CRA&I	<input checked="" type="checkbox"/>
DTIC TAB	<input type="checkbox"/>
Unannounced	<input type="checkbox"/>
Justification	
By	
Distribution /	
Availability Codes	
Dist	Avail and/or Special
A-1	

DTIC REPORT NUMBER 1194

**NAVAL COMMAND, CONTROL AND
OCEAN SURVEILLANCE CENTER
RDT&E DIVISION
San Diego, California 92152-5001**

**J. D. FONTANA, CAPT, USN
Commanding Officer**

**R. T. SHEARER
Executive Director**

ADMINISTRATIVE INFORMATION

This is the first revision of a Technical Report published in 1988. This work was done under project CH01, for the U.S. Army.

Released under authority of
D. W. Murphy, Head
Advanced Systems Division

CONTENTS

1.0 INTRODUCTION	1
2.0 BACKGROUND	5
2.1 RANGING TECHNIQUES	5
2.1.1 Proximity	5
2.1.2 Triangulation	7
2.1.2.1 Stereo Disparity	9
2.1.2.2 Active Triangulation	10
2.1.2.3 Structured Light	10
2.1.2.4 Known Target Size	11
2.1.2.5 Optical Flow	12
2.1.3 Time of Flight	14
2.1.4 Phase Shift Measurement	15
2.1.5 Frequency Modulation	16
2.1.6 Interferometry	17
2.1.6.1 Fringe Counters	17
2.1.6.2 Diffraction Gratings	19
2.1.7 Swept Focus	22
2.1.8 Return Signal Intensity	23
2.2 APPLICABLE TECHNOLOGIES	24
2.2.1 Acoustical	24
2.2.2 Optical	27
2.2.3 Electromagnetic	29
2.2.3.1 Microwave Radar	31
2.2.3.2 Millimeter Wave Radar	31
3.0 CANDIDATE SYSTEMS	33
3.1 COMMERCIALY AVAILABLE	33
3.1.1 Cybermotion Ultrasonic Collision Avoidance System CA-2	33
3.1.2 Polaroid Ultrasonic Ranging Unit	33
3.1.3 Pentax Near-Infrared Autofocus Sensor	35
3.1.4 Hamamatsu Range-Finder Chip Set	37
3.1.5 Hamamatsu H3065-10 Optical Displacement Sensor	38
3.1.6 Honeywell HVS-300 Three Zone Distance Sensor	39
3.1.7 Honeywell Visitronic Autofocus System	41
3.1.8 Honeywell Through-the-Camera-Lens Autofocus System	43

3.1.9 Robot Defense Systems' OWL	45
3.1.10 NAMCO LASERNET Smart Sensor	46
3.1.11 ERIM Adaptive Suspension Vehicle Sensor	49
3.1.12 CLS Laser Ranger	51
3.1.13 CLS Laser Profiler	52
3.1.14 CLS Laser Coordinate Measuring System	53
3.1.15 Odetics Scanning Laser Imaging System	55
3.1.16 ESP ORS-1 Optical Ranging System	57
3.1.17 SEO Scanning Laser Rangefinder	60
3.1.18 SEO LRF-X Laser Rangefinder Series	61
3.1.19 SEO Multi-Channel Laser Imaging System	62
3.1.20 Optech G150 Laser Rangefinder	63
3.1.21 Laser Systems Devices MR-101 Missile Rangefinder	64
3.1.22 IBEO Pulsar Survey Series Rangefinders	64
3.1.23 Azimuth LRG-90 Laser Rangefinder Transceiver	66
3.1.24 Banner Near-Infrared Proximity Sensors	67
3.1.25 TRC LABMATE Proximity Sensor Subsystem	67
3.1.26 TRC Strobed Light Triangulation System	68
3.1.27 TRC Light Direction and Ranging System, LIDAR	69
3.1.28 NOMADIC Sensus 300 Infrared Proximity System	70
3.1.29 NOMADIC Sensus 500 Vision System	71
3.1.30 VRSS Automotive Collision Avoidance Radar	72
3.1.31 AM Sensors Microwave Range Sensors	73
3.1.32 VORAD Vehicle Detection and Driver Alert System	75
3.1.33 Nissan Diesel Motor Company's Traffic Eye	75
3.1.34 National Semiconductor's LM1812 Ultrasonic Transceiver	75
3.2 UNDER DEVELOPMENT	77
3.2.1 FMC Ultrasonic Imaging Sensor	77
3.2.2 Honeywell Displaced Sensor Ranging Unit	79
3.2.3 Quantic Wide Angle Optical Ranging System	80
3.2.4 SEO Helicopter Obstacle Proximity Sensor System	84
3.2.5 RVSI Ship Surface Scanner	86
3.2.6 Multispectral ALV Sensors	88
3.2.7 RVSI Long Optical Ranging and Detection System	92
3.2.8 Digital Signal Laser Radar Sensor	95
3.2.9 Passive Swept-Focus Three-Dimensional Vision	96
3.2.10 JPL Range-From-Focus Optical System	98
3.2.11 JPL Stereo Vision System	100
3.2.12 TOSC Passive Stereo Ranging	101

3.2.13 Millitech Modular MMW Radar Sensor	102
3.2.14 Battelle Steerable-Beam Millimeter Wave Radar	103
3.2.15 K-MEC Low Cost Millimeter-Wave Radar	106
3.2.16 NASA Capaciflector Proximity Sensor	107
3.3 INTERESTING RESEARCH	110
3.3.1 Ultrasonic Scanning System	110
3.3.2 HILARE	111
3.3.3 Ultrasonics For Object Recognition	112
3.3.4 Ultrasonic Phased Array Rangefinder	113
3.3.5 University of Michigan Ultrasonic and Infrared Sensor Fusion	113
3.3.6 University of Minnesota Ultrasonic Range Sensing Array	115
3.3.7 Error Eliminating Rapid Ultrasonic Firing	118
3.3.8 Potential Field Obstacle Avoidance for Large Mobile Robots	118
3.3.9 Ground Vehicle Automatic Guidance System	121
3.3.10 Vehicle Location By Laser Rangefinding	122
3.3.11 Australian National University Laser Ranger	123
3.3.12 Case Western Reserve University Scanning Rangefinder	123
3.3.13 Rutgers Wide Field Of View Rangefinder	123
3.3.14 Obstacle Avoidance For Mobile Robots	124
3.3.15 Laser-Based Hazard Detection Sensor	124
3.3.16 Active Two-Dimensional Stereoscopic Ranging System	124
3.3.17 Programmable Near-Infrared Proximity Sensor	126
3.3.18 Return Signal Intensity Rangefinder	127
3.3.19 MIT Near-Infrared Ranging System	127
3.3.20 Passive Ranging and Collision Avoidance Using Optical Flow	128
3.3.21 Recovering 3D Scene Structure from Visual Data	128
3.3.22 Edge Detection by Active Defocusing	131
3.3.23 MnSCAN: 3D Multipoint and Multibody Motion Tracking System ...	132
3.3.24 Active Triangulation Rangefinder for a Planetary Rover	134
4.0 REFERENCES	137

FIGURES

1. Taxonomy of noncontact ranging methods for mobile robots (Everett, 1987).	3
2. Break-beam optical proximity sensor.	6
3. Reflective optical proximity sensor.	6
4. A special case of the diffuse type, the convergent optical proximity sensor.	7
5. Triangulation ranging. Observed angles at P_1 and P_2 can be used in conjunction with known separation A , to calculate the range to P_3	7
6. Stereoscopic ranging. Bearings to a common point of interest are measured using two cameras with known baseline separation A	8

7. Laser triangulation. Measured angle ϕ decreases as the object moves closer to the camera and laser source.	10
8. Known target size. The angle subtended by an object of known dimension is observed to increase as distance decreases in moving from position 2 to position 1 and can be used to calculate unknown range.	12
9. Optical flow field due to translation (Heeger & Jepson, 1990a).	13
10. Frequency modulation. The reflected signal (dashed line) is displaced along the time axis by an amount proportional to the target range.	16
11. Interferometer block diagram. A retroreflector must be placed on the target of interest.	18
12. Diffraction grating geometry. The higher order diffraction image perceived at point C appears at angle V from the central optical axis OC (DeWitt, 1989).	20
13. Diffraction rangefinder. Multiple images of an object appear when viewed through a grating; their displacement is proportional to distance D (DeWitt, 1991). .	21
14. Block diagram of a passive swept-focus ranging system (Courtesy Associates and Ferren Corporation).	22
15. Ultrasonic ranging error due to beam divergence.	26
16. Ultrasonic ranging error due to specular reflection.	27
17. Illustration of FMC-A autofocus principle (Courtesy Pentax Corporation).	36
18. Block diagram of the Hamamatsu's Range-Finder Chip Set, which applies the principle of triangulation (Hamamatsu Corporation, 1990).	37
19. Block diagram of Hamamatsu's Displacement Sensor (Hamamatsu Corporation, 1991).	38
20. The HVS-300 distance sensor gauge uses dual active near-infrared emitters to detect if an object is in the adjustable OK zone (Courtesy Honeywell Corporation). .	40
21. <i>Illustration of the Visitronic Autofocus System (Courtesy Honeywell Corporation).</i>	41
22. Schematic diagram of Visitronic Autofocus System (Courtesy Honeywell Corporation).	42
23. Light from two separate sectors of the same lens is compared to determine the position of best focus in the TCL Autofocus System (Courtesy Honeywell Corporation).	44
24. A row of microlenses focuses light on the pairs of detectors, forming two separate signatures for comparison (Courtesy Honeywell Corporation).	44
25. Target range.	47
26. Target bearing.	47
27. Scanning and nodding mirrors arrangement in the ERIM laser rangefinder (Courtesy Environmental Research Institute of Michigan).	50

28. Chesapeake laser-scanning range measurement system.	52
29. Chesapeake Laser's CMS-1000 Space Location System installed on the Intelligent Robotic Inspection System built for the Navy by MTS Systems Corporation (Courtesy MTS Systems Corporation).	54
30. Block diagram of Odetics Scanning Laser Rangefinder (Courtesy Odetics Incorporated).	56
31. Schematic block diagram of ESP's ORS-1 Optical Ranging System (ESP Technologies Incorporated, 1992).	58
32. A representative ranger scan taken in a laboratory environment (ESP Technologies Incorporated, 1992).	59
33. Schwartz Electro-Optics Scanning Laser Rangefinder (Schwartz Electro-Optics Incorporated, 1991a).	60
34. Schwartz Electro-Optics LRF-X Laser Rangefinder (Courtesy Schwartz Electro-Optics Incorporated, 1991b).	61
35. Schwartz Electro-Optics Multi-Channel three-dimensional image of a tank next to a bush (Schwartz Electro-Optics Incorporated, 1991c).	62
36. A block diagram of Transitions Research Company's Strobed Light Triangulation System mounted on the HELPMATE mobile platform (Courtesy Transitions Research Company).	68
37. The Sensus 300 configured for 360-degree coverage (Courtesy NOMADIC Technologies Incorporated).	71
38. The Sensus 500 light vision system (Courtesy NOMADIC Technologies Incorporated).	72
39. FMC Corporation's Ultrasonic Imaging Sensor (Courtesy FMC Corporation). ..	77
40. The imaging sensor mounted on an Army M113 armored personnel carrier used by FMC as an autonomous mobile testbed (Courtesy FMC Corporation).	78
41. Quantic's Wide Angle Optical Ranging System will be employed on this modular robot developed by NCCOSC.	80
42. A block diagram of the transmitter and receiver subsystems of Quantic's sequentially scanned active triangulation system. (Courtesy Quantic Industries Incorporated).	81
43. The pattern of the LED beams and their positioning behind the lens (Courtesy Quantic Industries Incorporated).	82
44. Planned placement for the Helicopter Optical Proximity Sensor System in a U.S. Army Helicopter (Schwartz Electro-Optics Incorporated, 1991d).	84
45. The laser beam is reflected from a surface that is rotating about the vertical axis with angular velocity ω (Schwartz Electro-Optics Incorporated, 1991e).	85
46. The beam pattern if the prism rotation rate, β , is greater than the angular velocity, ω , of the reflecting surface (Schwartz Electro-Optics Incorporated, 1991e). ..	86

47. RVSI Ship Surface Scanner was designed to digitize the interior of ship spaces for overhaul planning (Courtesy Robotic Vision Systems Incorporated).	87
48. Hexagonal rotating mirror used in the multispectral scanner reduces crosstalk and simplifies mirror alignment (Courtesy Environmental Research Institute of Michigan).	90
49. Block diagram of the multispectral ALV scanner (Courtesy Environmental Research Institute of Michigan).	91
50. Block diagram of the RVSI LORDS ranging concept (Courtesy Robotic Vision Systems Incorporated).	93
51. Swept-Focus Camera subsystem developed for the Navy for passive three-dimensional vision applications (Courtesy Associates and Ferren).	96
52. Video and high-pass filter output when viewing a piece of expanded metal (left) and a pencil (right).	97
53. A focus-based optical ranging sensor (Wilcox, 1990).	99
54. NASA's Planetary Rover with stereo vision system using a one-dimensional penalty function to model smoothness (Courtesy NASA Jet Propulsion Laboratory).	101
55. A rotating drum forms the heart of the Battelle diffraction antenna beam steering concept (Courtesy Battelle Columbus).	105
56. NASA's capaciflector mounted on the robot arm (Courtesy NASA Goddard Space Flight Laboratory).	107
57. Illustrating the principle of the capaciflector; electric field lines without a reflector (Vranish, McConnell & Mahalingham, 1991).	108
58. Electric field lines when a reflector is present (Vranish et al., 1991).	108
59. Schematic of the electronics of the capaciflector (Vranish et al., 1991).	109
60. Block diagram of the Honeywell displaced sensor ranging system.	110
61. Target position is more precisely determined through a combination of time-of-flight ranging and triangulation using an array of four transducers (Ma & Ma, 1984).	111
62. Vertical retroreflective cylinders used for navigation (Banzil et al., 1981).	112
63. Detected reflection pattern confirms acquisition.	112
64. Simultaneous beam projections when the measurements differ (University of Michigan Mobile Robotics Laboratory, 1991a).	114
65. Simultaneous beam projections when the measurements coincide (University of Michigan Mobile Robotics Laboratory, 1991a).	114
66. Ultrasonic range sensing array system design (University of Minnesota Robotics Laboratory, 1992).	115

67. Schematic of ultrasonic processing board (University of Minnesota Robotics Laboratory, 1992).	116
68. Ultrasonic sensor timing diagram (University of Minnesota Robotics Laboratory, 1992).	117
69. Schematic of the Virtual Force Field concept (University of Michigan Mobile Robotics Laboratory, 1991b).	119
70. Schematic of the laboratory obstacle course (Borenstein & Raschke, 1991).	120
71. After interrogating the environment, a composite schematic is generated from a polar histogram overlaying the cartesian histogram grid (Borenstein & Raschke, 1991).	121
72. Retroreflectors placed alongside a roadway are used as reference in a proposed automatic lateral positioning scheme (Tsumura et al., 1984).	122
73. Active Stereoscopic Ranging System used on ROBART II.	125
74. Programmable Near-Infrared Proximity Sensor used on ROBART II.	126
75. Recovery of 3D Range from Binocular Imagery (Wildes, 1991).	129
76. Recovery of 3D Attitude from Binocular Imagery (Wildes, 1990a).	130
77. Recovery of 3D Surface Curvature from Binocular Imagery (Wildes, 1990b).	131
78. Block diagram of the active defocussing edge extraction system (Zhu et al., 1991).	132
79. MnScan: 3D Multi-Point and Multi-Body Motion Tracking System Configuration (Sorensen et al., 1989).	133
80. Photo of Draper Lab active laser rangefinding system.	134

1.0 INTRODUCTION

The past few years have brought about a tremendous rise in the envisioned potential of robotic systems and a significant increase in the number of proposed applications. In the nonindustrial arena, numerous programs have evolved, each intending to harness some of this promise in hopes of solving some particular application need. Many of these efforts are government sponsored, aimed at the development of systems for fighting fires, handling ammunition, transporting materials, conducting underwater search and inspection operations, and patrolling warehouses and storage areas, etc. Many of the resulting prototypes, which were initially perceived as logical extensions of the traditional industrial robotic scenarios, have met with unexpected difficulty due to an insufficient supporting technology base.

One problem area common to many of these efforts arises from the need of a mobile system to interact with the physical objects and entities in its environment. The platform must be able to navigate from a known position to a desired new location and orientation, while avoiding any contact with fixed or moving objects while enroute. There has been a tendency to oversimplify these issues, and assume the natural growth of technology will provide the needed solutions. While such solutions will ultimately come to pass, it is important to pace the evolution of the platform with a parallel development of the needed collision avoidance and navigation technology. Fundamental in this regard are the required sensors with which to acquire high resolution data describing the robot's physical surroundings, in a timely yet practical fashion, in keeping with the limited onboard energy and computational resources of a mobile vehicle.

The difficulty can be directly related to the unstructured nature of the operating environment. Industrial process control systems used in high-volume manufacturing scenarios rely on carefully placed sensors that exploit the target characteristics. Background conditions are arranged to provide minimal interference, and often aid in the detection process by increasing the on-off differential or contrast. The introduction of industrial robots and the accompanying shift toward flexible versus hard automation has led to increasing use of vision systems as opposed to the more simplistic proximity and breakbeam sensors. More intelligent process and quality control decisions are made possible, but at the expense of increased system complexity.

Trying to directly carry this specialized assembly-line technology over into the unstructured world of a mobile robot makes little sense; the problems are fundamentally different. For example, in the collision avoidance problem, the nature and orientation of the target surface is not known with any certainty; the system must detect a wide variety of surfaces under varying angles of incidence. Control of background and ambient conditions may not be possible. Preprogrammed information regarding the relative positions, orientations, and nature of objects within the sensor's field of view becomes difficult for a moving platform. Specialized sensors intended to cope with these problems are needed to provide a mobile platform with sufficient environmental awareness of its surroundings to allow it to move about in a realistic fashion.

Possible considerations for such sensors are summarized (Everett, 1987):

Field of view. Wide enough with sufficient depth of field to suit the application.

Range capability. The minimum range of detection, as well as the maximum effective range, must be appropriate for the intended use of the sensor.

Accuracy and resolution. Must be in keeping with the needs of the given task.

Ability to detect all objects in environment. Objects can absorb emitted energy; target surfaces can be specular as opposed to diffuse reflectors; ambient conditions and noise can interfere with the sensing process.

Operate in realtime. The update frequency must provide rapid, realtime data at a rate commensurate with the vehicle's speed of advance.

Concise, easy to interpret data. The output format should be realistic from the standpoint of processing requirements; too much data can be as meaningless as not enough; some degree of preprocessing and analysis is required to provide output only when action is required, with threat ranking.

Redundancy. The system should provide a graceful degradation and not become incapacitated due to the loss of a sensing element; a multimodal capability would be desirable to ensure detection of all targets, as well as to increase the confidence level of the output.

Simplicity. The system should be modular to allow for easy maintenance and evolutionary upgrades, not hardware specific, and low in cost.

Power consumption. The power requirements should be minimal in keeping with the limited resources onboard a mobile vehicle.

Size. The physical size and weight of the system should be practical with regard to the intended vehicle.

Mobile ranging needs can be broken down into two issues: navigation and collision avoidance. Navigational sensors typically require high angular and/or range resolution over fairly long distances, with a relatively narrow field of view. Collision avoidance sensors, on the other hand, would operate over shorter ranges, with less resolution required. The field of view should provide sufficient coverage for a turning vehicle and allow enough time for the vehicle to stop or alter course.

This document provides some basic background on the various noncontact distance measurement techniques available (figure 1), with related discussion of implementation in the acoustical, optical, and electromagnetic portions of the energy spectrum. An overview of candidate systems, both commercially available and under development, is provided; followed by a brief summary of research currently underway in support of the collision avoidance and noncontact ranging needs of a mobile robot.

NONCONTACT RANGING TECHNOLOGIES

PROXIMITY

- MAGNETIC
- INDUCTIVE
- ULTRASONIC
- CAPACITIVE
- OPTICAL
 - BREAK-BEAM
 - REFLECTIVE
 - DIFFUSE

TRIANGULATION

- STEREO DISPARITY
- ACTIVE TRIANGULATION
- STRUCTURED LIGHT
- KNOWN TARGET SIZE

OPTICAL FLOW

TIME OF FLIGHT

PHASE SHIFT MEASUREMENT

FREQUENCY MODULATION

INTERFEROMETRY

FRINGE COUNTERS

DIFFRACTION GRATINGS

SWEPT FOCUS

RETURN SIGNAL INTENSITY

Figure 1. Taxonomy of noncontact ranging methods for mobile robots (Everett, 1987).

2.0 BACKGROUND

2.1 RANGING TECHNIQUES

2.1.1 Proximity

Proximity sensors are used to determine the presence (as opposed to actual range) of objects moving near a sensing probe. Such sensors were developed to gain position information in the close-in region (between a fraction of an inch and several inches), extending the sensing range beyond that afforded by direct-contact tactile or haptic sensors. Advances in electronic technology have improved the performance and reliability of these devices, thereby increasing the number of possible applications. Many installations, which historically have used mechanical limit switches, can now use proximity switches for their close-in sensing needs.

The reliability characteristics displayed by these instruments make them suited for operation in harsh or otherwise adverse environments, while providing high-speed response and long service lives. Instruments can be designed to withstand significant shock and vibration, with some capable of handling forces over 30,000 Gs and pressures of nearly 20,000 psi (Hall, 1984). Because of the inherent ability to sense through nonferrous materials, magnetic and inductive proximity switches can be coated, potted, or otherwise sealed permitting their operation in contaminated work areas or even submerged in fluids. In addition, proximity devices are valuable when detecting objects moving at high-speed, when contact with an object may cause damage, or when differentiation between metal and nonmetal objects is required.

Proximity switches are classified into several types related to the specific properties used to initiate a switching action. Permanent-magnet sensors are good for sensing ferrous objects over very short distances, and generally consist of a steel armature positioned between two permanent-magnetic fields. These fields hold the armature in a constant position until a ferrous object approaches, that diverts one of the fields and allows the remaining field to become dominant. The dominant field draws the armature to a contact, thereby closing a switch. This type of sensor has no applicability on a mobile robotic platform for purposes of external obstacle detection, due to the limited range and need for a ferrous target.

Continuing, induction-type proximity switches are applied to the detection of metal objects located at short-range. Typical inductive sensors generate an oscillatory radio-frequency (RF) field around a coil of wire. When a metal object enters the field, the effective inductance of the coil changes, resulting in an oscillator frequency shift that is converted into an output signal. Sensing range is approximately equal to the diameter of the sensing coil (Koenigsburg, undated).

Inductive sensors have limited use for purposes of object detection, except in application-specific instances. One such example involves a large industrial manipulator that cleans the exterior hulls of ships in drydock (Everett, 1985c). Inductive sensors are used to sense the presence of the steel hull surface, controlling a servomechanism that keeps the manipulator under pre-loaded contact as it traverses the hull removing rust and marine growth.

Ultrasonic proximity sensors (not to be confused with ultrasonic ranging systems) are useful over longer distances (several feet) for detecting most objects, liquid and solid. Typical systems consist of two transducers, one to transmit and one to receive the return energy. When no object

is present, the control circuitry indicates no output; when an object enters the acoustical field, energy is reflected back to the receiver. When the received signal reaches the preset threshold, the sensor output changes state, indicating detection.

The capacitive type proximity sensor is effective for short-range detection (a few inches) of most objects. Such sensors measure the electrical capacitance between a probe and its surrounding environment. As an object draws near, the changing geometry and/or dielectric characteristics within the sensing region cause the capacitance to change, affecting the current flow through the probe. The distance between the sensor and the target is inversely proportional to the probe current (Hall, 1984). The use of this type of sensor for collision avoidance purposes is again extremely limited and very application specific.

Optical proximity sensors can be broken down into three basic groups: (1) break beam, (2) reflective, and (3) diffuse. In the first of these categories, separate transmitting and receiving elements are physically located on either side of the region of interest. The transmitter emits a beam of light, often supplied by a light-emitting diode (LED), that is focused on the photosensitive receiver (figure 2). Any object passing between the emitter and receiver breaks the beam, disrupting the circuit.

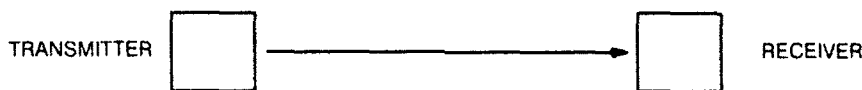


Figure 2. Break-beam optical proximity sensor.

Figure 3 shows reflective optical proximity sensors that evolved from break beam through the use of a mirror to reflect the transmitted energy back to a detector collocated with the transmitter. Corner-cube and cat's-eye retroreflectors quickly replaced the mirrors to cut down on critical alignment needs. In most cases, the object of interest is detected when it breaks the beam, although some applications call for placing the retroreflector on the object itself.

Sensors in the diffuse category operate in similar fashion to reflective, except that energy is returned from the surface of the object of interest as opposed to a cooperative target reflector. Modulated near-infrared energy is typically employed to reduce the effects of ambient lighting, thus achieving the required signal-to-noise ratio for reliable operation.

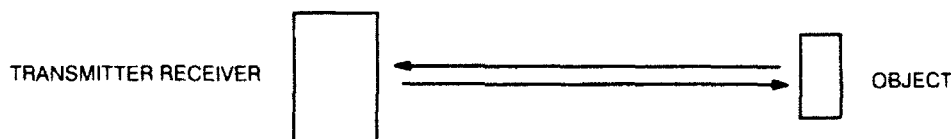


Figure 3. Reflective optical proximity sensor.

A subcategory of diffuse is the convergent optical proximity sensor. This sensor employs a special geometry in the configuration of the transmitter with respect to the receiver to ensure more precise positioning information. Figure 4 shows the optical axis of the transmitting LED is angled with respect to that of the detector, so the two intersect only over a narrowly defined region. It is only at this specified distance from the device that a target can be in position to

reflect energy back to the detector. Consequently, targets beyond this range are not detected. This feature decouples the proximity sensor from any dependence on the reflectivity of the target surface, and is useful where targets are not well displaced from background objects. Sensors of this type were used on ROBART II (Everett, 1985a) to detect discontinuities in the floor surface, such as a descending stairway.

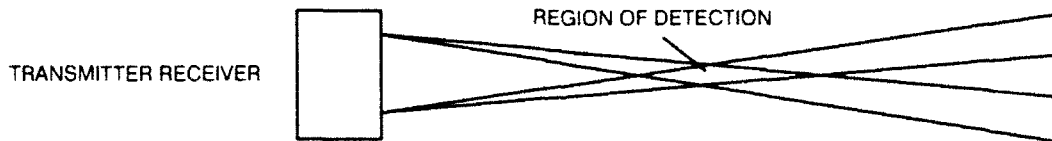


Figure 4. A special case of the diffuse type, the convergent optical proximity sensor.

The performance specifications of proximity sensors depend on several factors. Effective range is a function of the physical characteristics (size, shape, and material) of the object to be detected, its speed and direction of motion, the design of the sensor probe, and the quality and quantity of energy it radiates or receives. Distance resolution is dependent upon object size, speed, and generally reduces with increased range. Finally, repeatability in detection is based on the size of the target object, changes in ambient conditions, variations in reflectivity or other material characteristics of the target, and the stability of the electronic circuitry of the sensor.

2.1.2 Triangulation

This common ranging technique with ancient Greek and Egyptian origins has historically been used in ship navigation, surveying, and civil engineering applications. Triangulation presents a simple trigonometric method for calculating the distances and angles needed to determine object location. An important premise of plane trigonometry is that given the length of a side and two angles of a triangle, it is possible to determine the length of the other sides and the remaining angle. The basic Law of Sines can be rearranged as shown to represent the length of side B as a function of side A, and the angles θ and Φ :

$$B = A \frac{\sin \theta}{\sin \alpha} = A \frac{\sin \theta}{\sin(\theta + \phi)}$$

In practical applications, length B would be the range to a desired object (figure 5).

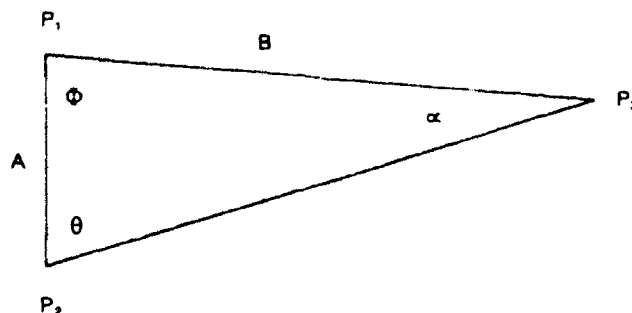


Figure 5. Triangulation ranging. Observed angles at P_1 and P_2 can be used in conjunction with known separation A, to calculate the range to P_3 .

Ranging systems using triangulation for robot navigation and collision avoidance are classified as either passive or active. Passive stereoscopic ranging systems that use only the ambient light of the scene to illuminate the target, position directional detectors such as TV cameras, solid-state imaging arrays, or photodetectors at positions corresponding to locations P_1 and P_2 (figure 6). Both imaging sensors are focused on the same object point, P_3 , forming an imaginary triangle. The distance between the detectors as well as their orientation angles can be measured and used to calculate the range to the object of interest.

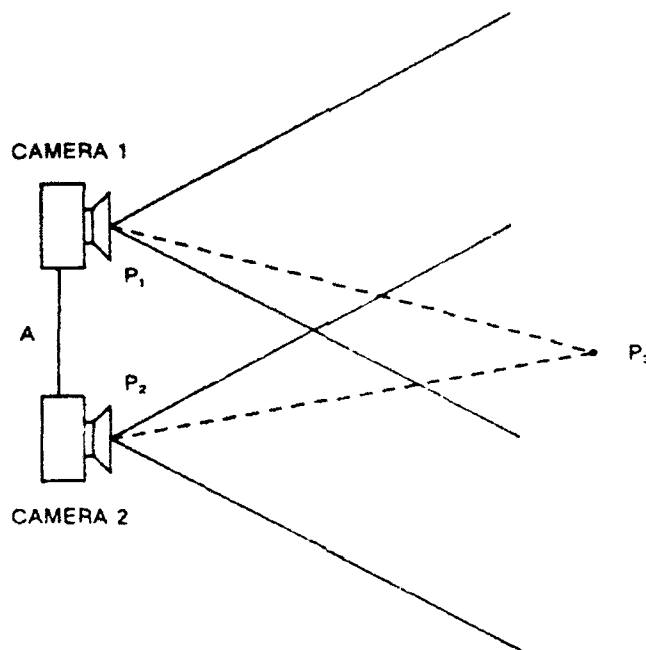


Figure 6. Stereoscopic ranging. Bearings to a common point of interest are measured using two cameras with known baseline separation A .

Active triangulation systems position a controlled light source, such as a laser, at either point P_1 or P_2 that is directed at the observed point, P_3 . A directional imaging sensor is placed at the remaining triangle vertex and is also aimed at P_3 . Illuminating energy from the source light will strike the target and be reflected, with a portion of the light falling on the detector, permitting range determination by the Law of Sines. In both passive and active systems, an array of range points can be determined by adjusting the incident angles of the detectors and/or the light source in a raster sequence. The resulting range map is a three-dimensional image of the environment in front of the sensor.

The performance characteristics of triangulation systems are to some extent dependent on whether the system is active or passive in nature. Passive triangulation systems require special ambient lighting conditions that must be artificially provided if the environment is too dark. Furthermore, these systems suffer from a correspondence problem resulting from the difficulty in matching points viewed by one image sensor with those viewed by the other. On the other hand, active triangulation techniques employing but a single detector do not require special

ambient lighting, nor do they suffer from the correspondence problem. Active systems, however, encounter instances of no recorded strike because of specular reflectance or surface absorbance of the light.

Limiting factors common to all triangulation sensors include angular measurement inaccuracies and a *missing parts* problem. *Missing parts* refers to the occurrence where particular portions of a scene can be observed by only one viewing location (P_1 or P_2). This situation arises because of the offset distance between the viewing locations causing partial occlusion of the target. The design of triangulation systems must include a tradeoff analysis of the offset; as this baseline measurement increases, the range accuracy increases but problems due to directional occlusion worsen.

2.1.2.1 Stereo Disparity. The first of the triangulation schemes to be discussed, stereo disparity, (also referred to as stereo vision, binocular vision, and stereopsis) is a passive ranging technique modeled after the depth-measuring capabilities of the human eye. When a three-dimensional object is viewed from two locations on a plane normal to the direction of vision, the image when observed from one position will shift laterally when viewed from the other. This displacement of the image, known as disparity, is inversely proportional to the distance to the object.

Practical ranging devices based on stereopsis use a pair of identical television cameras (or a single camera with the ability to move laterally) to generate the two disparity images. The cameras are typically aimed straight ahead, view approximately the same scene, and do not possess the capability to converge their center of vision on an observed point like the human eye can. This limitation makes *placement of the cameras critical* because stereo ranging can take place only in the region where the fields of view of the two camera positions overlap. A reference point corresponding to the center of vision is determined for both images, from which the displacement of the point of interest is measured. The difference in the displacements between the two images, the focal length of the cameras, and the distance between camera locations are used to calculate range.

Four basic steps are involved with this ranging process. First, a point in the image of one camera must be identified and located. Second, the same point must be located in the image of the other camera. Third, their positions must be measured with respect to a common reference, and fourth, the distance to the point must be calculated from the disparity in the measurements (Poggio, 1984). On the surface this procedure appears straightforward. However, a major obstacle arises when attempting to locate the specified point in the second image, due to the same binocular disparity that is being used to determine range. The effort to match the two images of the point is called correspondence, and methods for minimizing this computationally expensive procedure are widely discussed in the literature (Poggio, 1984; Jarvis, 1983a; Nitzan, 1981; Loewenstein, 1984; Wildes, 1991).

Correspondence between images can occur only when the identified point lies in both views, giving rise to the *missing parts* problem where the range cannot be determined for a point seen in one view, but otherwise occluded or not present in the other. To compensate, the baseline distance between the cameras can be shortened to increase the overlap area; however, measurement accuracy is decreased as separation diminishes. Matching is further complicated in regions where the intensity or color are uniform (Jarvis, 1983b). Additional factors affecting

performance include the presence of shadows in only one scene and the variation in image characteristic resulting from viewing environmental lighting effects from different angles.

2.1.2.2 Active Triangulation. Ranging by active triangulation is a variation on the stereo disparity method of distance measurement. In place of one camera is a laser (or LED) light source aimed at the surface of the object of interest. The remaining camera is offset from this source by a known distance, and configured to hold the illuminated spot within its field of view (figure 7).

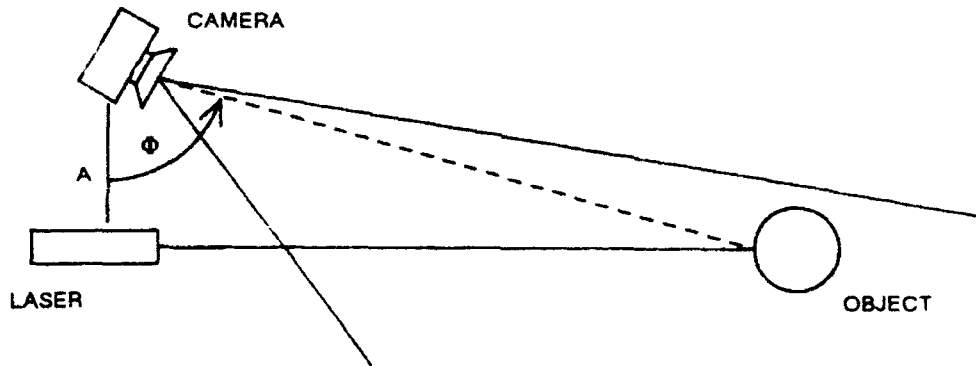


Figure 7. Laser triangulation. Measured angle ϕ decreases as the object moves closer to the camera and laser source.

From this image, the range to the surface can be determined. For one- or two-dimensional array detectors such as vidicon or charge-coupled-device cameras, the range is typically determined from the known baseline distance and the position of the laser spot image on the array relative to some reference. For mechanically scanned single element detectors such as photodiodes or phototransistors, range is generally determined by measuring the rotational angles of the detector and/or source at the exact moment when the detector observes the illuminated spot. The trigonometric relationship between these angles and the baseline value are used to compute the distance.

To obtain three-dimensional information for an entire scene, laser triangulators can be scanned in both azimuth and elevation. In systems where the source and photodetector are fixed, the entire sensing configuration can be moved mechanically. In systems with movable optics, the mirrors, lenses, etc., are generally moved in synchronization. The major drawbacks to active triangulation include the situation where points illuminated by the light source cannot be seen by the camera and vice versa (*missing parts*) (Jarvis, 1983b), as well as surface absorption or specular reflection of the irradiating energy. On the positive side, however, the point source illumination of the image effectively eliminates the correspondence problem encountered in stereo disparity rangefinders.

2.1.2.3 Structured Light. Ranging systems that employ structured light are a further refined case of active triangulation ranging. An active source projects a pattern of light (either a line, a series of spots, or a grid pattern) onto the object surface, while the camera observes the pattern from its offset vantage point. Range is determined by triangulation and manifests itself in the distortions visible in the projected pattern due to variations in the depth of the scene. The use of

these special lighting effects reduce the computational complexity and improve the reliability of three-dimensional object analysis (Jarvis, 1983b). The technique is commonly used for rapid extraction of limited quantities of visual information of moving objects (Kent, 1985), and thus lends itself well to collision avoidance applications.

The most common structured light ranging configuration, projecting a line of light onto a scene, was originally introduced by P. Will and K. Pennington of IBM Research Division Headquarters, Yorktown Heights, NY (Schwartz, undated). Their system created a plane of light by passing a collimated, incandescent source through a slit that projected a line across a scene viewable by an offset camera. (This line can also be formed by passing a laser beam through a cylindrical lens or by rapidly scanning the beam in one dimension.)

Where the line intersects an object, the camera view will show displacements or kinks in the light stripe that are proportional to the depth of the scene. The result is a two-dimensional contour line representing a narrow segment of the surface. The proportionality constant between the light stripe displacement and depth is dependent on the length of the baseline between the source and the detector. Like any triangulation system, when the baseline separation increases, the accuracy of the sensor increases; but the *missing parts* problem worsens.

Three-dimensional range information for an entire scene can be obtained in relatively simple fashion through striped lighting techniques. By assembling a series of rapidly produced, closely spaced two-dimensional contours, a three-dimensional description of a region within the camera field of view can be constructed. The third dimension is typically provided by scanning the laser plane across the scene. Compared to a single-point triangulation, striped lighting generally requires less time to scan over a surface, with fewer moving parts because of the need to scan only in one direction. Such systems have been able to construct images of a scene on the order of 200 times faster (Simmons, 1986). The drawback to this concept is that range extraction is time consuming and difficult, due to the necessity to store and analyze many frames.

An alternative structured light technique involves projecting a rectangular grid of high-contrast light points or lines onto a surface. Variations on depth cause the grid pattern to distort, providing a means for range determination. The extent of the distortion is ascertained by comparing the displaced grid with the original projected patterns as follows: (1) identify the intersection point of the distorted grid image, (2) label these intersections according to the coordinate system established for the projected pattern, (3) compute the disparities between the intersection points and/or lines of the two grids, and (4) convert the displacements to range information (Le Moigue & Waxman, 1984).

The comparison process requires correspondence between points on the image and the original pattern, which can be troublesome. However, by correlating the image grid points to the projected grid points, this problem can be somewhat alleviated. A critical design parameter is the thickness of the lines that make up the grid and their spacing. Excessively thin lines will break up in busy scenes, causing discontinuities that adversely affect the intersection points labeling process. Thicker lines will produce less observed grid distortion resulting in reduced range accuracy (Le Moigue & Waxman, 1984). The sensor's intended domain of operation will determine the density of points required for adequate scene interpretation and resolution.

2.1.2.4 Known Target Size. A stadimeter is a hand-held nautical instrument used for optically measuring the distance to objects of known heights, between 50 and 200 feet, covering ranges

from 200 to 10,000 yards. The stadimeter measures the angle subtended by the object, and converts it into a range reading taken directly from a micrometer drum (Dunlap & Shufeldt, 1969).

The final variation on the triangulation-ranging method to be discussed makes use of this same technique. Range is calculated through simple trigonometry; the known baseline, instead of being between two cameras (or a detector and a light source) on the robot, is now the target itself. The concept is illustrated in figure 8. The only limiting constraint (besides knowing the size of the target) is the target must be normal to the optical axis of the sensor, which in the case of a passive system can be an ordinary CCD camera.

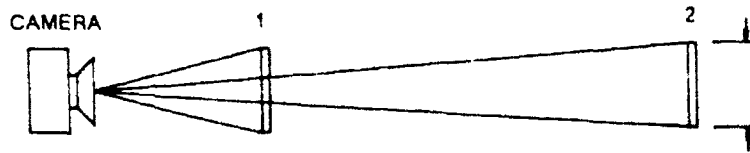


Figure 8. Known target size. The angle subtended by an object of known dimension is observed to increase as distance decreases in moving from position 2 to position 1 and can be used to calculate unknown range.

The standard lens equation applies:

$$\frac{1}{r} + \frac{1}{s} = \frac{1}{f}$$

where r = distance from lens to object viewed
 s = distance from lens to image plane
 f = focal length of the lens.

Now, suppose the camera views an open doorway of known width A . If A is relatively small compared to the unknown distance r , then the range can be approximated by the formula (Nitzan et al., 1986):

$$r = \frac{Af}{w}$$

where A = known width
 w = perceived width in image plane.

If the view angle for the object of interest is wide (i.e., A is not small with respect to r), then local geometric features should be examined (Nitzan et al., 1986).

One implementation of this ranging concept used on automated guided vehicles (AGVs) employs a scanning laser source mechanically coupled to a similarly rotating detector (section 3.1.11). A retroreflective target of known width is placed in a strategically located position to serve as a navigational aid. As the rotating laser scans across the retroreflector, energy is returned to the receiving detector. The length of the arc of rotation, during which the detector senses reflected energy, is directly related to the distance of the target: the closer the target, the longer the perceived arc.

2.1.2.5 Optical Flow. Range information can also be derived through the optical flow in the image sequence. Optical flow is the apparent motion of the brightness pattern produced by the

relative motion between the camera and the objects in the environment. Figure 9 shows an optical-flow field resulting from the translational movement of a camera mounted on a vehicle traveling on a planar surface. The optical-flow vectors from closer objects will have greater magnitudes than the vectors from distant objects. One of the main advantages of using optical flow is that the ratio of distance to speed (e.g., time-to-collision) can be easily obtained and used for obstacle avoidance (Young et al., 1992; Heeger & Jepson, 1990a, 1990b).

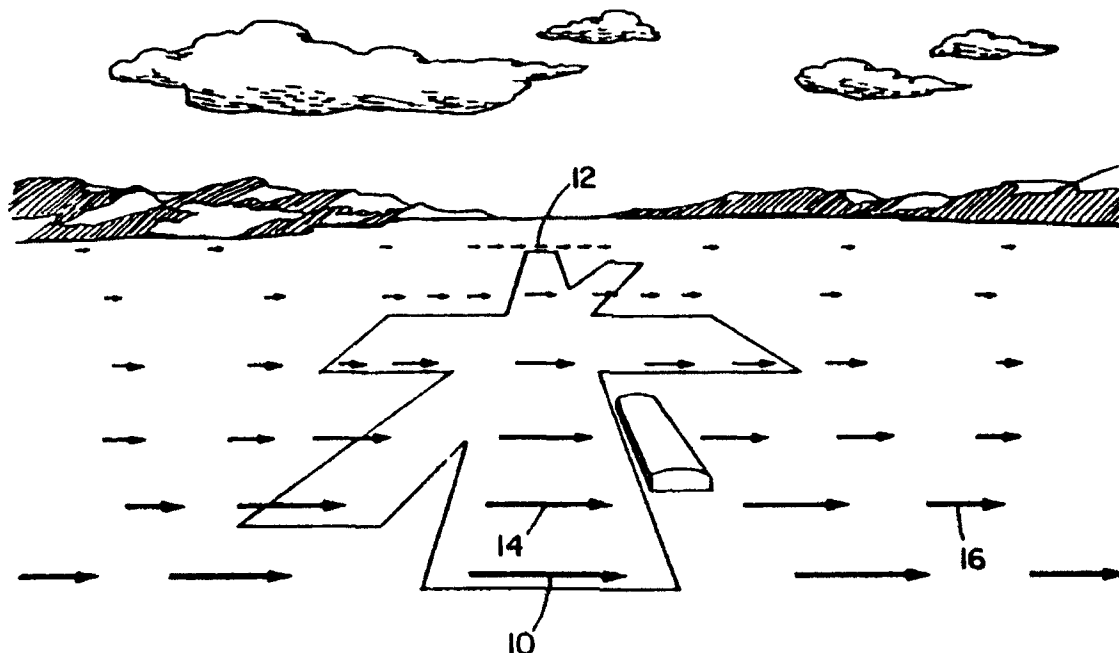


Figure 9. Optical flow field due to translation (Heeger & Jepson, 1990a).

The optical flow often cannot be found by local computations on the image pixels due to a phenomenon known as the aperture problem. However, the component of the optical flow in the direction of the local brightness gradient (also known as the normal flow, since it is perpendicular to the brightness edge) can always be computed locally and easily. The magnitude of the normal flow vector is

$$M_n = \frac{E_t}{\sqrt{(E_x^2 + E_y^2)}}$$

Where: M_n = magnitude of normal flow vector

E_t = time derivative of the pixel brightness

E_x = spatial derivative along the x axis

E_y = spatial derivatives along the y axis.

When the motion of the camera is known, distances to points in the scene can be computed directly from the normal flow, with the most accurate results at points where both the brightness gradient and the normal flow are greatest (Nguyen, 1993).

When camera motion is not known, the camera motion and distances to points in the scene can be recovered from the optical flow, but only up to a scaling factor. That is, we can find the

ratios between the distances to different points in the image, but not their absolute distances. If the distance to one point can be pinpointed by another method (such as by active sonar), then the distances to all points will be known. The computations are easiest if the camera motion is purely translational or purely rotational (Horn, 1986). Iterative and approximation schemes for estimating camera motion and distances from visual motion are still being actively investigated (Fermuller & Aloimonos, 1991; Duric & Aloimonos, 1991).

2.1.3 Time of Flight

Another rangefinding technique originally used in surveying applications to accurately measure distance is time of flight (TOF), referring to the time it takes for a pulse of energy to travel from transmitter to an observed object then back to a receiver. The energy transmission typically originates from an ultrasonic, radio, or light source. The relevant parameters involved in range calculation, therefore, are the speed of sound (roughly 1 foot/millisecond), and the speed of light (1 foot/nanosecond). TOF systems measure the round-trip time between an energy pulse emission and the return of the echo resulting from reflectance off an object. Using elementary physics, distance d is determined by multiplying the velocity v of the energy wave by the time t required to travel the distance:

$$d = vt$$

In this case, the measured time is representative of traveling twice the distance and must therefore be reduced by half to result in actual range to the target.

The advantages of TOF systems arise from the direct nature of their active sensing. Transmissions are in a straight-line fashion from the transducer to the object. The returned signal follows essentially the same direct path back to the receiver, which is generally located coaxially with or in close proximity to the transmitter. In fact, it is possible for the transmitting and receiving transducers to be the same device. The absolute range to an observed point is directly available as output with no complicated analysis required, and the technique is not based on any assumptions concerning the planer properties of objects. The *missing parts* problem of triangulation does not arise because minimal or no offset distance between transducers is needed for the range calculation. Furthermore, TOF sensors maintain range accuracy in a linear fashion as long as reliable echo detection is maintained, while triangulation schemes suffer diminishing accuracy as range increases.

The limitations of TOF systems are primarily related to the properties of the emitted energy, which vary across the spectrum. When light, sound, or radio waves strike an object, only a small portion of the original signal returns to be detected. The remaining energy reflects in scattered directions or is absorbed, depending on the characteristics of the object's surface and the angle of incidence (angle of approach) of the source transmission. The scattered signals can reflect from secondary objects as well and return to the detector at various times, resulting in false signals yielding questionable or otherwise noisy data. To compensate, repetitive measurements are averaged to bring the signal/noise response within acceptable levels, but at the expense of additional time required to determine a single range value.

Instances where no return signal is received can occur because of specular reflection by the object surface, especially in the ultrasonic region of the energy spectrum. (In specular reflection, the angle of incidence equals the angle of reflection.) If the transmission source approach angle

meets or exceeds a certain critical value, the reflected energy will be deflected outside of the sensing envelope of the receiver. This threshold angle is a function of the wavelength of the energy and the topographical characteristics of the target (Everett, 1985b).

Finally, the propagation speed of electromagnetic energy can place severe requirements on associated control and measurement circuitry. As an example, TOF sensors based on the speed of light require subnanosecond timing circuitry to measure distances with a resolution of about a foot (Koenigsburg, undated). This capability is expensive to realize and may not be cost effective for certain applications, particularly at close range where high accuracies are required.

Such laser-based TOF ranging systems (also known as light or laser radar (LIDAR)) first appeared in work performed at the Jet Propulsion Laboratory in the 1970s (Lewis & Johnson, undated). Laser energy is emitted in a rapid sequence of short bursts aimed directly at the object being ranged. The time required for a given pulse to reflect off the object and return is measured, and used to calculate range based on the known speed of light. Ranging is direct and the calculations are not computationally difficult. Accuracies for sensors of this type approach a few centimeters over the range of 1 to 5 meters (Depkovich & Wolfe, 1984).

2.1.4 Phase Shift Measurement

Laser-based continuous wave (CW) ranging originated out of research performed at the Stanford Research Institute in the 1970s (Nitzan et al., 1977). This method of distance measurement requires the transmission of CW energy in contrast to the pulsed outputs used in direct measurement TOF systems, and involves a determination of the shift in phase of the signal as it returns from a reflecting object.

A continuous beam of modulated laser energy is directed towards the target: a portion of this wave is reflected by the object and returned to the detector along a direct path. This returned energy is compared to a simultaneously generated reference beam that has been split off from the original signal, and the relative phase shift between the two is measured. This phase shift is a function of the round-trip distance the wave has traveled. Accuracies approach those achievable by pulsed laser TOF methods.

Further improved confidence in the accuracy of range data can be obtained by integrating over many measurements for each observed location. This process is relatively time consuming, making it difficult to achieve realtime sensor systems. As with TOF rangefinders, the paths of the source and the reflected beam are coaxial. This characteristic ensures objects cannot cast shadows when illuminated by the energy source, preventing the *missing parts* problem.

Even greater measurement accuracy and overall range can be achieved when cooperative targets, such as retroreflectors, are attached to the objects of interest. These specular reflectors are geometrically configured so incident light striking them will reflect back along a path parallel to the source beam, thereby increasing maximum range capabilities because of the resulting increase in power density of the return signal.

The CW phase-shift technique is the one most often found in electronic distance measuring instruments and automatic inspection systems; however, it possesses only a slight advantage over pulsed TOF rangefinding because the time-measurement problem is replaced by the need for sophisticated phase-measurement electronics (Depkovich & Wolfe, 1984). Because of the

limited information obtainable from a single range point, these sensors are often scanned in one or more directions by either electromechanical or acousto-optical mechanisms.

2.1.5 Frequency Modulation

An alternative to the phase shift measurement scheme discussed in section 2.1.4 is frequency modulation (FM). Widely used in radar altimeter applications, FM radar involves the transmission of a continuous electromagnetic wave, modulated by a periodic triangular signal that varies the carrier frequency linearly above and below the mean frequency f_0 as shown in figure 10. The transmitter emits a signal that varies in frequency as a linear function of time:

$$f(t) = f_0 + at$$

where a = some constant
 t = elapsed time

This signal is reflected from a target and arrives at the receiver at time $t + T$:

$$T = 2\frac{d}{c}$$

where T = round-trip propagation time
 d = distance to target
 c = speed of light

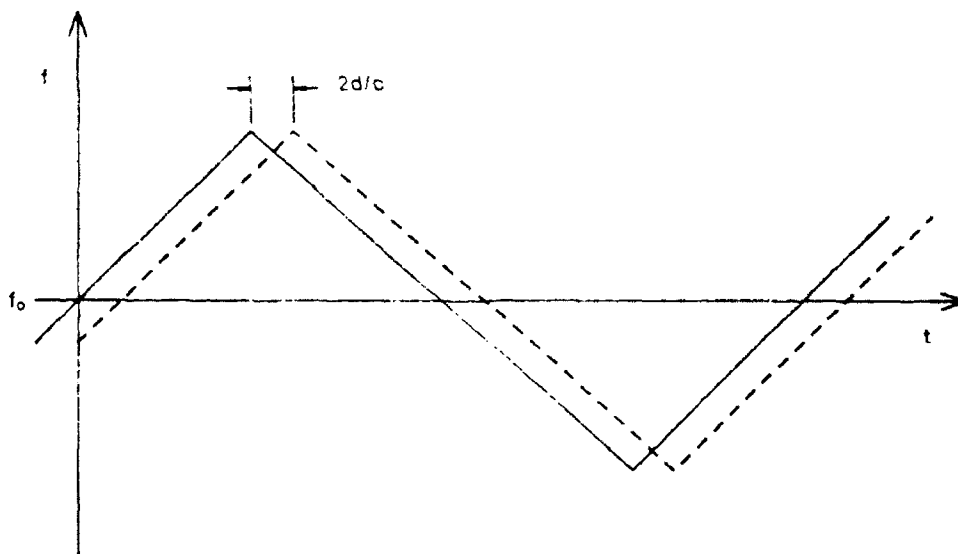


Figure 10. Frequency modulation. The reflected signal (dashed line) is displaced along the time axis by an amount proportional to the target range.

The received signal is compared with a reference signal taken directly from the transmitter. The received frequency curve will be displaced along the time axis relative to the reference frequency curve by an amount equal to the time required for wave propagation to the target and back. (There might also be a displacement of the received waveform along the frequency axis, due to the Doppler effect.) These two frequencies, when combined in the mixer, produce a beat frequency B_F :

$$B_F = f(t) - f(t + T) = aT$$

This beat frequency is measured and used to calculate the distance to the object:

$$d = B_F \frac{c}{2a}$$

Distance measurement is as accurate as the linearity of the frequency variation over the counting interval.

Advances in wavelength control of laser diodes now permit this radar ranging technique to be used with lasers. The frequency or wavelength of a laser diode can be shifted by varying its temperature. Consider an example where the wavelength of an 850-nanometer laser diode is shifted by 0.05 nanometers in 4 seconds. The corresponding frequency shift is 5.17 MHz/nanosecond; this laser beam, when reflected from a surface 1 meter away, would produce a beat frequency of 34.5 MHz. The linearity of the frequency shift controls the accuracy of the system. A frequency linearity of one part in 1000 yards yields an accuracy of 1 millimeter.

The frequency modulation system has an advantage over the phase-modulation technique in that a single distance measurement is not ambiguous. Phase-modulation systems must perform two or more measurements at different modulation frequencies to be unambiguous. However, frequency modulation has several disadvantages associated with the requirements of coherence of the laser beam and the linearity and repeatability of the frequency ramp. It is not clear at this point in the development of the technology if the frequency modulation scheme is as simple as other ranging techniques presently available.

2.1.6 Interferometry

2.1.6.1 Fringe Counters. One of the most accurate and precise distance ranging techniques known, interferometric methods of measurement, has existed for many years in laboratory scenarios that afforded the necessary controlled or otherwise structured environment (Brown, L. B., 1985). In such nonturbulent atmospheric conditions, laser interferometers can achieve fractional wavelength accuracies. Developments in optical technologies are now making possible applications of interferometry outside of the laboratory.

This ranging method is based on the resulting interference patterns that occur when two energy waves caused to travel different paths are compared. The primary energy source used to produce these waves is light. If the length of one of the optical paths is changed, the two beams will interact in such a way so that clearly visible constructive and destructive interference fringes are produced. (Fringes are patterns or disturbances in the combined waveform that alternate between maximum and minimum intensity.)

Figure 11 shows a typical system consisting of a laser emitter, a series of beam splitters and directional mirrors, and a fringe counter. (Beam splitters simultaneously reflect and transmit portions of a light beam.) Retroreflectors must be attached to objects that are to be tracked to provide a reliable return signal for the interferometer.

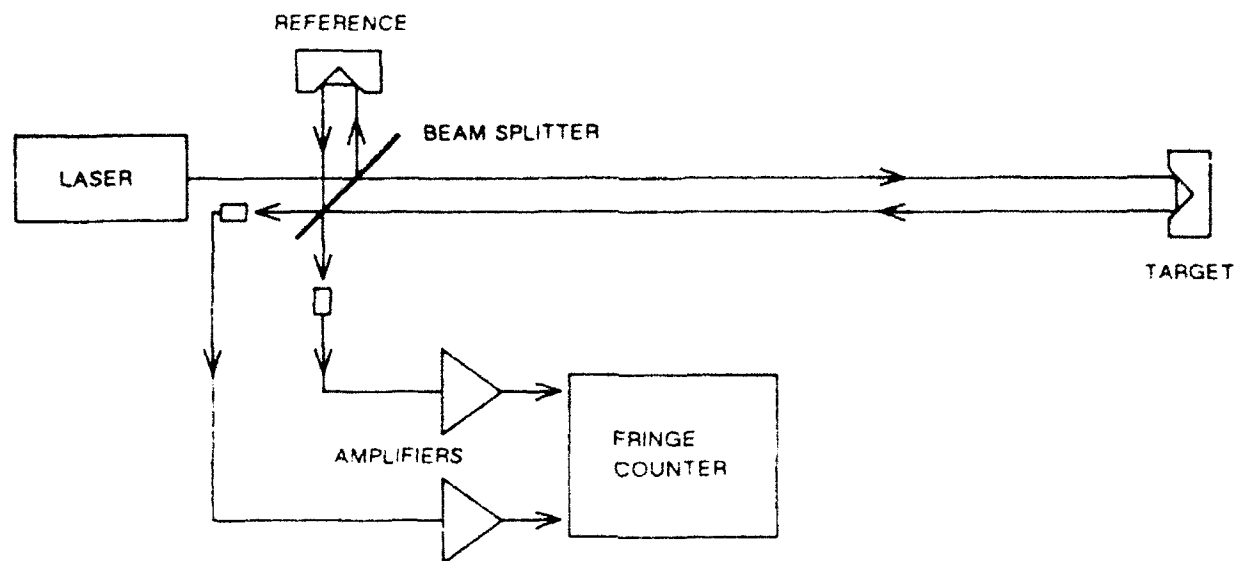


Figure 11. Interferometer block diagram. A retroreflector must be placed on the target of interest

Initially the transmission of a single coherent light source is split into a reference beam and an output beam. The reference beam is immediately directed into the fringe counter for future recombination with the reflected beam. The second beam exits the instrument and travels through the air to a retroreflector located on the object of interest. The returned signal is then sent directly back to the instrument by the retroreflector, where it is optically combined with the reference beam in the fringe counter. By counting the number of fringes passing a detector and knowing the wavelength of the light source in air, it is possible to calculate with extreme accuracy the distance the retroreflector (i.e., the object) has traveled along the line of the source beam. When the object moves a distance equal to half the light source wavelength, the movement and detection of one fringe will result (Beesley, 1971).

Interferometers do not measure absolute range, but the relative distance an object has moved from its previous location; therefore, the distance from the sensor to the target is not directly known. However, by initializing the retroreflector to a specified reference point, it becomes possible to determine absolute distance to an object. All subsequent measurements will be distances from the reference point, provided the beam is never broken and the target momentarily lost.

In conventional interferometers, target displacement of 1 centimeter can result in the movement of approximately 10 million fringes past a detector capable of measuring changes on the order of one tenth of a fringe (Beesley, 1971). Potential accuracies over a distance of 10 meters can approach 1/1,000,000; however, to achieve this, similar accuracy is required for the wavelength of the energy source. The maximum distance that can be measured by such instruments is therefore dependent on the coherent qualities of the source used. In theory, distances of hundreds of kilometers can be measured; however, this goal cannot be practically achieved using current technology (Beesley, 1971).

Important constraints on applying this ranging technique include (Brown, L. B., 1985) the following:

- Technique provides only relative distance measurement.
- Measurements are cumulative and therefore require continuous line-of-sight contact between the target and system.
- Measured distances lie along straight-line paths, unless an automatic beam-tracking system is employed.
- A retroreflector must be installed on the object of interest.

Limitations of interferometers result from environmental factors as well as component characteristics. Air turbulence effectively reduces the practical range distance of such systems to 10 meters (Beesley, 1971). The turbulence causes large enough variations in the path lengths of the light beams so that no spatial coherence exists between the interfering beams; therefore, there are no fringes produced. Temperature changes and microphonic disturbances can cause fluctuations in components of the light source delivery system that alter the wavelength and intensity of the output (Beesley, 1971). The laser output must, therefore, be stabilized to realize the full potential of interferometric measuring. Further functional limitations result from the nature of the light energy. For example, nonlaser light sources possess coherent lengths restricted to a few centimeters wavelength, consequently reducing the range of measurable distance.

The speed at which an interferometer can measure distances depends on the velocity of the object. The maximum detectable object velocity is, in turn, restricted by the maximum frequency response of the fringe counter detector. The use of interferometers in robotic applications was initially limited only to measurement of single-axis linear motion. Recent developments have expanded their applicability to three-dimensional six degree-of-freedom (DOF) systems, known as *tracking* interferometers, because the returning beam is also used by the system to track the lateral motion of retroreflective mirrors mounted on the object. Robotic tracking systems currently in existence are capable of precision tracking of manipulators performing nonrectilinear motions in six degrees of freedom (Everett, 1985c; Brown, L. B., 1985; Lau et al., 1985). While extremely precise, limiting factors of this method include the need for a continuous line-of-sight between source and retroreflectors, and the system is constrained to measuring only relative distance.

2.1.6.2 Diffraction Gratings. Diffraction rangefinding is a method of distance measurement based on the observation of higher order diffraction spectra. This method requires target illuminated by energy radiating with a periodic waveform: electromagnetic (light or radio) or sonic. Diffraction occurs when a wavefront transits an aperture or grating; diffraction gratings are a series of ruled lines that retransmit an intersected wavefront as many new wavefronts, one new wavefront for each slit in the grating. The new waveforms are phase related and create interference patterns observed as diffraction spectra (Dewitt, 1987, 1988).

Diffraction rangefinding exploits the fact that the curvature of a wavefront incident on the grating varies with the separation distance between grating and source. To an observer viewing the diffracted wave, there are discrete points along the grating where constructive wavefront interference produce maxima or diffraction orders. The zero-order image occurs along the axis between the viewer and source. The higher orders appear off the zero-order central axis at angles described by the classic diffraction equation:

$$n\lambda = p(\sin I + \sin V)$$

where n = diffraction order
 λ = wavelength
 p = pitch of grating
 I = angle of incidence of wavefront on grating
 V = perceived angle of diffraction

When there is infinite separation between source and grating, the wavefront is flat, and therefore in phase at all points across the grating. In this case, only the zero order diffraction spectra is produced and no range information is available. At finite separations, however, the wavefront is curved and arrives out of phase with itself across the grating. This phase shift gives rise to higher order spectra, whose position relative to the zero-order central axis is proportional to the target range (see figure 12). The angle of perceived diffraction, or deflection angle, is related to the target range in the following manner (DeWitt, 1989):

$$D = \frac{d \tan V \sqrt{1 - \left(\frac{n\lambda}{p} - \sin V\right)^2}}{\frac{n\lambda}{p} - \sin V}$$

where D = distance from grating to target along OC
 d = distance from grating to observer

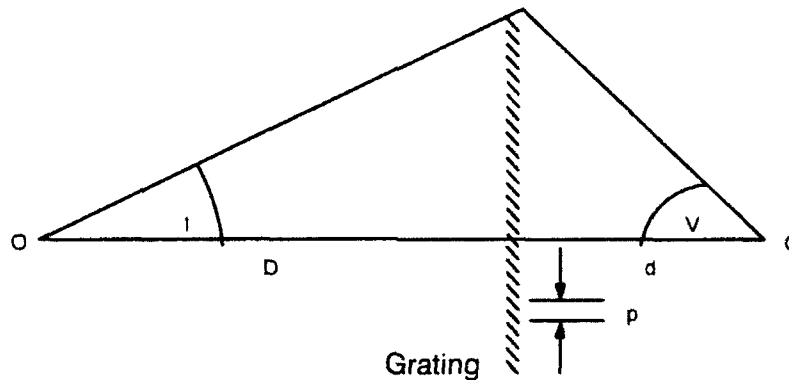


Figure 12. Diffraction grating geometry. The higher order diffraction image perceived at point C appears at angle V from the central optical axis OC (DeWitt, 1989).

By way of example, consider the hypothetical rangefinder working in the light flux regime as shown in figure 13. The perspective center can be formed by conventional optics and the model for measurement can be made by a camera. By measuring the horizontal displacement x of higher order spectra across the focal plane, the range D of the target can be computed as (DeWitt, 1991):

$$D = \frac{xd \sqrt{1 - \left(\frac{n\lambda}{p} - \frac{x}{\sqrt{x^2 + F^2}}\right)}}{F \left(\frac{n\lambda}{p} - \frac{x}{\sqrt{x^2 + F^2}}\right)}$$

where F = camera focal length

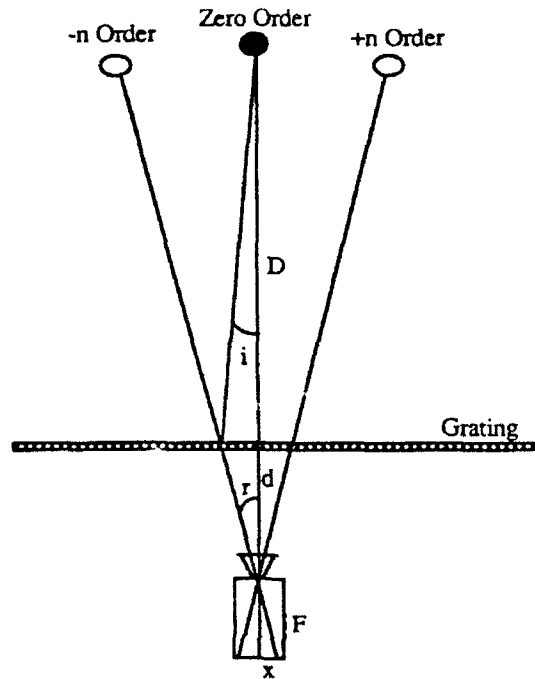


Figure 13. Diffraction rangefinder. Multiple images of an object appear when viewed through a grating; their displacement is proportional to distance D (DeWitt, 1991).

The diffraction method of ranging is similar to focus analysis in that both depend on the curvature of the incident waveform, are monocular, and are limited in accuracy by the length of intersection across the wavefront. Where focus analysis works best when using large telephoto lenses with narrow fields of view, diffraction gratings are no more massive than the substrates that support them, and increased accuracy does not require a consequent reduction in field of view. Moreover, as gratings are simple geometric rulings, their manufacturing costs are minimal. Furthermore, the computational requirements of focus analysis that requires the recovery of the circle of confusion are greater than that required by the measurement of displacement of higher order diffraction spectra. Ranging through diffraction gratings has advantages over triangulation in the near field (DeWitt, 1989). Working to point-of-contact range, the grating method provides redundant views of the target on either side of the zero order image, overcoming any occlusion artifacts.

Because this method of ranging requires the detection of the wavefront curvature, it is effective only over ranges : which this phenomena can be observed. A lower limit can be set for increments on the order of a wavelength; an upper limit can be set where the physical size of the

grating becomes impractically large (Dewitt, 1989). The grating method lends itself to scanning, allowing the acquisition of arrays of surface coordinates, something that is difficult to accomplish with triangulation because of the requirement for scanner synchronization. Where triangulation can be made increasingly accurate with longer focal length lenses, there is a tradeoff between cost, weight, and field of view. With the diffraction ranging method, distance readings are most accurate nearest the grating, the standard diffraction equation shown previously describes this hyperbolic dependence (DeWitt, 1989). Overall system accuracy is improved by decreasing the grating pitch and increasing grating size, with a lesser cost and weight penalty, and no sacrifice in field of view.

2.1.7 Swept Focus

The swept focus technique uses a modified video camera with a single lens of very short depth of field to produce an image in which only a narrow interval of range in object space is in focus at any given time. By means of a computer-controlled servo drive, this lens can be positioned with great accuracy over a series of positions to view different range slices. (Some systems operate with a fixed-location lens, and vary the position of the detector element to achieve the same effect.) The distance between the lens and the image plane at the detector is related to the range the camera is focused (standard lens equation). Thus, if the lens is mechanically positioned to bring the desired object into focus, then the range to that object could be derived from the position of the lens.

An analog signal processor filters the video signal from the camera to obtain only the high-frequency portion, representing information that changes rapidly across the scene, such as in-focus edges or textured material (figure 14). The out-of-focus portions of an image do not contribute to the high-frequency information. This filtered signal is integrated during each video field time.

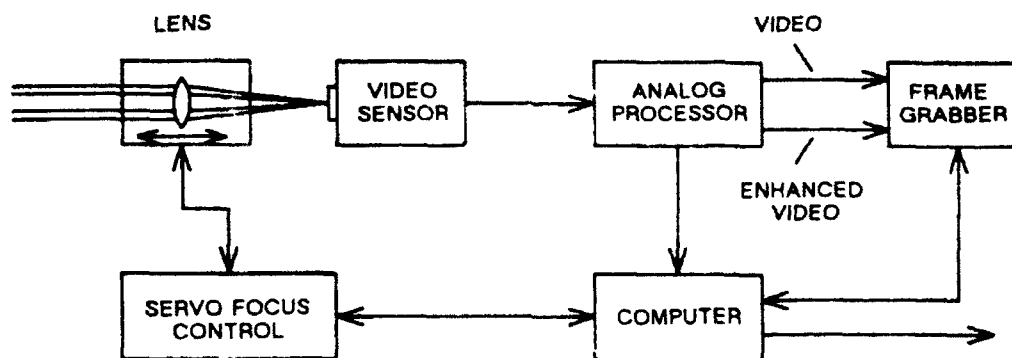


Figure 14. Block diagram of a passive swept-focus ranging system (Courtesy Associates and Ferren Corporation).

To perform ranging, the lens is successively positioned at hundreds of discrete, precalculated positions, reading and storing the integrated high-frequency data as it becomes available at each position before moving to the next. At the end of this process, the resultant profile of high-frequency response with range is processed to reduce noise effects, and then analyzed to determine the locations of all significant peaks. Each peak in high-frequency response represents the

best-focus location of a target. The distance to each target can be found simply by reading from a look-up table the object range corresponding to the lens position where the peak occurred.

The speed of this type of sensor is currently limited by the standard video frame rate (60 frames/second). Ranging accuracy and the ability to separate targets closely spaced in range are limited by physical constraints of the lens. The greater the desired accuracy and resolution, the shorter the required depth of field, which can be achieved by using a lens of longer focal length or larger aperture. The tradeoffs involved are, respectively, reduced field of view and increased size and weight.

Thus, through use of optical preprocessing, the swept focus technique provides the advantages of a visual sensor, while eliminating many of the major disadvantages of other visual methods. Swept focus has acceptable accuracy for most applications, will locate multiple targets at different ranges, is not computation intensive, does not suffer from the *missing parts* problem, and operates passively provided there is sufficient ambient light.

2.1.8 Return Signal Intensity

Ranging techniques involving return signal intensity determine the distance to an object based on the amplitude of energy (usually light) reflected from the object's surface. The inverse square law for emitted energy states that as the distance from a point source increases, the intensity of the source diminishes as a function of the square of the distance. If Lambertian surfaces are assumed (Lambertian surfaces are ideal surfaces that in theory scatter reflected energy with equal probability in all directions (Jarvis, 1983b)), then this principle results in a computationally simple range calculation algorithm.

The Lambertian assumption eliminates problems of specular reflection due to surface topography. Requiring only a single detector, this ranging technique does not suffer the *missing parts* problem common to triangulation systems. Unfortunately, however, objects in the real world are not ideally Lambertian in nature. The varying reflectivities of typical object surfaces preclude simple measurement of signal strength from being a reliable indicator of distance under most conditions.

One implementation of this ranging technique developed at the Massachusetts Institute of Technology (MIT) Artificial Intelligence Lab involves using a pair of identical point-source LEDs positioned a known distance apart, with their incident light focused on the target surface. The emitters are individually fired, and the returned energy from each is measured by a photodetector in a sequential manner. According to the inverse square law of emitted energy, if the power of both sources was the same, then the intensity of the return signal as sensed by the receiver should be the same, if the sources were colocated. However, in this case one emitter is closer to the scene than the other, resulting in a difference in the return signal intensity produced by the two sources. This measurable difference can be exploited to yield absolute range values, and the effects of varying surface reflectivities (which attenuate returned energy for both LEDs) cancel out.

Range is determined by relating the two intensities through a factor known as the brightness ratio, B_1/B_2 . B_1 is the return intensity produced by the more distant light source and B_2 is the return intensity produced by the closer source. By the inverse square law:

$$\frac{B_1}{B_2} = \left(\frac{L_2}{L_1}\right)^2$$

where L_1 = distance between farther emitter and object

L_2 = distance between close emitter and object

d = known distance between two light sources

Realize that L_1 is equal to L_2 plus the distance d between the two light sources. Substituting this new value for L_1 and evaluating the resulting quadratic produces an equation for the range L_2 , as a function of d and the returned intensities, B_1 and B_2 . Range is calculated after measuring the intensities, since d is a known quantity set by the design of the sensor. Assumptions used in the above derivation are that all surfaces are Lambertian in nature, and the width of observed objects is greater than or equal to the footprint of the incident illumination.

2.2 APPLICABLE TECHNOLOGIES

2.2.1 Acoustical

Acoustical energy has been established as an effective sensing medium since 1918. With the development of sonar (sound navigation and ranging), high-frequency acoustic waves have been used to determine the position, velocity, and orientation of underwater objects. Though sensor systems for operation in air have been developed using acoustic transmission in the audible frequency ranges, ultrasonic energy (sound waves above the limits of human hearing) has been the most widely applied. Ultrasonic transducers typically transmit at frequencies greater than 20,000 Hz, generated by both mechanical and electronic sources.

Acoustical ranging can be implemented using triangulation, time-of-flight, phase-shift-measurement, or a combination of these techniques. The direction and velocity of a moving object can also be determined by measuring Doppler shift in frequency of the returned energy caused by objects moving toward or away from the observer. A minimum 10-Hz Doppler shift is necessary to determine an object's velocity with respect to its environment (Hall, 1984).

Typically, triangulation and time-of-flight methods transmit sound energy in pulses and are effective at longer distances for navigation and positioning, and at shorter distances for object detection. The phase-shift ranging technique involving the transmission of a continuous sound wave is better suited for situations where a single dominant target is present.

The performance of ultrasonic ranging systems is significantly affected by environmental phenomenon and sensor design characteristics. Of primary concern is the attenuation of sound energy over distance. As an acoustical wave travels away from its source, its intensity decreases according to the inverse square law (also known as spherical divergence) and due to absorption of the sound by the air. (By the inverse square law, intensity of acoustic energy will drop 6 dB as the distance from the source is doubled (Ma & Ma, 1984)). The absorption of sound energy varies with the humidity and dust content of the air as well as the frequency of the transmitted wave. Absorption can also occur at the reflecting surface and is a function of the topographical characteristics of the target.

Consequently, the maximum detection range for an ultrasonic sensor is dependent on the emitted power and frequency of operation; the lower the frequency, the longer the range. For a

20-KHz transmission, the absorption factor in air is approximately 0.02 dB/foot, while a 40-KHz transmission losses between 0.06 and 0.09 dB/foot (Ma & Ma, 1984). However, resolution is dependent on the bandwidth of the transmitted energy, and greater bandwidth can be achieved at higher frequencies. Minimum ranging distance is also a function of bandwidth, and thus greater bandwidth and higher frequencies are required as the distance between the detector and target decreases.

Another parameter affected by the ambient properties of air is the velocity of sound. The principal factors involved are air temperature (determines the interactivity of air molecules), and the wind direction and velocity, which have a push or delay effect on sound energy. Correction for wind effect errors must treat crosswind components as well as those which travel on a parallel path either with or against the sound. Crosswind effects are significant because they cause the beam center to be offset from its targeted direction, diminish the intensity of returned echoes, and result in a slightly longer beam path due to deflection.

The speed of sound in air is proportional to the square root of temperature in degrees Rankine:

$$c = \sqrt{g k R T}$$

where c = speed of sound
 g = gravitational constant
 k = ratio of specific heats
 R = gas constant
 T = temperature in degrees Rankine (F + 460).

For the temperature variations encountered in robotic ranging applications, this results in a significant effect even considering the short distances involved. Temperature variations over the span of 60 to 80 degrees Fahrenheit can produce a range error as large as 7.8 inches at a distance of 35 feet (Everett, 1985b). Fortunately, this situation can be remedied through the use of a correction factor based upon the actual ambient temperature, available from an external sensor mounted on the robot. The formula is simply:

$$R_a = R_m \sqrt{\frac{T_a}{T_c}}$$

where R_a = actual range
 R_m = measured range
 T_a = actual temperature (R)
 T_c = calibration temperature (R)

However, the possibility does still exist for temperature gradients between the sensor and the target to introduce range errors, in that the correction factor is based on the actual temperature in the immediate vicinity of the sensor.

Still another factor to consider is the beam dispersion angle of the selected transducer. The width of the beam is determined by the transducer diameter and the operating frequency. The higher the frequency of the emitted energy, the narrower and more directional the beam and, hence, the higher the angular resolution. Unfortunately, an increase in frequency also causes a corresponding increase in signal attenuation in air, and decreases the maximum range of the

system. The beam-dispersion angle is directly proportional to the transmission wavelength (Brown, M. K., 1985), as shown:

$$\theta = 1.22 \frac{\lambda}{D}$$

where θ = desired dispersion angle
 λ = acoustic wavelength
 D = transducer diameter

Best results are obtained when the beam centerline is maintained normal to the target surface. As the angle of incidence varies from the perpendicular, however, note that the range actually being measured does not always correspond to that associated with the beam centerline (figure 15). The beam is reflected first from portion of the target closest to the sensor. For a 30-degree beam-dispersion angle at a distance of 15 feet from a flat target, with an angle of incidence of 70 degrees, the theoretical error could be as much as 10 inches. The actual line of measurement intersects the target surface at point B as opposed to point A (Everett, 1985b).

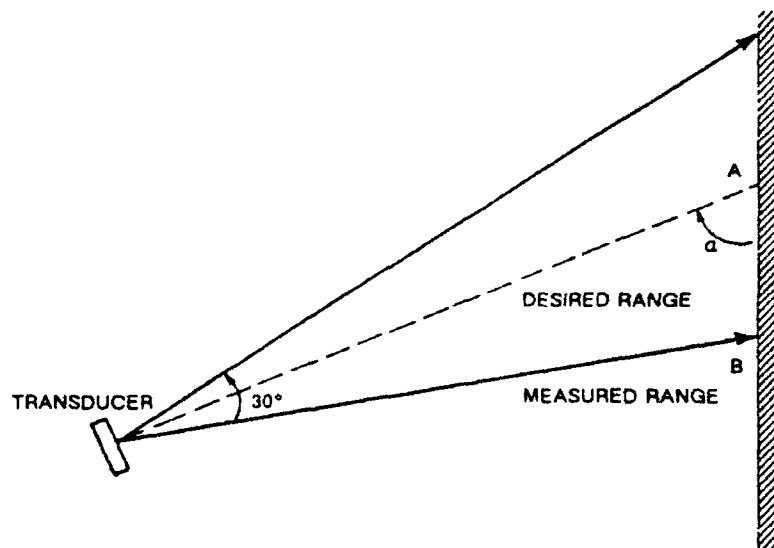


Figure 15. Ultrasonic ranging error due to beam divergence.

The width of the beam introduces an uncertainty in the perceived distance to an object, but an even greater uncertainty in the angular resolution of the object's position. A very narrow vertical target such as a long wooden dowel maintained perpendicular to the floor would have associated with it a relatively large region of floor space that would essentially appear to the sensor to be obstructed. Worse yet, an opening such as a doorway may not be discernible at all when only 6 feet away, simply because at that distance the beam is wider than the door opening.

Finally, errors due to the topographical characteristics of the target surface must be considered. When the angle of incidence of the beam decreases below a certain critical value, the reflected energy does not return to strike the transducer (figure 16). This phenomenon occurs because most targets are specular in nature with respect to the relatively long wavelength (roughly 0.25 inch) of ultrasonic energy, as opposed to being diffuse. In the case of specular reflection, the angle of reflection is equal to the angle of incidence. In contrast, diffuse reflection

energy is scattered in various directions caused by surface irregularities equal to or larger than the wavelength of incident radiation. The critical angle is a function of the operating frequency chosen, and the topographical characteristics of the target surface. Transducer offset from the normal will result either in a false echo as deflected energy returns to the detector over an elongated path, or no echo as the deflected beam dissipates.

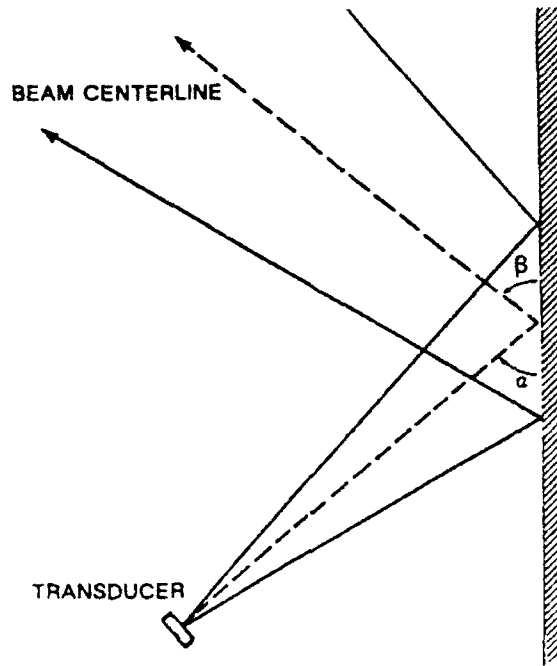


Figure 16. Ultrasonic ranging error due to specular reflection.

In summary, ultrasonic sensors are a powerful and practical method of range determination for selected applications. Simple construction of the transducers makes them reliable and economical. The low-cost factor also makes design redundancy feasible, further improving system reliability and effectiveness. These points combined with the extensive use of ultrasonics in cameras, aids for the blind, health care, and other endeavors demonstrate the low technical risk involved in applying the technology where applicable.

2.2.2 Optical

Active optical sources employed in rangefinding include broadband incandescent, narrow-band LEDs, and coherent lasers. The actual source should be chosen according to the following guidelines: (1) it must produce with sufficient intensity, (2) at the required wavelength (or within an appropriate spectrum), and, (3) with the desired radiation pattern (Dokras, 1987). The design is optimized around these features to extract the necessary information from ambient noise and clutter with a comfortable signal-to-noise ratio.

Super luminescent diodes (SLDs) are a new development that can best be described as midway between the coherent laser diode and the more simplistic LED. The construction of all three of these devices is similar; a forward-biased p-n junction leads to a recombination of holes with

electrons accompanying emission of photon energy. An LED produces spontaneous emission in its active region, with a moderate spectrum about a central wavelength. Laser diodes, on the other hand, are physically configured so emissions in the active region oscillate back and forth several times between the specially designed front and back facets, with the characteristic laser *gain* on each forward pass. This results in a primary wavelength or mode of operation, and what is termed a coherent output (Dokras, 1987).

LEDs have no such amplification mechanism; the output intensity simply increases with an increase in current density. Surface-emitting LEDs have a wide solid angle output beam, and the beam intensity is Lambertian. Edge-emitting LEDs have a waveguide mechanism built into their structure, that results in a narrow Gaussian intensity pattern (Dokras, 1987).

An SLD, on the other hand, is like an edge-emitting LED, but with a single-pass gain feature similar to the laser. This results in an increased power output over a conventional LED, but as current density is increased, the device is unable to attain the threshold for multiple-pass gain as does a laser diode (Dokras, 1987).

Most optical proximity detectors employ near-infrared LEDs operating between 800 and 900 nanometers. SLDs have only recently emerged in the rapidly expanding field of fiber-optic communications and optical-disc technology, and thus do not yet appear in applications involving noncontact ranging, although it's only a matter of time.

At present, the majority of active optically based distance measuring devices employ laser sources. Such systems are generally considered to be the quickest and most accurate way to obtain range information (Depkovich & Wolfe, 1984). Lasers are found in ranging equipment based on triangulation, time of flight, phase modulation, proximity, interferometry, and return signal intensity. This dynamic expansion in usage can be better understood by recognizing some of the inherent qualities of laser light (Depkovich & Wolfe, 1984).

First, lasers produce a bright, intense output important to long-distance ranging and for distinguishing the signal from the background. Second, by nature or through use of corrective optics, laser beams are narrow and collimated, with little or no divergence. This property allows the source to be highly directional or spatially selective, because an intense beam of energy can be concentrated on a small spot at long distances.

Furthermore, lasers generally transmit light of a single wavelength (spectrally pure), and therefore are void of extraneous signals and noise. This quality can be exploited in rangefinders by placing narrowband optical filters, that match the wavelength of the beam, in front of the detector component. Filters of this type will reject the ambient light, resulting in an improved signal-to-noise ratio for the system.

Along with these advantages there also exist some disadvantages that must be taken into account (Dopkovich & Wolfe, 1984). All laser-based systems represent a potential safety problem in that the intense and often invisible beam can be an eye hazard. Furthermore, gas lasers require high-voltage power supplies that present some danger of electrical shock. Another liability is that performance is dependent on the presence of a highly accurate beam-delivery system for pointing, tracking, and scanning functions.

In addition, the wide dynamic range of the returning energy (between 80 to 100 dB) complicates the design of the detector electronics. Laser sources typically suffer from low overall

power efficiency. Lasing materials are often unstable and possess short lifetimes, resulting in reliability problems. Finally, some laser-based ranging techniques require the use of retroreflective mirrors or prisms at observed points, effectively eliminating selective sensing in unstructured surroundings.

Lasers exist in a variety of types. The more well known are gas lasers like helium-neon (HeNe) or the solid-state variety like neodymium: yttrium aluminum garnet (Nd:YAG). The recent advent of semiconductor-based laser diodes has had significant impact on the rangefinder instrument community (Depkovich & Wolfe, 1984). Although they typically have reduced power output and poorer spectral quality relative to other lasers, solid-state devices are compact, rugged, reliable, and efficient, with sufficient quality of performance for most sensing needs. An often used semiconductor laser of this type is the gallium arsenide (GaAs) laser diode, which emits in the near-infrared region.

The use of energy from the optical portion of the spectrum minimizes the specular reflectance problems encountered with acoustics, with the exception of polished surfaces (Jarvis, 1983b). Similarly, glass, clear plastic, and other transparent substances with little or no reflectance properties can cause problems. In fact, the unknown reflectivity of observed targets is perhaps the most significant problem in optical range measurement. This varying reflectivity coupled with the changing angle of incidence of the transmitted laser beam causes the returned energy to vary significantly in amplitude, requiring detection capabilities over a wide dynamic range.

To be used with mobile robotic systems, an optical ranging system must function effectively under normal ambient light conditions, which makes the choice of light sources critical. Some structured light systems use an incandescent source which is directed through a slit or patterned mask and projected onto the surface. Others use laser beams that are mechanically or electronically scanned at high rates to create the desired illumination. The major criterion for selecting a light source is to be sure that its intensity peaks at a spectral frequency other than that of the ambient energy (Zhao et al., undated). The camera (or detector) should be outfitted with a matching narrowband filter to complement the source and improve detection.

For example, ultraviolet light with a wavelength of 0.2 and 0.3 micron is effective outdoors because the atmosphere absorption of ozone blocks the transmission of sunlight energy less than 0.3 micron in length. However, an ultraviolet source of the required power density level would be hazardous in indoor environments (not eyesafe). Contrast this with infrared light near 2.8 microns, which is better suited to indoor activities because man-made objects tend to reflect infrared energy well. Infrared loses its usefulness outdoors due to the inherent radiation emitted by the natural terrain, roadways, and objects (Le Moigue & Waxman, 1984). Ambient light effects can also be reduced by modulating the source over time, then demodulating the received energy at the detector, which effectively subtracts off the constant illumination of the background.

2.2.3 Electromagnetic

Radar (radio detecting and ranging) determines the distance and bearing to an object and/or its speed relative to an observer calculated through the measurement of reflected electromagnetic waves. The properties of the received echoes are used to form a picture or determine certain

information about the objects causing the echoes. Common uses include detection and location of ships and aircraft, as well as weather forecasting.

Specific advantages of radar sensing include the ability to *see* through smoke, dust, or haze-filled environments such as battlefields, a strong base of existing knowledge originating prior to World War II, and the ability to be made radiation hard. When combined with computerized signal processing, radar systems can produce astonishing accuracies in terms of target discrimination and range computation (Nowogrodzki, undated). Radars are also effective at measuring the speed of moving objects by Doppler-shift methods, wherein the magnitude of the frequency shift of an energy wave reflected off a mobile target is proportional to its relative velocity.

Ranging is accomplished by pulsed TOF methods, or CW phase or frequency modulation. Pulsed energy systems can detect targets up to distances on the order of tens of miles, relying on the measurement of the round-trip time of a propagating wave. The high-speed propagation of the emitted energy makes short distance measurements difficult for this type of system because the extremely sharp short-duration signals that must be generated and detected are expensive and complicated to realize. CW systems, on the other hand, are effective at shorter ranges because the phase-shift measurements are not dependent on the wave velocity. Power consumption drops because lower transmitter intensity levels are needed for shorter distances.

The basic radar equation expresses the relationship between the signal power received at the antenna as a function of the antenna size and the emitted power of the system:

$$S = \left(\frac{PG}{4\pi R^2} \right) \left(\frac{\sigma}{4\pi R^2} \right) \left(\frac{G\lambda^2}{4\pi} \right)$$

where S = signal power received
 P = transmitted power
 G = antenna gain
 λ = wavelength
 σ = radar cross section of target
 R = range to target

The quantity in the first parenthesis represents the power density in the incident wave at the target. The first two terms in parentheses together give the power density of the returning wave at the radar antenna, and the last factor is the cross section of the receiving antenna (Ridenour, 1947). This equation assumes the same antenna is used for transmission and reception. For a more detailed explanation of terms, and treatment of separate antennae, see Blake (1990).

A major consideration on the implementation of radar ranging capability is the configuration of the transmitting and receiving antenna. Systems employing a single antenna typically feature a large concave reflector with the detector or *feed* positioned at the focal point of the dish. This set-up is exactly analogous to an optical telescope at its prime focus. The principal advantage of this arrangement is that the antenna will collect all the returned energy which falls upon it from the beam that is inversely proportional to the diameter of the reflector (Miller et al., 1985). The relationship is expressed in the following equation:

$$\theta = 1.22 \frac{\lambda}{d}$$

where θ = beamwidth
 λ = wavelength
 d = diameter of the reflector

The disadvantages include the need to manipulate a large-diameter antenna system when the application requires narrow beams, and the effects of vibration and wind, which can necessitate a massive supporting structure.

Phased-array antenna configurations present an alternative arrangement, which creates an array of multiple small antennae separated by distances of a few wavelengths. The transmissions from each antenna diverge and overlap with neighboring transmissions in a constructive and destructive fashion based on their phase relationships. By properly adjusting the phases, the overall antenna can be tuned to a desired direction and intensity, as well as electronically scanned across the field of view. The small size of the individual transmitter-receivers reduces the problems due to wind effects; however, the resulting smaller coverage area decreases overall effectiveness. Also, the requirement for electronically variable phase control increases the system complexity.

2.2.3.1 Microwave Radar. The portion of the electromagnetic spectrum considered to be the useful frequency range for practical radar is between 3 and 100 GHz (Miller et al., 1985). The primary electromagnetic source used in most modern conventional radar systems is microwave energy (Nowogrodzki, undated). This form of radiation, with wavelengths falling between 1 millimeter and 1 meter, is extensively employed for surveillance, tracking, and navigation applications.

Microwaves are also used for shorter-range sensing needs such as tail warning radar and ground control radar for aircraft, typically involving distances in hundreds of feet. Other uses include level indicators, presence detectors, and obstacle avoidance radars, operating over ranges from a few feet to several yards. Equipment for the transmitting, receiving, and processing of the waveform is widely available. Microwave systems have been in the experimental stage for quite some time but only came into their prime within the last 15 years or so with the advent of inexpensive, reliable solid-state components as alternatives to the typically fragile, power-consuming thermionic devices (Nowogrodzki, undated).

Microwave energy is ideally suited for long-range sensing because the resolution is sufficient, attenuation of the beams in the atmosphere is minimal, and low-mode guiding structures can be constructed. The relatively long microwave wavelengths provide radar systems with an *all-weather* capability because they overcome the absorption and scattering effect of the air, weather, and other obscurants. However, they are susceptible to specular reflections at the target surface, requiring receivers and signal processors with wide dynamic ranges. Shorter wavelengths (i.e., higher frequencies) can be used to produce systems with high-angular resolution and small-aperture antennae. High-angular resolution is possible at longer wavelengths; but, the antenna size becomes very large. For these reasons, conventional radar systems operating in the microwave portion of the energy spectrum have less applicability to the high-resolution collision avoidance needs of a mobile robotic platform.

2.2.3.2 Millimeter Wave Radar. The rapidly evolving millimeter wave technology involves that portion of the electromagnetic energy spectrum from wavelengths of about 500 micrometers to 1 centimeter. Millimeter waves possess several properties that differ substantially from microwave

radiation. First, the shorter wavelengths result in a narrow beamwidth, with relatively small-sized antenna apertures for a given bandwidth. Consequently, more information can be obtained about the nature of targets than at larger wavelengths because of reduced scattering of the reflected signal by objects. The overall physical size of the system is reduced, but the smaller apertures result in less collected energy, which limits the effective range of the system.

Second, millimeter waves possess a wide frequency bandwidth (the entire microwave frequency range could be encompassed by a single band of the millimeter wave region), which translates into greater resolution and sensitivity for radar applications, larger data transmission rates for communications, reduced interference between mutual users of the band, and improved security.

Relative to microwaves, millimeter waves display greater interaction with the environment. This attribute is good in that millimeter wave sensors can detect small particles and can carry on frequency selective interaction with gases; however, the resulting atmospheric attenuation limits the range and prevents operation of such devices in all weather conditions. Likely applications of this technology include remote environmental sensing, interference-free communications and radar, low-angle tracking radar, high resolution and imaging radar, spectroscopy (Sentizky & Oliner, 1970), and mobile platform collision avoidance.

In tracking radar systems the antenna gain is frequency dependent; therefore, for a given antenna aperture, the wavelength should be small if the range is to be long, which favors millimeter wave sources. Furthermore, the narrow beamwidth of millimeter wave transmissions is highly immune to ground reflection problems when following targets at low-elevation angles, making such radars highly effective at low-angle tracking. In imaging radar, the wide bandwidth of the millimeter wave region can sense the size and shape of an object with high resolution.

Although there are no current commercial sources of millimeter wave ranging devices, several contractors are involved in supplying such equipment to the military. While development costs may run as high 1 million, with lead times approaching a year or more, the indication is that individual transmitter, receiver, and antenna units may eventually cost as little as \$100, and fit into packages as small as an 8-inch cube (Miller et al., 1985).

3.0 CANDIDATE SYSTEMS

3.1 COMMERCIALY AVAILABLE

This section is largely composed of information submitted by the respective vendors, or taken directly from their product literature, and is understandably somewhat positive in tone.

3.1.1 Cybermotion Ultrasonic Collision Avoidance System CA-2

The CA-2 Collision Avoidance System is a dual-channel ultrasonic ranging module developed by Cybermotion, Inc., Roanoke, VA, for use on indoor vehicles operating at speeds up to 10 mph. The CA-2 achieves a maximum detection range of 8 feet, with programmable resolution over the span of interest (Cybermotion, 1991).

Selected Specifications:

Ranging technique	Time of flight
Maximum range	8 feet (programmable)
Minimum range	1 foot
Update rate	up to 10 Hz
Resolution	0.084 inch (standard)
Operating frequency	75 KHz
Number of beams	2
Beamwidth	70-degree cone
Power consumption	11.5 to 14.5 volts DC at 150 mA
Size	1.2 by 8.1 by 5.85 inches
Sensitivity	programmable to 1 square-inch surface at 5 feet

Point of Contact:

John Holland
Cybermotion, Inc.
5457 Aerospace Rd.
Roanoke, VA 24014
(703) 982-2641

3.1.2 Polaroid Ultrasonic Ranging Unit

The Polaroid ranging module is an active time-of-flight device developed for automatic camera focusing, and determines the range to target by measuring elapsed time between transmission and the detected echo. This system is the most widely found in mobile robotic literature (Koenigsburg, undated; Kim, 1986; Irwin & Caughman, undated) and is representative of the general characteristics of such ranging devices.

A very thin metalized diaphragm mounted on a machined backplate forms a capacitive transducer (Polaroid Corporation, 1981; Biber et al., 1987). The system operates in the transceiver mode so that only a single transducer is necessary to acquire range data. Polaroid offers both the transducer and ranging module circuit board for less than \$50, which partially accounts for the widespread usage. A ruggedized *environmental transducer* has been introduced for applications

that may be exposed to rain, heat, cold, salt spray, and vibration. A new, smaller diameter transducer has also been made available, developed for the Polaroid Spectra camera.

The original Polaroid system functioned by transmitting a 1-millisecond *chirp* consisting of four discrete frequencies transmitted back-to-back: 8 cycles at 60 KHz, 8 cycles at 56 KHz, 16 cycles at 52.5 KHz, and 24 cycles at 49.41 KHz. This technique was employed to increase the probability of signal reflection from the target, since certain surface characteristics could absorb and cancel a single-frequency waveform, preventing detection. It should be recognized, however, that the 1-millisecond length of the *chirp* was a significant source of potential error, in that sound travels roughly 1100 feet/second at sea level, which equates to about 13 inches/millisecond. The uncertainty and, hence, the error arises from not knowing which of the four frequencies making up the *chirp* actually returned to trigger the receiver, but timing the echo always began at the start of the *chirp* (Everett, 1985b).

For the initial application of automatic camera focusing, designers were more concerned about missing a target altogether due to surface absorption of the acoustical energy; the depth of field of the camera optics would compensate for any small range errors that might be introduced due to this *chirp* ambiguity. In actual practice, such errors rarely showed up, which suggests the theoretical absorption problem had been somewhat overestimated.

In fact, Polaroid subsequently developed an improved version of the ranging module circuit board (SN28827) with reduced parts count and power consumption, and simplified computer interface requirements. This second-generation board transmits only a single frequency at 49.1 KHz. A third-generation board was introduced in 1990, that provided yet a further reduction in interface circuitry, with the ability to detect and report multiple echoes (Polaroid Corporation, 1990).

The range of the Polaroid system runs from about 1 foot out to 35 feet, with a beam dispersion angle of approximately 30 degrees. The typical operating sequence is as follows:

- The control circuitry fires the transducer and waits for indication that transmission has begun.
- The receiver is blanked for 1.6 milliseconds to prevent false detection due to transmit signal ringing.
- The received signals are amplified with increased gain over time to compensate for the decrease in sound intensity over distance.
- Returning echoes that exceed a threshold value are recorded, and the associated distances calculated.
- The receiver will listen for 62.5 milliseconds then prepare for subsequent transmissions.

Selected Specifications:

Ranging technology	Time of flight			
Input voltage	4.7 to 6.8 volts DC			
	6500 Series	Single Frequency	TI SN28827	
Power				
operating	100	200	100	milliamps
peak transmit	2.5	2.5	2.0	amps
Maximum range	35	35	35	feet
Minimum range	6	10.5	6	inches
Pulses transmitted	16	56	16	
Blanking time	2.38	0.6	2.38	milliseconds
Resolution	+1	+1	+2	percent
Gain lines	4	3	4	
Gain steps	12	16	12	
Multiple echo capacity	Yes		Yes	
Programmable frequency	Yes	No	No	

Point of Contact:

Jack O'Brien
Polaroid Corporation
119 Windsor St.
Cambridge, MA 02139

3.1.3 Pentax Near-Infrared Autofocus Sensor

The Pentax Corporation developed in the late '70s an autofocusing mechanism used in its Sport 35 camera that illustrates the potential for application of such systems to the close-in ranging needs of mobile robotic platforms. The Focus Control Module (FCM-A) is an active distance-measuring device that determines range by simple triangulation. The autofocusing unit consists of a near-infrared light-emitting diode (LED) with collimating optics, a single silicon photodiode detector offset from the light source, a position-determining scanning plate that traverses across the detector's surface, and the associated circuitry (figure 17).

The LED emits a CW source beam through its focusing lens along the optical axis to the target. A portion of the energy is reflected back to the sensor where the beam illuminates a spot on the surface of the photodiode. The output of the detector then normalizes to the photo-electric current produced by the light, whereupon the scanning plate is electromechanically moved across the detector's surface in discrete increments or steps until it blocks the path of the reflected beam. This shadowing action prevents the reflected light spot from reaching the photodiode and effectively drops the output current to zero.

At that moment, the near-infrared source is converted to pulsed energy to limit the effects of ambient light. The scanning plate continues across the detector until the spot strikes the surface again and the current rises back to normal. The current profile across the photodiode is analyzed by the detection circuitry; the point where the current drops to its maximum negative value (minus peak detection) is the centroid of the spot.

The lateral location of the spot is representative of the sensor-to-object range. In the case of distant objects, the return beam travels along a path (figure 17), and the spot falls on the far right side of the detector. As an object moves closer, the spot moves across the detector from right to left. The minimum measurable distance is obtained when the spot falls on the far left side of the photodiode.

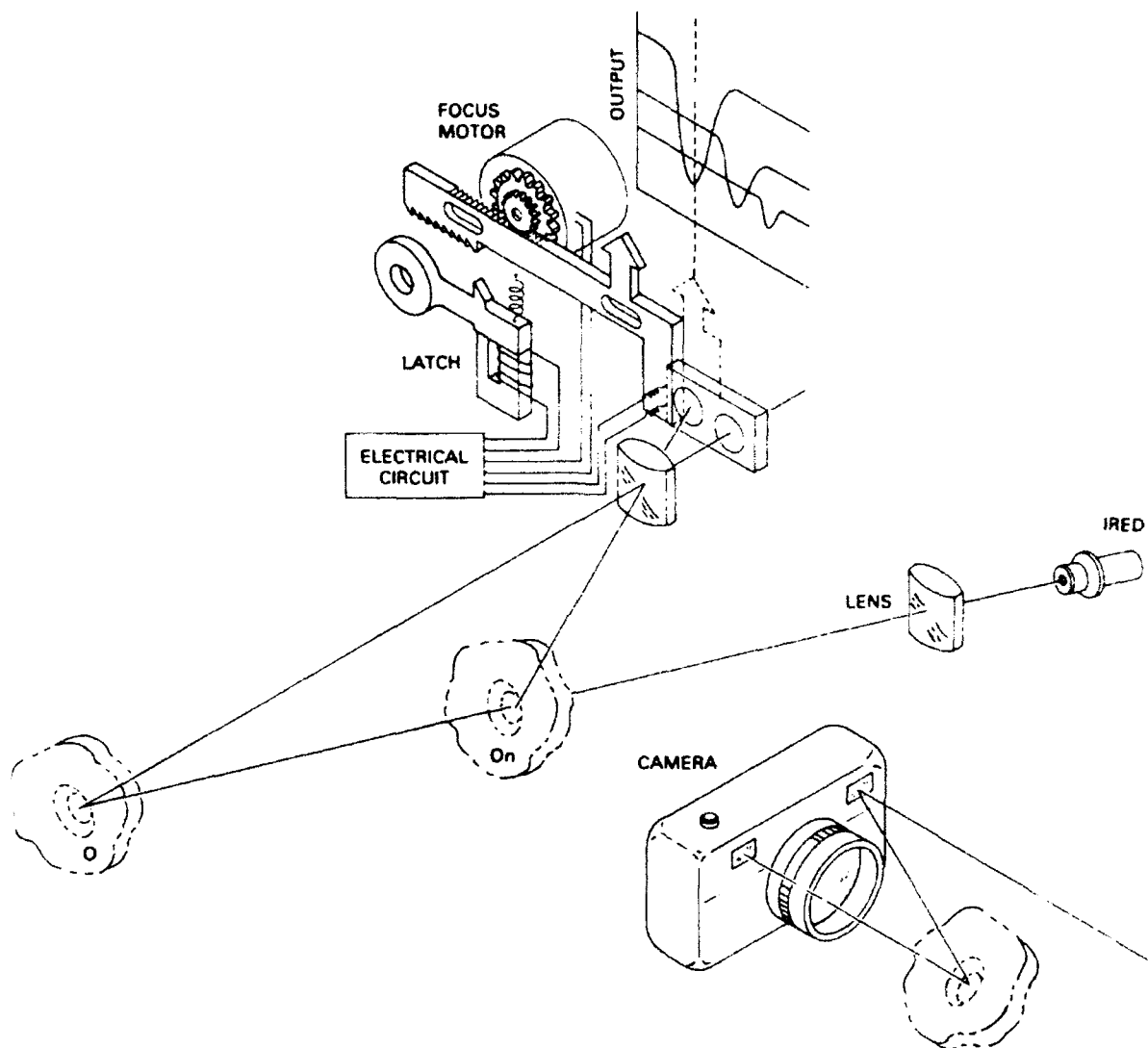


Figure 17. Illustration of FMC-A autofocus principle (Courtesy Pentax Corporation).

Selected Specifications:

Ranging technique	Active triangulation
Maximum range	4 meters
Minimum range	0.75 meter
Range increment	8 steps
Range accuracy	± one step
Measuring time	70 milliseconds

Light source	Near-infrared LED modulated at 4 KHz
Beam projection angle	1 degree, 20 minutes
Power	3.5 volts DC at 50 ma (250 ma peak)
Operating temperature	-20 to +50 degrees C

Point of Contact:

Pentax Corporation
 55 Inverness Drive East
 Englewood, CO 80112
 (303) 773-1101

3.1.4 Hamamatsu Range-Finder Chip Set

The diagram for the chip-set manufactured by Hamamatsu Corp. is shown in figure 18. It consists of three related components: the position sensitive detector (PSD), the range finder IC, and an LED light source. Applying the principles of triangulation in an integrated circuit chip set, this 16-step rangefinder works at high speed, offering a maximum sample rate of 700 Hz. Near-infrared energy is emitted by the LED source, and reflected energy received by the PSD, a continuous light-spot position detector. The highly sensitive circuitry is capable of detecting pulsed light returns generating approximately 1 nanoampere or more of output current in the PSD.

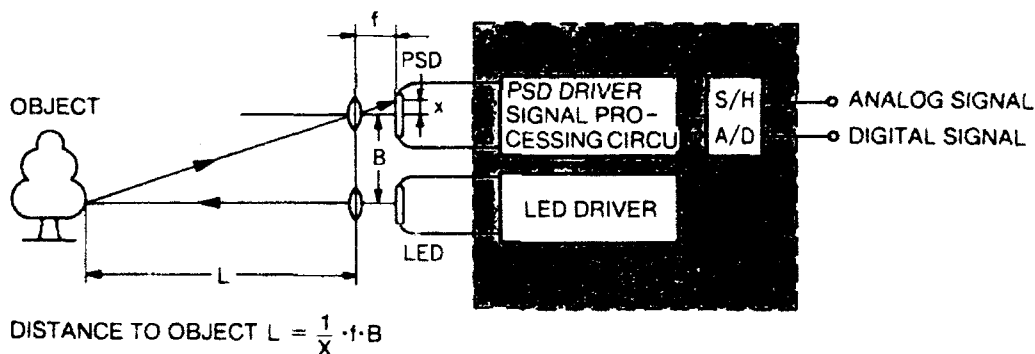


Figure 18. Block diagram of the Hamamatsu's Range-Finder Chip Set, which applies the principle of triangulation (Hamamatsu Corporation, 1990).

This 16-step rangefinder chip provides both analog and digital signal outputs. The analog output is produced by a sample-and-hold circuit; the digital output is determined by an A/D converter with 4-bit discrimination, corresponding to 16 analog-range zones. A similar 3-step IC converts range into 3 zones (Hamamatsu Corporation, 1990).

Selected Specifications (16-step version):

Ranging technique	Active triangulation
Sample frequency	700 Hz maximum
Temperature range	-15 to 55 degrees C
Input power	3.0 volts DC
Analog output	0.24 to 0.46 volt
Size	44-pin molded-plastic package, 16 by 13 millimeters

Point of Contact:

Mr. Norman H. Schiller
Hamamatsu, Corporation
360 Foothill Rd.
Bridgewater, NJ 08807
(908) 231-0960

3.1.5 Hamamatsu H3065-10 Optical Displacement Sensor

Hamamatsu's H3065-10 Optical Displacement Sensor detects in the range from 350 to 650 millimeters. The system consists of a sensor head and a controller unit; the sensor head incorporates a pulsed near-infrared LED, and uses a segmented photodiode as the lateral position detector. When coupled with one of two recommended controller units (figure 19), the resulting displacement measurement provides an analog output spanning 10 volts; the relationship between output voltage and object range is linear. Range resolution can be increased by incorporating a low-pass filter with cutoff frequency of 60 Hz (Hamamatsu Corporation, 1991).

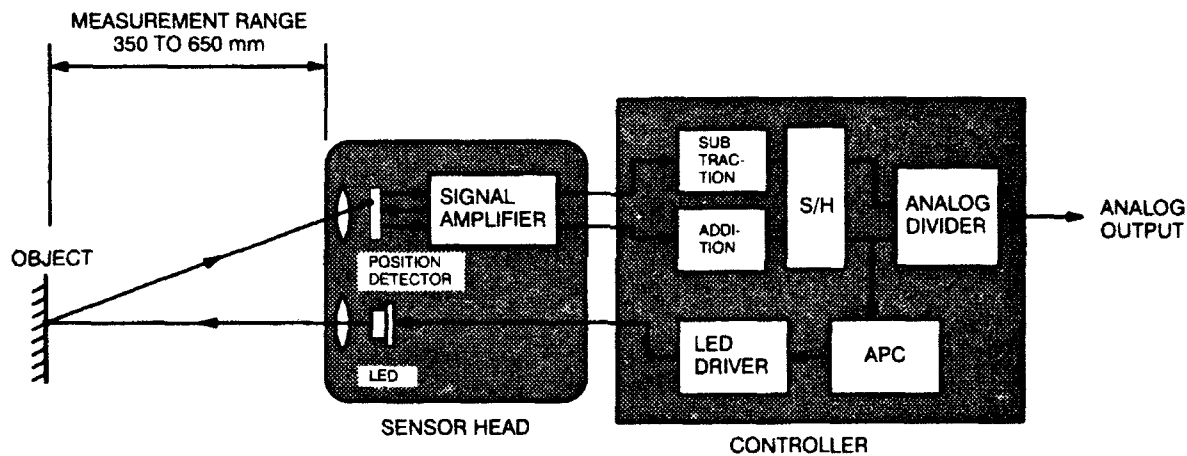


Figure 19. Block diagram of Hamamatsu's Displacement Sensor (Hamamatsu Corporation, 1991).

Selected Specifications:

Ranging technique	Active triangulation
Maximum range	650 millimeters
Minimum range	350 millimeters
Resolution	±5 millimeters 0.8 millimeter with LPF
Light source	Near-infrared LED
Light spot diameter	15 millimeters (maximum)
Pulse repetition rate	2 KHz
Analog output	±5 volts
Sensor head	
Size	20 by 75 by 45 millimeters
Weight	80 grams

Controller (C2935-10)

Size	55 by 255 by 230 millimeters
Weight	2.2 kilograms
Power	115 Volts AC

Point of Contact:

Mr. Norman H. Schiller
Hamamatsu, Corp.
360 Foothill Road
Bridgewater, NJ 08807
(908) 231-0960

3.1.6 Honeywell HVS-300 Three Zone Distance Sensor

Honeywell Visitronics of Englewood, Colorado, has developed a noncontact, near-infrared proximity gage that employs a triangulation ranging technique to determine relative distance as well as the presence or absence of an object. The HVS-300 Three Zone Distance Sensor is capable of indicating whether a surface within its field of view is close to the sensor, at an intermediate distance, far from the sensor, or out of range. Conventional diffuse proximity detectors based on return signal intensity display high repeatability only when target surface reflectivity is maintained constantly. The HVS is capable of higher range accuracy under varying conditions of reflectivity and ambient lighting due to the use of the triangulation ranging scheme (Honeywell Visitronic, undated). Intended applications include low-cost inspection for zero-defect manufacturing systems, small-part position detection, conveyor system parts location, tool position indicators, robot arm position indicators, depth inspection, and fill-level detectors.

The HVS-300 proximity sensor consists of a pair of near-infrared LED sources, a dual-element silicon photodetector, directional optics, and control logic circuitry. The LED emitters transmit coded light signals at differing angles of incidence through one side of a directional lens and into the environment. If emitted energy strikes an object, a portion of the transmission is returned through the other side of the lens and focused onto the detector assembly.

The detector employs two photodiode elements placed side by side, separated by a narrow gap. Depending on the range to the reflective surface, a returning reflection will either fall exclusively on one photodetector (indicating the reflecting surface is close to the sensor), or the other (indicating the surface is far from the sensor), or equally on both (meaning the object is on the boundary between these two regions). Changing the incidence angle changes the distance this boundary lies from the sensor.

With two transmissions projected onto the scene at different angles of incidence, two such boundaries are created. The first distinguishes between the near and intermediate regions, while the second distinguishes between the intermediate and far regions (figure 20). Because both transmissions use the same detector, the sources must be coded so that the control electronics can distinguish between them and determine which regions they represent.

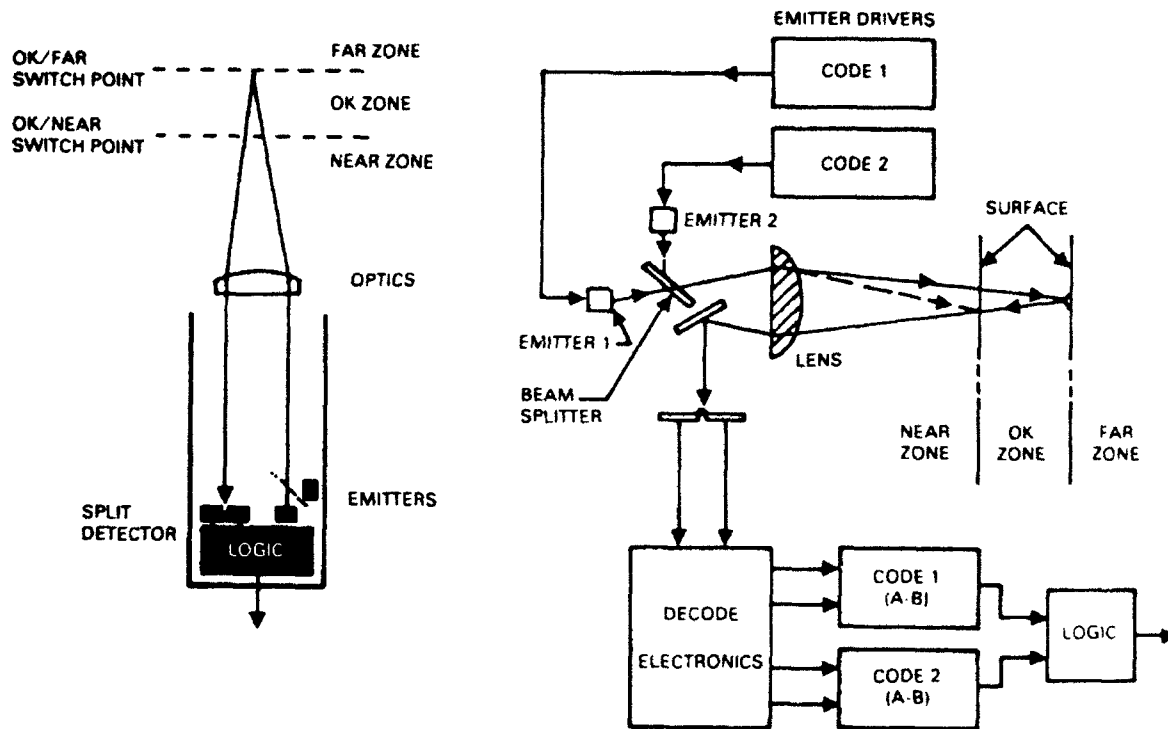


Figure 20. The HVS-300 distance sensor gauge uses dual active near-infrared emitters to detect if an object is in the adjustable OK zone (Courtesy Honeywell Corporation).

System response is on the order of 10 milliseconds. The HVS-300 can be set to operate between the ranges of 2.5 and 30 inches. Adjustment is manual and fixed prior to operation. At maximum range, the system switch point repeatability approaches 1 percent, but can be better than 0.05 percent at a range of 6 inches. The size of the intermediate region is limited and determined by the emitter that sets the closest boundary. The irradiation pattern of the light source is 1.5 by 0.5 degrees, which forms an oblong spot on the target of interest; spot size is dependent on object range. Sensor output is in the form of a logic signal representing the possible range states: near, OK, far, or out of range.

In general, the HVS-300 is insensitive to changes in surface texture or color and unaffected by ambient light conditions. Such a system would find potential application as a close-in proximity sensor for the collision avoidance needs of an indoor mobile robot, where speed of advance would be limited and in keeping with the sensor's maximum range of 30 inches. The four discrete range zones would give a relative feel for the distance to a threatening object, allowing for more intelligent evasive maneuvering.

Selected Specifications:

Ranging technique	Active triangulation
Maximum range	30 inches
Minimum range	2.5 inches
Repeatability	1 percent
Light source	820 nanometer near-infrared LED (2)

Beamwidth 1.5 by 0.5 degrees
Update rate 10 milliseconds

Point of Contact:

Honeywell Visitronics
P.O. Box 5077
Englewood, CO 80155
(303) 850-5050

3.1.7 Honeywell Visitronic Autofocus System

The first practical autofocus system for lens-shutter cameras was developed by the Honeywell Visitronic Group in 1976. The system employs a variation of the stereoscopic ranging technique, nicely optimized for low-cost implementation through the development of a special purpose integrated circuit (IC) for autocorrelation. Two five-element photosensitive arrays are located at each end of the Visitronic IC, that measures about 0.1 by 0.25 inch in size (Stauffer & Wilwerding, 1982). Figure 21 shows a pair of mirrors reflecting the incoming light from two viewing windows at either end of the camera housing onto these arrays. One of these images remains fixed while the other is scanned across its respective array through the mechanical rotation of the associated mirror. The angular orientation of the moving mirror at the precise instant that the IC indicates the two images are matched is directly related to the range to the subject, and used to position the camera lens.

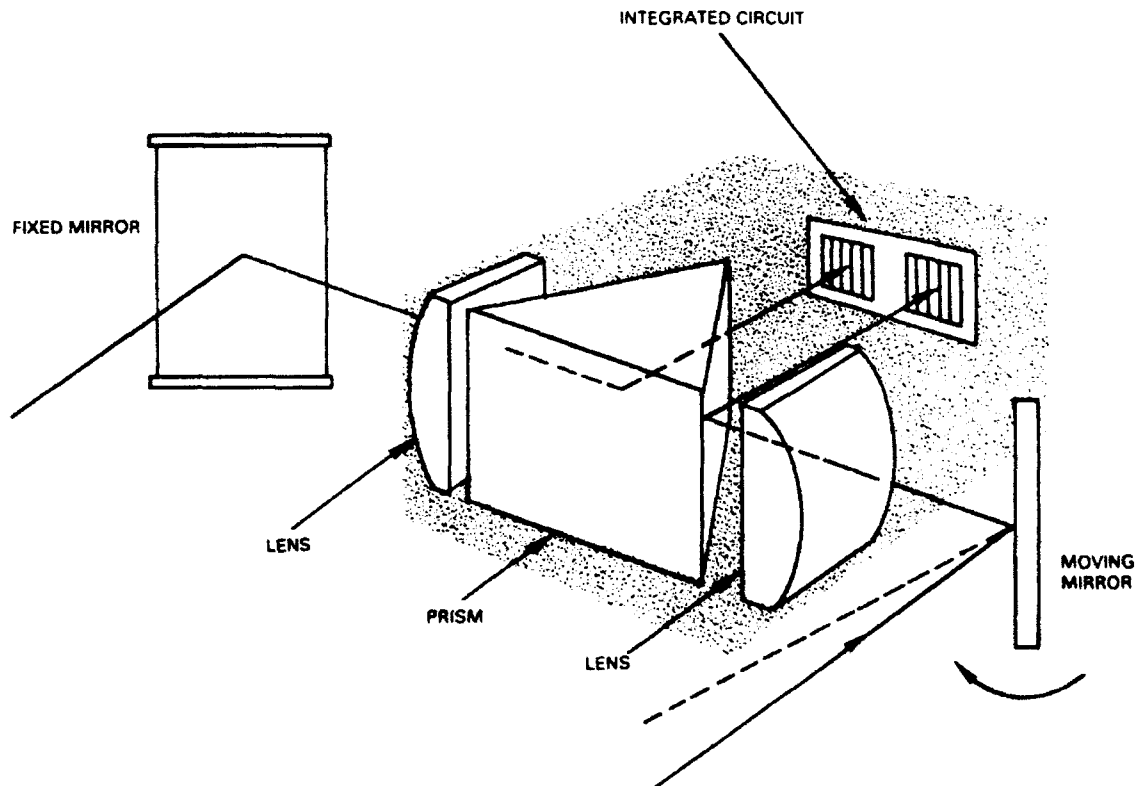


Figure 21. Illustration of the Visitronic Autofocus System (Courtesy Honeywell Corporation).

The photocurrents from corresponding elements in each array are passed through a string of diodes on the IC and thus converted to voltages proportional to the log of the current. The resulting pair of voltages is then fed to a differential amplifier, which produces a difference signal proportional to the ratio of the two light intensities as seen by the respective detectors (Stauffer & Wilwerding, 1982). For four of the five-element array pairs, the absolute values of these difference signals are summed and the result subtracted from a reference voltage to yield the correlation signal. The better the scene match, the lower the differential signal for each array pair, and the higher the correlation signal.

The peak value of the correlation signal corresponds to the best scene match. An operational amplifier on the IC makes a continuous comparison between the correlation output and the previous highest value, which is stored in a capacitor. The output from this comparator is high as long as the correlation signal is lower than the previously stored peak value. The last low-to-high transition (figure 22) represents the mirror angle corresponding to the highest peak.

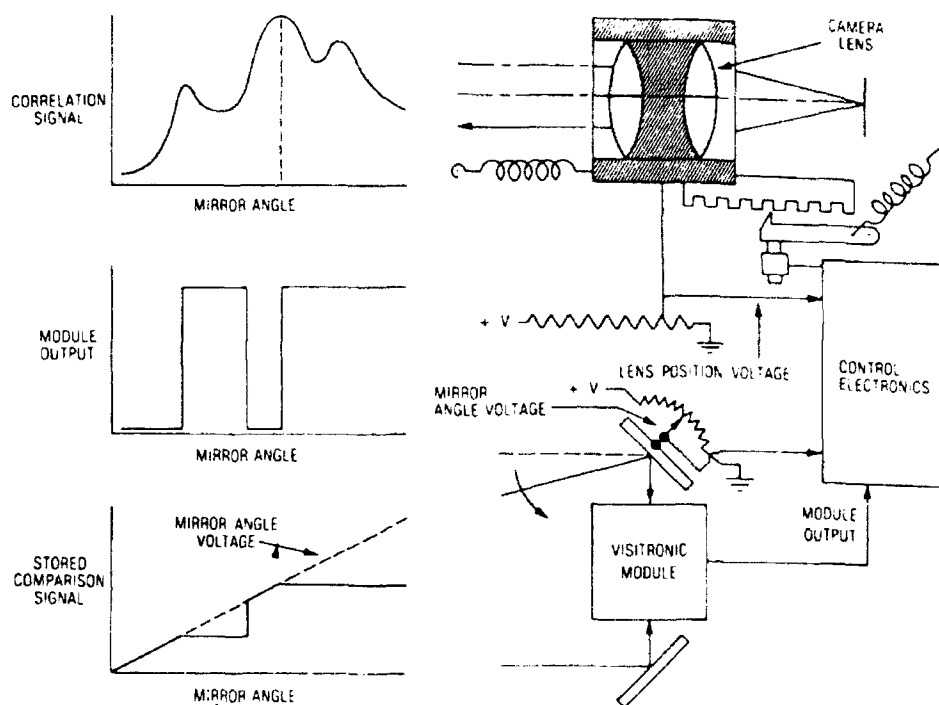


Figure 22. Schematic diagram of Visitronic Autofocus System (Courtesy Honeywell Corporation).

The output of the autofocus system was used to position the camera lens for best focus. A potentiometer on the moving mirror produced a voltage that varied as a linear function of mirror position. The output of this potentiometer was sampled and stored when the IC indicates the peak correlation signal was present. A similar potentiometer coupled to the camera lens positioning mechanism was used to stop the lens travel when its output matched the stored voltage signifying mirror position at best focus.

Like the active triangulation scheme employed in the Pentax autofocus system discussed in section 3.1.3, the passive Honeywell System was developed for a short-range application where accuracy was not critical. The camera application clearly illustrates, however, the

feasibility of a small, low-cost, low-power passive ranging system, and suggests improved results more suitable to the needs of a mobile robot could be readily achievable, as discussed in section 3.1.8.

No specifications are available.

Point of Contact:

Honeywell Visitronics
P.O. Box 5077
Englewood, CO 80155
(303) 850-5050

3.1.8 Honeywell Through-the-Camera-Lens Autofocus System

The Honeywell Through-the-Camera-Lens (TCL) autofocus system is a second-generation refinement of the Visitronic System, comparing the signatures of light passing through two different sectors of the camera lens, as opposed to two separate viewing windows. Instead of five, there are 24 pairs of detectors arranged in an array about 5 millimeters long. Two complete arrays are provided to accommodate camera lenses with different aperture sizes (Stauffer & Wilwerding, 1982).

Light from any given point in the field of view of a camera passes through all sectors of the camera lens, and subsequently arrives at the image plane from many different angles. If the lens is in focus, these components all converge again to a single point in the image plane. If the lens is not in focus, these components are displaced from one another, and the image becomes fuzzy.

Similarly, light from every point in the scene of interest passes through each sector of the lens. Thus, each sector of the lens will contribute a recognizable signature of light to the image plane, in keeping with the image viewed. (Early pinhole cameras made use of this principle; essentially there was only one sector, and so there was only one image, which was always in focus.) Practically speaking, these signatures are identical, and if the lens is in focus, they will be superimposed. As the lens moves out of focus, the signatures will be displaced laterally, and the image blurs.

The Honeywell TCL system detects this displacement for two specific sectors (A and B) located at opposite sides of the lens as shown in figure 23. Light from these two sectors falls upon a series of 24 microlenses mounted on the surface of the integrated circuit, and in the camera image plane. An array of sensors is positioned within the IC at a specified distance behind the image plane in such a fashion that light incident upon the row of microlenses and their associated image sampling apertures will diverge again to isolate the respective components arriving from each of the two lens sectors (figure 24). Within each aperture image in the detector plane are two detectors, one for each of the two sectors (A and B). Output of all 24 of the A detectors is used to construct the A signature; the 24 B detectors are read to form the B signature (Stauffer & Wilwerding, 1982).

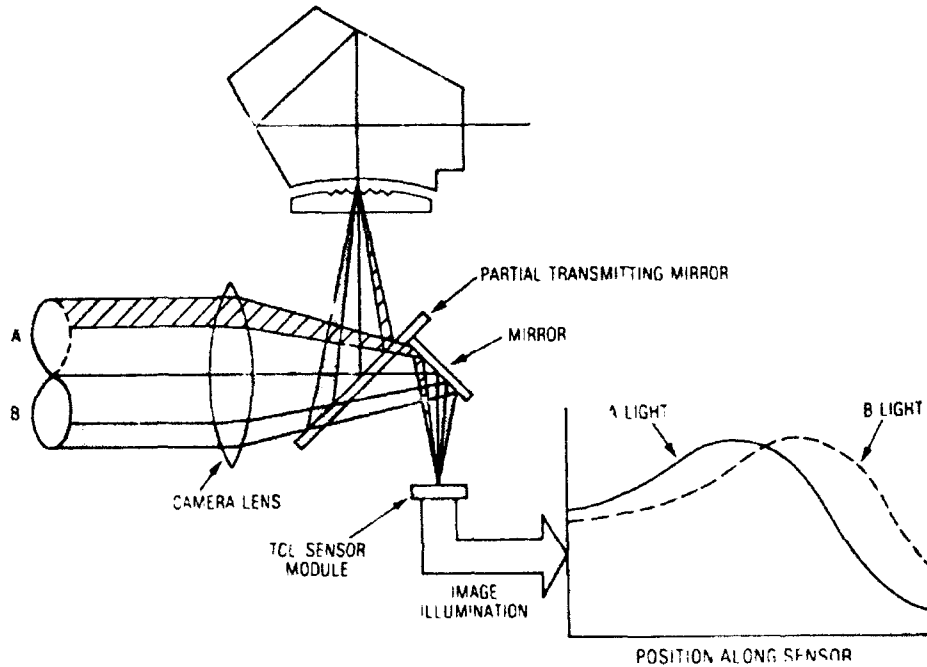


Figure 23. Light from two separate sectors of the same lens is compared to determine the position of best focus in the TCL Autofocus System (Courtesy Honeywell Corporation).

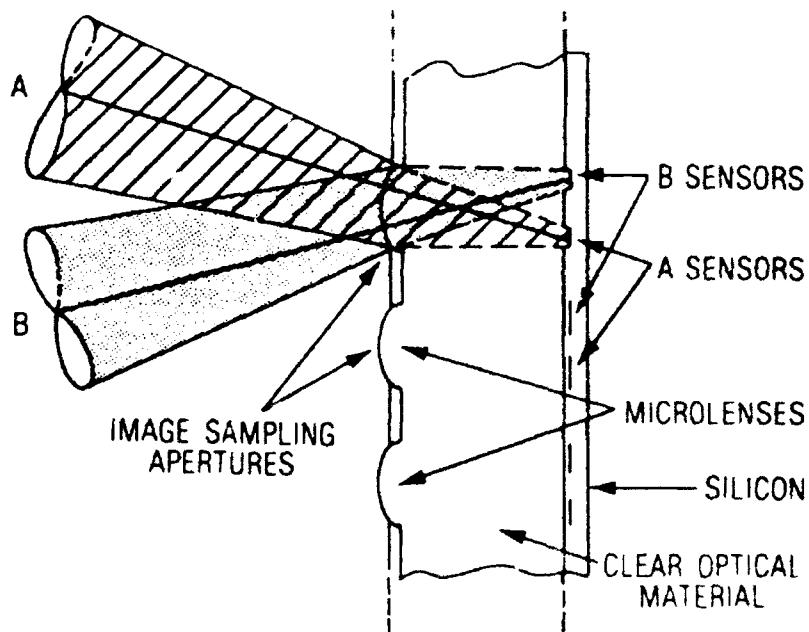


Figure 24. A row of microlenses focuses light on the pairs of detectors, forming two separate signatures for comparison (Courtesy Honeywell Corporation).

The signatures of light passing through the two camera lens sectors can then be compared and analyzed. The distance between these lens sectors is the base of triangulation for determining range to the subject. Which signature appears to be leading the other and to what degree indicates how far and in what direction the lens must be moved to bring the images into superposition. The output of the CCD detector array is fed to a CMOS integrated circuit which contains the CCD clock circuitry and an A/D convertor that digitizes the analog output for further processing.

The TCL system can sense that the image is in focus to where the plane of the image is within 0.05 millimeter of the position of correct focus (Stauffer & Wilwerding, 1982). This point of focus can be directly converted to range resolution through the standard lens equation, and varies with the focal length of the lens used. The detector pairs in the TCL system can discriminate light differences of one part in 100; the human eye is limited to one part in 10 (Stauffer & Wilwerding, 1982).

The Honeywell TCL circuitry operates on a 5-volt power supply, and the sensor and companion ICs together draw less than 60 milliwatts. The TCL system can potentially provide a low-cost, noncontact distance sensing capability for robotic applications provided there is adequate ambient illumination, and the scene being viewed has sufficient contrast.

No specifications are available.

Point of Contact:

Honeywell Visitronics
P.O. Box 5077
Englewood, CO 80155
(303) 850-5050

3.1.9 Robot Defense Systems' OWL

The OWL (no longer available) was a computer-controlled, three-dimensional, laser-based imaging device developed by Robot Defense Systems, Thornton, CO, intended initially for intrusion detection applications (Robot Defense Systems Incorporated, undated). The system mechanically scanned a wide field of view in a raster sequence to produce images used to map a scene and detect objects. The observed objects were then categorized by threat level, and an alarm triggered if the threat exceeded a set threshold. The process of data collection, analysis, and classification occurred at a rate of approximately 1.5 frames per second.

The sensor determined range through phase shift measurement, and used the returned signal amplitude of the scanned points to display the outline and dimensions of an object. The maximum range for the system was 140 feet; objects larger than 3 inches could be detected at a distance of 70 feet.

Horizontal scanning was performed by a pair of gear-synchronized, counterrotating, mirrored wedges; one wedge directed the transmitted beam while the other collected the returning energy. This action combined with a vertical scanning motion carried out by a nodding mirror resulted in a total field of view of 256 by 128 pixels. The laser light source, classified as eye-safe due to the constant scanning motion of the beam, reportedly allowed operation under conditions including adverse weather, smoke, and darkness.

Selected Specifications:

Ranging technique	Phase-shift measurement
Maximum range	140 feet
Minimum range	10 feet
Light source	800 nanometer laser diode
Beam divergence	<0.2 degree
Field of view	45 degrees (horizontal), 30 degrees (vertical)
Scan rate	5760 degrees/second (horizontal), 30 degrees/second (vertical)
Power requirements	24 volts DC at 6 amps
Temperature range	-20 to +140 degrees F
Enclosure	1728 cubic inches

Point of Contact:

Robot Defense Systems, Inc.
471 East 124th Avenue
Thornton, CO 80241-2402

NOTE: Company is no longer in business. Included for information purposes only.

3.1.10 NAMCO LASERNET Smart Sensor

NAMCO Controls of Mentor, OH, developed LASERNET (Laskowski, 1988) for applications in industrial environments. The laser-based sensor is an active scanning device that employs retroreflective targets to measure range and angular position. Multiple targets can be processed simultaneously, and it is also possible to specifically identify objects through the use of uniquely identifiable codes.

A helium-neon (HeNe) laser source, photodetector, mechanical scanner, beam-forming optics, and control electronics are housed in an enclosure measuring 5 by 6.5 by 3.4 inches for the standard range unit, and 5 by 9 by 3.4 inches for the long-range unit. The detector is a photodiode with an operational bandwidth of 1.0 MHz, tailored to receive inputs only from the 632.8-nanometer region of the spectrum. A servo-controlled rotating mirror horizontally pans the laser beam through an arc of 90 degrees (45 degrees either side of centerline) at a rate of 20 scans/second. Directional mirrors route the beam from the laser tube to the scanning mirror; a collecting lens focuses the return signal onto the photodetector.

Retroreflectors positioned within the sensor's environment are necessary for the effective application of the LASERNET ranging system. A standard retroreflective target is provided by the developer, essentially a 4- by 4-inch square surface of corner cube prisms with an overall 90-percent reflection coefficient. The LASERNET system operates by panning a beam of light across the scene at a constant rate through a 90-degree field of view. When the laser beam sweeps across a retroreflective target, a return signal of finite duration is sensed by the detector. Since the targets are all the same size, the return generated by a close target will be of longer duration than that from a distant one (figure 25). In effect, the target appears larger.

Range is calculated from the equation (NAMCO Controls, 1989):

$$d = \frac{W}{2 \tan\left(\frac{VT_s}{2}\right)}$$

where: d = range to target
 W = target width
 V = scan velocity (7200 deg/sec)
 T_a = duration of the returned pulse

Because the target width and angular scan velocity are known, the equation reduces to an inverse function of the pulse duration, T_a . With 4-inch targets, the effective range of the sensor is from 1 to 20 feet (2 to 50 feet for the long-range model), and range resolution for either model is 9.6 inches (1.57 inches using digital output) at 20 feet down to 0.1 inch (0.017 inch using digital output) at 1 foot. LASERNET produces an analog output ranging from 0 to 10 volts over the range 0 to 20 feet, and an inverse range function (representing T_a rather than d) digital output on an RS-232 serial port.

Angle measurement is initiated when the scanner begins its sweep from right to left; the laser strikes an internal synchronization photodetector that starts a timing sequence. The beam is then panned across the scene until returned by a retroreflective target in the field of view. The reflected signal is detected by the sensor, terminating the timing sequence (figure 26). The elapsed time is used to calculate the angular position of the target in the equation (NAMCO Controls, 1989):

$$\theta = VT_b - 45^\circ,$$

where: θ = target angle
 V = scan velocity (7200 deg/sec)
 T_b = interval between scan initiation and target detection

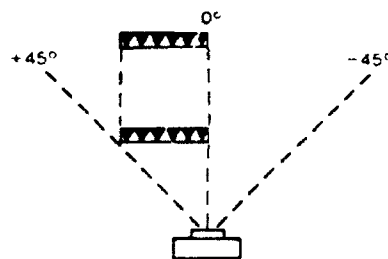


Figure 25. Target range.

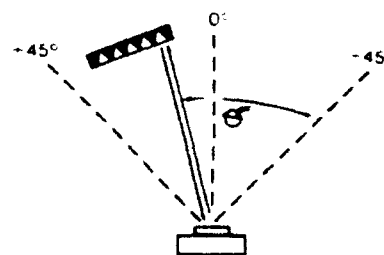


Figure 26. Target bearing.

This angle calculation determines either the leading edge of the target, the trailing edge of the target, or the center of the target, depending upon the option selected within the LASERNET software option list. The angular accuracy for LASERNET is ± 1 percent, and the angular resolution is 0.1 degree for the analog output; accuracy is within ± 0.05 percent with a resolution of 0.006 degree when the RS-232 serial port is used. The analog output is a voltage ranging from 0 to 10 volts over the range of from -45 to $+45$ degrees, whereas the RS-232 serial port reports a proportional *count value* from 0 to 15360 over this same range.

The Multiple-Target model of LASERNET can track up to eight retroreflective targets simultaneously for range and/or angle information. While the analog outputs of range and angle report on only the first several targets seen, the RS-232 serial port digital output reports angle and/or

range information for all targets seen in the 90-degree field of view. Navigation, using triangulation based on data from several targets, coupled with range and distance information from one target, is possible using the data from the serial port. The Multiple-Target models are available with RS-485 multidrop networking protocols for the serial output port. Up to 16 sensors can be connected into a single twin-wire cable and addressed with a simple master-slave protocol.

By masking a target in specific ways, some limited height information can be obtained as well as angular position. With a mask that falls along the diagonal and blocks the lower left portion of the square target, the height and angle can be measured. This configuration is ideal when the range to a target is a known constant. The height is a function of the duration of the returned pulse, which varies with the vertical position of the laser scan. The leading edge of the target is not masked so the angle calculation is identical to that discussed previously.

Note, all of the above calculations assume the target is positioned perpendicular to the angle of incidence of the laser source. If a target happens to be rotated or otherwise skewed away from the perpendicular, it will appear narrower than actual, with a resultant range measurement error. Errors in angle determination also occur because the leading edge is either positioned in front of or behind the center of the target.

With the proper placement of retroreflective targets or tape, the LASERNET system can guide AGVs using wall-following, center-of-the-path, or track-following methods. The sensor is also capable of aligning the lifting mechanisms of automated conveyors to desired storage locations, as well as providing identification of the contents of a particular location when coded targets are used. AGV applications employing fixed-position reflectors are used for factory, office, and mining vehicle navigation (Anderson, 1989; Horst, undated), (i.e., limited to facility work performed in known environments).

Selected Specifications (standard model):

Ranging technique	Known target size
Maximum range	20 feet
Minimum range	1 foot
Range	9.6 inches at 20 feet
Angular	0.1 degree
Field of view	90 degrees (horizontal plane)
Light source	632.8 nanometer HeNe laser
Scan rate	7200 degrees per second
Size	5 by 6.5 by 3.4 inches

Point of Contact:

Dr. Edward Laskowski
NAM.CO Controls
7567 Tyler Boulevard
Mentor, OH 44060
1-800-NAMTECH

3.1.11 ERIM Adaptive Suspension Vehicle Sensor

The Adaptive Suspension Vehicle (ASV) developed at Ohio State University and the Autonomous Land Vehicle (ALV) developed by Martin Marietta Denver Aerospace, Denver, CO, were the premier autonomous mobile robot projects sponsored by the Defense Advanced Research Projects Agency (DARPA) in the late '80s under the Strategic Computing Program. In support of these efforts, the Environmental Research Institute of Michigan (ERIM) was tasked to develop an advanced, three-dimensional vision system to meet the close-in navigation and collision avoidance needs of a mobile platform. The initial design, which is now commercially available under license from ERIM to the Daedalus Corporation, Ann Arbor, MI, is known as the Adaptive Suspension Vehicle Sensor. The sensor operates on the principle of optical radar and determines range to a point through phase-shift measurement, using a CW laser source.

The ranging sequence begins with the transmission of a modulated laser beam that illuminates an object and is partially reflected back to the receiver, where the returning light strikes the detector, generating a representative signal. This signal is amplified and then filtered to extract the modulation frequency. At this point, the amplitude of the signal is picked off to produce a reflectance image used to produce a video image for viewing or for two-dimensional image processing. A reference signal is then output by the modulation oscillator and both the detector and reference signals are sent to the comparator electronics.

The laser is modulated at an RF frequency (70 MHz), and it is the detection of phase shift on this signal, not the optical carrier, that is used to derive range. This phase difference is determined by a time-measurement technique, where the leading edge of the reference signal initiates a counting sequence that is terminated when the leading edge of the returned signal enters the counter. The resulting count value is a function of the phase difference between the two signals and is converted to an 8-bit digital word representing the range to the scene.

Three-dimensional images are produced by the ASV sensor through the use of scanning optics. The mechanism consists of a nodding mirror and a rotating polygonal mirror with four reflective surfaces (figure 27). The polygonal mirror pans the transmitted laser beam in azimuth across the ground, creating a scan line at a set distance in the front of the vehicle. The scan line is deflected by the objects and surfaces in the observed region and forms a contour of the scene across the sensor's horizontal field of view. The third dimension is added by the nodding mirror which tilts the beam in discrete elevation increments. A complete image is created by scanning the laser in a left-to-right and bottom-to-top raster pattern.

The returning signals share the same path through the nodding mirror and rotating polygon (actually slightly offset), but are split off through a separate glass optical chain to the detector. The scan rate of 180 lines per second is a function of the field of view and desired frame rate, determined by the vehicle's maximum forward velocity (10 feet/second in this case). The size, weight, and required velocities of the mirrors precluded the use of galvanometers in the system design; the rotating and nodding mirrors are servo driven.

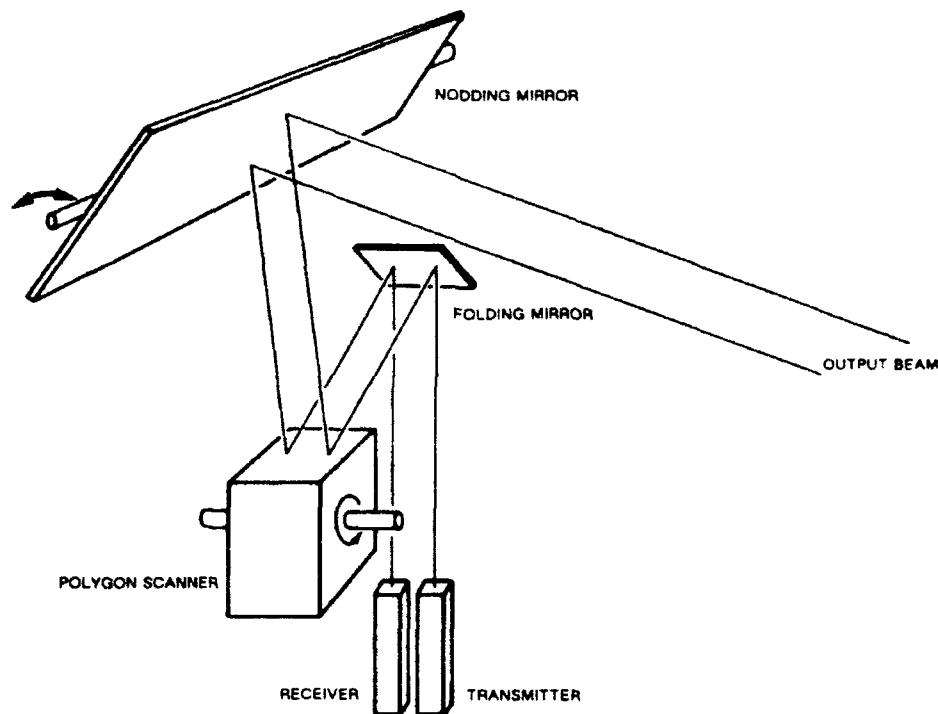


Figure 27. Scanning and nodding mirrors arrangement in the ERIM laser rangefinder (Courtesy Environmental Research Institute of Michigan).

The output beam is produced by a gallium arsenide (GaAs) laser diode emitting at a wavelength of 820 nanometers. The small size, internal modulation, low temperature, and limited eye hazard of this source resulted in its selection over an alternative carbon dioxide laser used in a trade-off analysis. The only significant drawbacks for the GaAs device were reduced effectiveness in bright sunlight, and only fair penetration capabilities in fog and haze. Collimating and expansion optics were required by the system to produce a 6-inch diameter laser footprint at 30 feet, which is the effective operating range of the sensor. The major factor limiting the useful range of the system is the measurement ambiguity that occurs when the phase difference between the reference and returned energy exceeds 360 degrees.

The detector is a silicon avalanche photodiode optically matched to the laser wavelength. The laser source, detector, scanning optics, and drive motors are housed in a single enclosure, designed to be situated at a height of 8 feet to look down upon the field of view. From this vantage point, the laser strikes the ground between 2 and 30 feet in front of the vehicle; at 30 feet, the horizontal scan line is 22 feet wide. The 2-Hz frame rate for the system creates a new image of the scene for every 5 feet of forward motion at the vehicle's maximum speed of 10 feet/second.

Following the design and fabrication of the ASV sensor, ERIM undertook the task of developing a similar device known as the ALV sensor for DARPA's autonomous land vehicle. The two instruments are essentially the same in configuration and function, but with modified specifications to meet the needs of the individual mobile platforms. The following selected specifications for each device illustrate their differences.

Selected Specifications:

	<u>ASV</u>	<u>ALV</u>
Ranging technique	Phase shift	Phase shift
Field of view		
horizontal	80 degrees	80 degrees
vertical	60 degrees	30 degrees
Beamwidth	1 degree	0.5 degree
Frame rate	2 frames/second	2 frames/second
Scan lines per frame	128	64
Pixels per scan line	128	256
Maximum range	32 feet	64 feet
Depression angle		
(Top of vertical scan)	-15 degrees	-15 degrees
Vertical scan increment	10 degrees	20 degrees
Wavelength	820 nanometers	820 nanometers
Power	24 volts 450 watts	24 volts 450 watts
Size (inches)	14 by 26 by 22	14 by 29 by 22
Weight	85 pounds	85 pounds

Point of contact:

Environmental Research Institute of Michigan (ERIM)
Box 8618
Ann Arbor, MI 48107-8618
(313) 994-1200

3.1.12 CLS Laser Ranger

Chesapeake Laser Systems of Lanham, Maryland, offers an active laser-based triangulation ranging system to measure the position of an object. The unit employs a laser diode emitting up to 30 milliwatts, a linear CCD detection array, and a high-speed preprocessor and micro-processor-based control system. Dynamic exposure control allows the system to function effectively over five orders of magnitude light intensity. The temperature stability of the linear CCD array facilitates extended operation without recalibration.

The optics and electronics are housed in a NEMA 12 drip-proof enclosure, with the optics protected by an over-pressure *air curtain* for applications involving extremely hostile environments. Several housing sizes are available depending on the range or accuracy desired. The CLS Laser Ranger can be configured to measure ranges of 10 feet or more.

Selected Specifications (LTG-2100 Series):

Ranging technique	Active triangulation
Maximum range	10 feet
Size	6 by 9 by 2 inches
Weight	4 pounds
Light source	Laser diode operating at 820 nanometers

	<u>Option 1</u>	<u>Option 2</u>
Range Interval	1 to 3 feet	5 to 6 inches
Accuracy	0.005 to 0.040 inch	0.001 inch

Point of Contact:

Lawrence B. Brown
 Chesapeake Laser Systems, Inc.
 4473 Forbes Boulevard
 Lanham, MD 20706
 (301) 459-7977

3.1.13 CLS Laser Profiler

Chesapeake Laser Systems has developed a laser-scanning range measurement system using a solid-state beam deflector (figure 28) that allows random beam positioning with a 10-micro-second response time (Chesapeake Laser Systems Incorporated, 1991a). This approach has a speed and accuracy advantage over systems relying on mechanical scanning mechanisms or CCD arrays to acquire three-dimensional data. This electro-optic camera was developed to replace conventional TV cameras in machine vision systems.

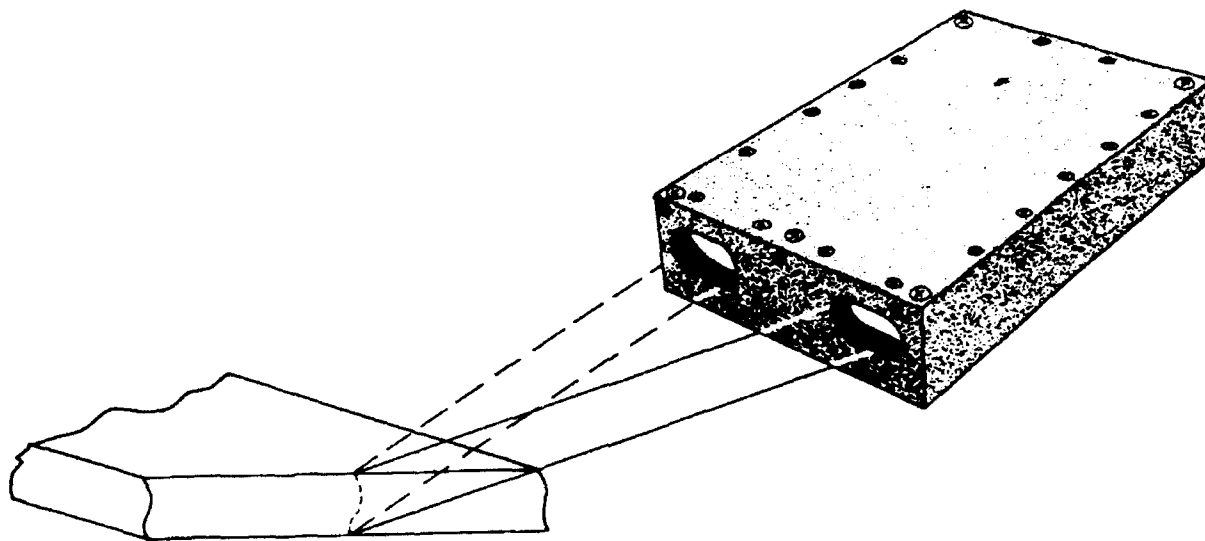


Figure 28. Chesapeake laser-scanning range measurement system.

The Chesapeake Profiler performs like a randomly accessible 1000 by 1000 two-dimensional array. Most conventional vision systems use a small CCD television camera that collects visual information, which is then fed to a computer which typically employs pattern recognition software to obtain geometrical data. Processing involves a minimum of 65,000 pieces of information that must be digitized and sorted, a relatively difficult and time consuming task which can take on the order of 0.1 or more seconds. The electronic and software complexity of the CCD TV approach thus unnecessarily limits the speed and precision of machine vision (Chesapeake Laser Systems Incorporated, 1991a).

The solid-state scanning mechanism removes these limitations by collecting only the useful information from the scene being viewed; processing time is cut to 0.001 second. The LPG-4100 shown in figure 28 gives high-accuracy measurement over a range interval of up to 1.5 inches, with as much as a 20-inch standoff.

Selected Specifications (LPG-4100 Series):

Ranging technique	Active triangulation
Standoff	2 to 20 inches
Range interval	0.5 to 2 inches
Accuracy	0.001 to 0.032 inch
Resolution	1:256 to 1:2000
Points of Profile	1 to 1000 (programmable)
Data rate	1 to 10 KHz
Size	3 by 6 by 8 inches
Power requirements	115 VAC or DC (+28V, +15V, +5V)

Point of Contact:

Lawrence B. Brown
Chesapeake Laser Systems, Inc.
4473 Forbes Boulevard
Lanham, MD 20706-4354
(301) 459-7977

3.1.14 CLS Laser Coordinate Measuring System

In an effort to improve the accuracy and speed of existing measurement technology, Chesapeake Laser Systems began development of the CMS-1000 in 1983 in conjunction with the U.S. Navy. Originally designed as a positioning control unit for a gantry robot, the CMS-1000 is a laser-based tracking interferometer system that can measure the location of a moving object to better than 10 microns over a volume of 3 by 3 by 3 meters (Brown, L. B., 1985; Cleveland, 1986; Chesapeake Laser Systems, undated; Brown, Merry & Wells, 1987). The system employs a servo-controlled beam steering mechanism to track a randomly moving target. (Standard interferometric ranging works only with nonrectilinear straight-line motion as discussed in section 2.1.5.1.)

Figure 29 shows the CMS-1000 using three laser beams to track a retroreflective target attached to the moving end effector. The tracking interferometer is rigidly fixed to the edge of the work area. After a brief calibration routine, the CMS-1000 continuously measures the distance to the retroreflector and calculates the x, y, z coordinates of the robotic arm at a 50-Hz rate.

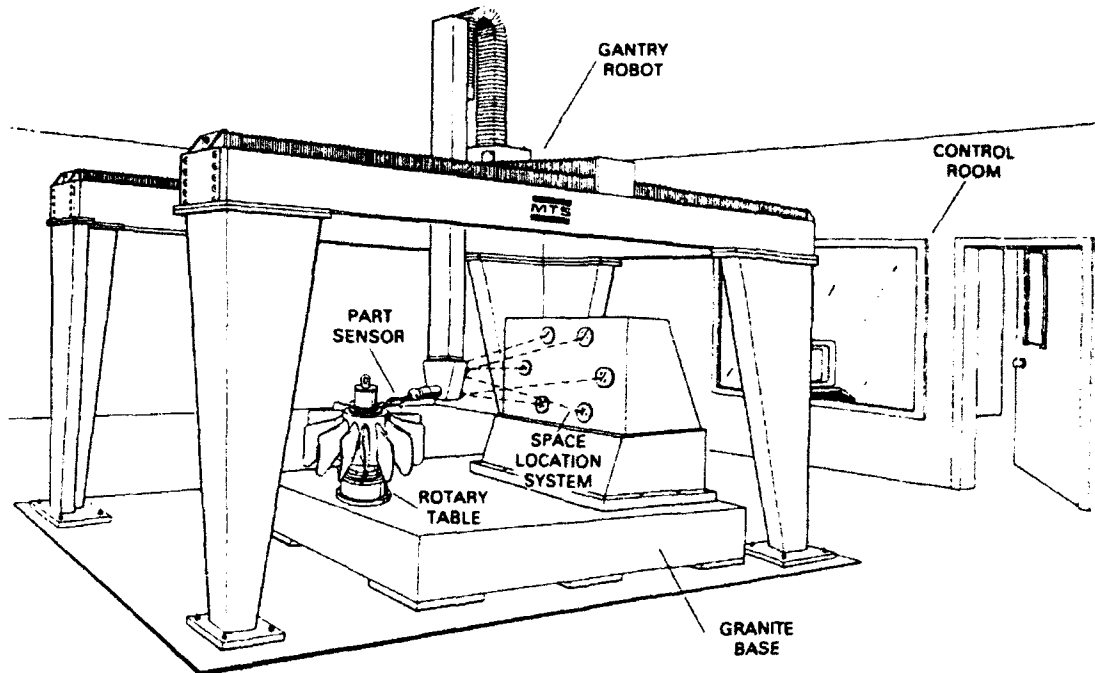


Figure 29. Chesapeake Laser's CMS-1000 Space Location System installed on the Intelligent Robotic Inspection System built for the Navy by MTS Systems Corporation (Courtesy MTS Systems Corporation).

To get positional accuracy of 0.001 inch at a distance of 10 feet using a conventional angle-measuring triangulation scheme requires an angular measurement accuracy of 1.7 seconds of arc. Experience in the optical instrumentation industry has shown such angular precision is not practical for distances over 10 feet, regardless of the precision of the shaft encoder used. The angular error is largely due to servo-loop tracking error (± 5 seconds of arc), atmospheric turbulence and gradient index effects due to temperature variations (± 10 seconds of arc), laser pointing inaccuracies (± 2 seconds of arc), and laser spot position uncertainty on the tracking mirror (± 2 seconds of arc).

Instead of measuring angles, the CMS-1000 uses a system of three tracking interferometers to measure distance to a special retroreflector via trilateration techniques. Such a system is inherently more accurate than any technique that incorporates angle measurement for the reasons mentioned above. When angular measurements are used, position errors appear as $r d\theta$, where r is the radial distance from the tracker to the retroreflector, and $d\theta$ is the angular error. For example, an angular error of 20 seconds of arc over 10 feet shows up as a position error of 1 micro-inch.

An improved system, the CMS-2000, combines laser interferometry with servo-controlled trackers to measure movement with submicron resolution at ranges up to 35 feet. The CMS-2000 was initially designed for use by the U.S. Air Force as part of the Strategic Defense Initiative. In this particular application, the stationary interferometer tracks a retroreflector mounted on a hovering rocket. The data obtained by the CMS-2000 is then used to check the vehicle's on-board control systems (Chesapeake Laser Systems Incorporated, 1991b). This application was unsuccessful due to the excessive heat and dust present in the hanger during launch.

A third-generation CMS-3000 system is currently being installed for Northrup Corporation at the Palmdale, CA site, for use as a precision-measurement device in conjunction with the B-2 bomber. The CMS-3000 also uses the trilateration scheme, wherein no angles are measured, only distances (i.e., r_1 , r_2 , and r_3). The position error shows up as

$$\text{error} = r (1 - \cos d\theta) = r d\theta^2,$$

which is orders of magnitude smaller than $r d\theta$.

Selected Specifications:

Ranging Technique	Interferometry
Range	35 feet
Resolution	Submicron
Accuracy	10 micrometer in 3 meter cube
Light source	HeNe laser
Update rate	50 Hz (CMS-1000) 100 Hz (CMS-2000)
Size	23 by 23 by 56 centimeters
Power	115 volts AC
Weight	27 kilograms

Point of Contact:

Jim Shaw
 Chesapeake Laser Systems, Inc.
 4473 Forbes Blvd.
 Lanham, MD 20706-4354
 (301) 459-7977

3.1.15 Odetics Scanning Laser Imaging System

Odetics, Inc., Anaheim, CA, recognized the need for an adaptive and versatile vision system for mobile robot navigation in the early '80s while developing ODEX 1, a six-legged walking robot. The ensuing 3-year research effort resulted in a scanning laser rangefinder capable of producing three-dimensional images of an observed scene. The system determines the distance to individual points by phase-shift measurement, constructing range pictures by panning and tilting the sensor across the field of view. This technique was selected over alternatives including acoustic ranging, stereo vision, and structured light triangulation because of the inherent accuracy, fast update rate, and simplified interface to robotic systems.

The imaging system consists of two major subelements: the scan unit and the electronics unit (figure 30). The scan unit houses the laser source, the photodetector and the scanning mechanism. The laser source is a CW, gallium aluminum arsenide (GaAlAs) laser diode emitting at a wavelength of 820 nanometers. The power output is adjustable under software control between 1 to 50 milliwatts. Detection of the returned energy is achieved through use of an avalanche photodiode whose output is routed to the phase-measuring electronics.

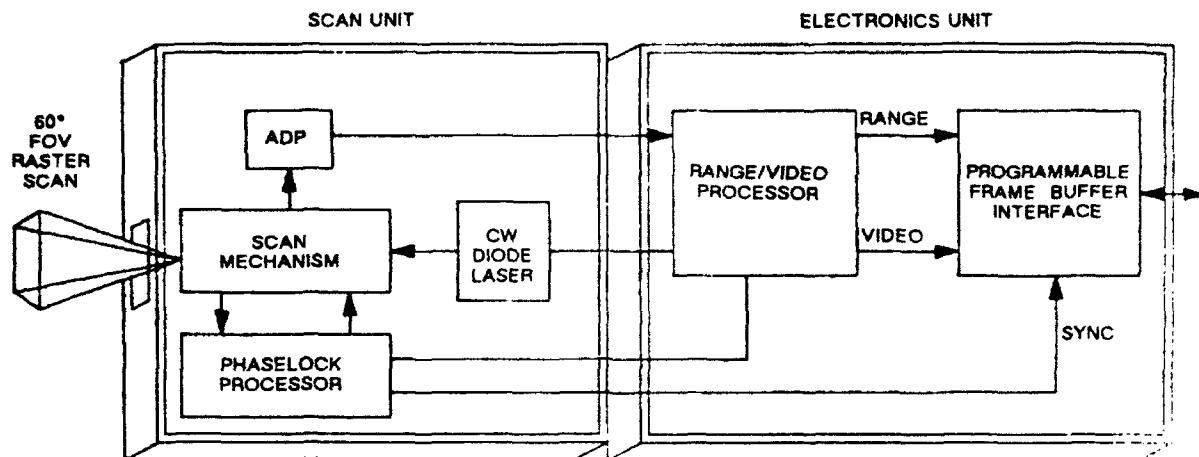


Figure 30. Block diagram of Odetics Scanning Laser Rangefinder (Courtesy Odetics, Incorporated).

The scanning hardware consists of a rotating polygonal mirror that pans the laser beam across the scene, and a planar mirror whose back-and-forth nodding motion tilts the beam for a realizable field of view of 60 degrees in azimuth and 60 degrees in elevation. The scanning sequence follows a raster-scan pattern, and can illuminate and detect an array of 128 by 128 pixels at a frame rate of 1.2 Hz (835 milliseconds per frame.)

The second subelement, the electronics unit, contains the range calculating and video processor as well as a programmable frame buffer interface. The range and video processor is responsible for controlling the laser transmission, the activation of the scanning mechanism, the detection of the returning energy, and the calculation of range values. Distance is calculated through a proprietary Odetics phase-detection scheme, reported to be high-speed, fully digital, and selfcalibrating with a high signal-to-noise ratio. The minimum observable range is 1.5 feet, while the maximum range without ambiguity due to phase shifts greater than 360 degrees is 30.74 feet.

For each pixel, the processor outputs a range value and a video reflectance value. The video data are equivalent to that obtained from a standard black and white television camera, except that interference due to ambient light and shadowing effects are eliminated. The format for these outputs is a 16-bit data word consisting of the range value in either 8 or 9 bits, and the video information in either 8 or 7 bits, respectively. The resulting range resolution for the system is 1.44 inches for the 8-bit format, and 0.72 inch with 9 bits.

The buffer interface provides interim storage of the data and can execute single word or whole block direct memory access transfers to external host controllers under program control. Information can also be routed directly to a host without being held in the buffer. Currently, the interface is designed to support VAX, VME-Bus, Multibus, and IBM-PC/AT equipment.

Selected Specifications:

Ranging technique	Phase shift measurement
Field of view	60 degrees (horizontal), 60 degrees (vertical)
Frame size	128 by 128 pixels
Frame rate	835 milliseconds/frame
Range resolution	1.44 inches (8 bit), 0.72 inch (9 bit)
Ambiguity range	30.74 feet
Minimum range	1.5 feet
Light source	820 nanometer GaAlAs laser diode
Enclosure	9 by 9 by 9.25 inches (scan unit) 7 by 7 by 2.5 inches (electronics unit)
Weight	28 pounds (scan unit), 3 pounds (electronics unit)
Power requirements	28 volts DC at 2 amps

Point of Contact:

Susan Boltinghouse
Odetics, Inc.
1515 South Manchester Avenue
Anaheim, CA 92802-2907
(714) 758-0300

3.1.16 ESP ORS-1 Optical Ranging System

A simple, low-cost near-infrared rangefinder (figure 31) was developed in 1989 by ESP Technologies, Inc., Lawrenceville, NJ, for use in autonomous robot cart navigation in factories and similar environments. A 2-milliwatt, 0.82- μm LED source is 100 percent modulated at 5-MHz and used to form a collimated 1-inch diameter transmit beam that is unconditionally eye-safe. Returning scattered radiation is focused by a 4-inch diameter coaxial Fresnel lens onto the photodetector. The system provides three outputs: range and angle of the target, and an automatic gain control (AGC) signal (Miller & Wagner, 1987).

Range is determined from the phase shift between the transmitted and received signals; range resolution at 20 feet is approximately 2.5 inches. Radial and angular resolution correspond to approximately 1 inch at a range of 5 feet, with an overall bandwidth of 1 KHz. The ORS-1 AGC output signal is inversely proportional to the received signal strength and provides information about a target's near-infrared reflectivity, warning against insufficient or excessive signal return (ESP Technologies, Incorporated, 1992). Usable range results are produced only when the corresponding gain signal is within a predetermined operating range. Use of a rotating mirror, mounted at 45 degrees to the optical axis, provides 360-degree polar-coordinate coverage. It is driven at 1 to 2 revolutions per second by a motor fitted with an integral incremental encoder and an optical indexing sensor that signals the completion of each revolution. The system is capable of simultaneous operation as a wideband optical communication receiver (Miller & Wagner, 1987).

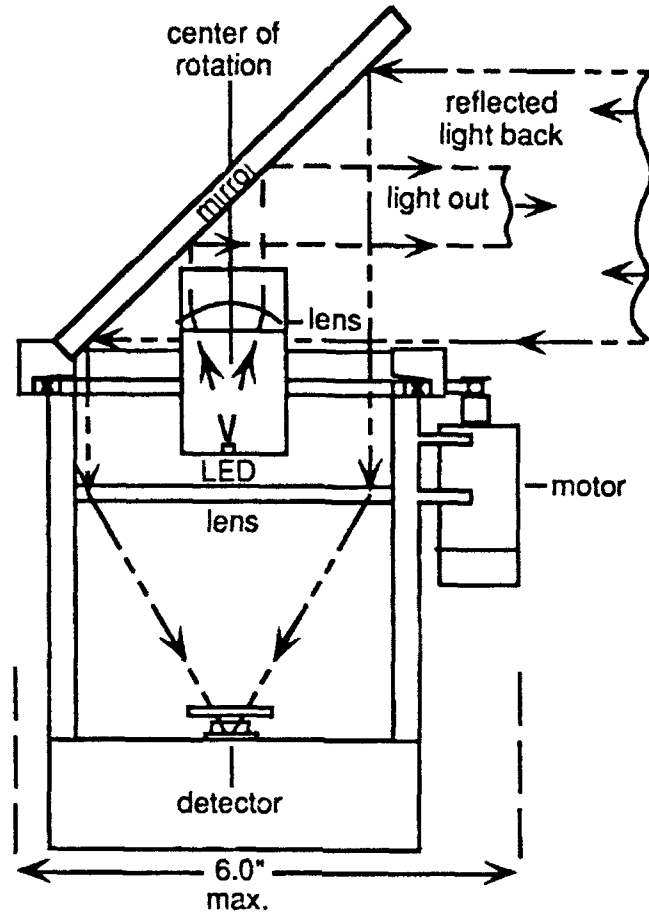


Figure 31. Schematic block diagram of ESP's ORS-1 Optical Ranging System (ESP Technologies Incorporated, 1992).

A representative ranger scan taken in a laboratory environment is shown in figure 32. The ranger is mounted on the robot cart and located at the (0.0) position, marked by a cross in the center of the plot. The data collection corresponded to a single mirror rotation taking approximately 1 second. The display computer program employed connects adjacent data points with straight line segments. The reason for the absence of any data points in regions such as that labelled AB in the figure is that in such ranges the signal is outside the AGC window; therefore, no data are accumulated. All of the objects in the room were found to correspond accurately to their positions as indicated by the ranger (Miller & Wagner, 1987).

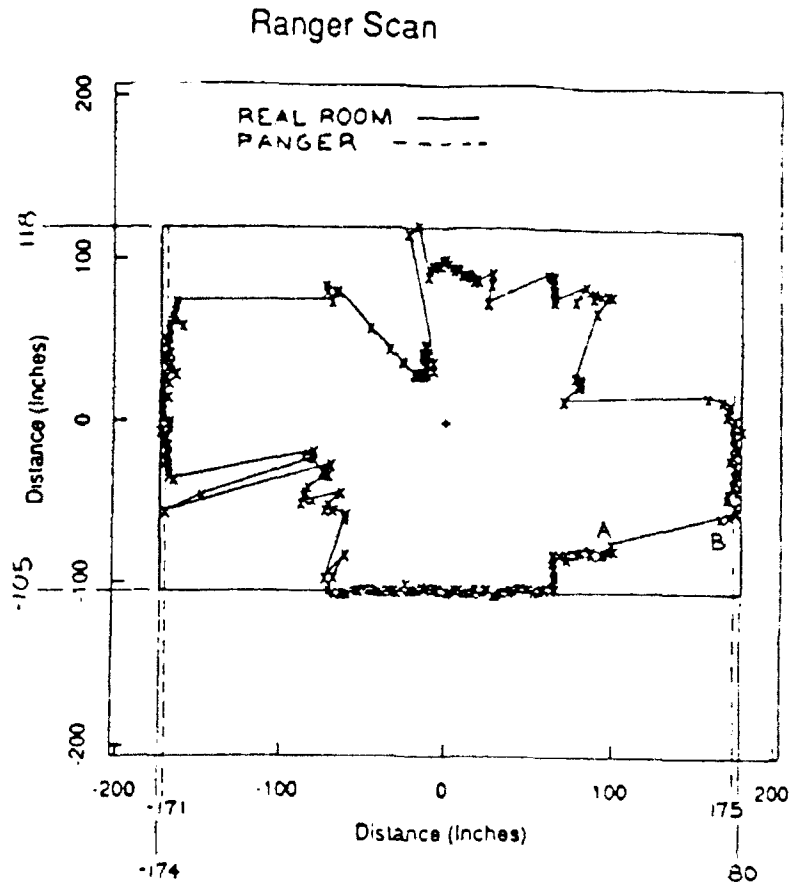


Figure 32. A representative ranger scan taken in a laboratory environment (ESP Technologies Incorporated, 1992).

Selected Specifications:

Ranging technique	Phase-shift measurement
Maximum range	20 feet
Minimum range	2 feet
Resolution	1 inch at 5 feet, 2.5 inches at 20 feet
Accuracy	< 6 inches typically
AGC output	1 to 5 volts
Light source	820-nanometer near-infrared LED
Output power	2 milliwatts

Output beamwidth	1-inch diameter
Scan rate	1 to 2 revolutions per second
Quantization	~1000 points/revolution
Power	12 volts DC at 2 amps
Dimensions	6 by 6 by 12 inches

Point of Contact:

Susan Cox
 ESP Technologies, Inc.
 21 Le Parc Drive
 Lawrenceville, NJ 06848-5135
 (609) 275-0356

3.1.17 SEO Scanning Laser Rangefinder

Figure 33 shows the Scanning Laser Rangefinder manufactured by Schwartz Electro-Optics, Inc., Orlando, FL. Originally developed for submunition sensor research, this single-channel rangefinder is currently installed aboard a remotely piloted vehicle (RPV) (Schwartz Electro-Optics, 1991a).

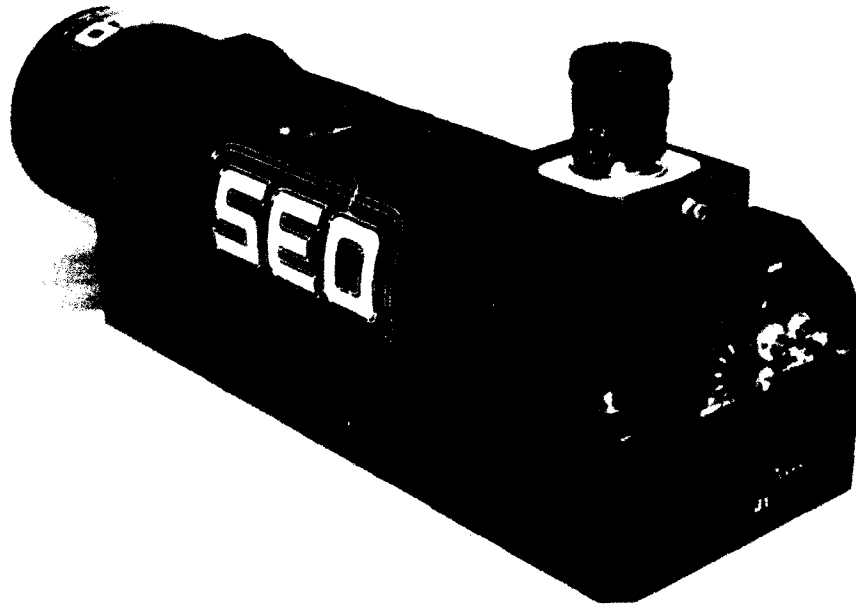


Figure 33. Schwartz Electro-Optics Scanning Laser Rangefinder
 (Schwartz Electro-Optics Incorporated, 1991a).

For this application, the sensor is positioned so the velocity of the RPV is perpendicular to the scan plane, since three-dimensional target profiles are required. In a second application, the rangefinder was used by Carnegie Mellon University's Field Robotic Center as a terrain mapping sensor onboard their unmanned autonomous vehicles.

Selected Specifications:

Ranging technique Phase shift measurement

Maximum range	256 meters
Minimum range	10 meters
Accuracy	±0.5 feet
Data rate	500 Kbps
Scan angle	±30 degrees
Scan rate	24.5 to 30.3 KHz
Samples per scan	175
Size	5-inch diameter, 17.52 inch length
Weight	11.75 pounds
Input voltage	8–25 VDC

Point of Contact:

Terry Meyers
 Schwartz Electro-Optics, Inc.
 3404 N. Orange Blossom Trail
 Orlando, FL 32804-3411
 (407) 298-1802

3.1.18 SEO LRF-X Laser Rangefinder Series

The LRF-X series rangefinder (figure 34) manufactured by Schwartz Electro-Optics, Inc., Orlando, FL, features a compact size, high-speed processing, and an ability to acquire range information from most surfaces. The following specifications detail the sensor's performance (Schwartz Electro-Optics, 1991b).



Figure 34. Schwartz Electro-Optics LRF-X Laser Rangefinder
 (Courtesy Schwartz Electro-Optics Incorporated, 1991b).

Selected Specifications:

Maximum range	10 to 300 meters
Minimum range	2 to 5 meters (5% reflectivity, Lambertian target)
Accuracy	±0.3 meter
Range jitter	±11.25 centimeters
Analog output	0 to 5.11 volts (0 to 30 meters)
Digital output	RS-232
Size	3.5-inch diameter, 7 inch length
Power	8 to 24 volts DC

Point of Contact:

Terry Meyers
Schwartz Electro-Optics, Inc.
3404 N. Orange Blossom Trail
Orlando, FL 32804-3411
(407) 298-1802

3.1.19 SEO Multi-Channel Laser Imaging System

Schwartz Electro-Optics, Inc., Orlando, FL, developed the Multi-Channel Imaging System for the U.S. Air Force (Schwartz Electro-Optics, 1991c), a submunition sensor array comprised of 25 laser-rangefinding elements whose transmit and return beams are reflected from a rotating mirror. The acquired three-dimensional images (figure 35) are processed using realtime algorithms developed by SEO, and identification and location information extracted.

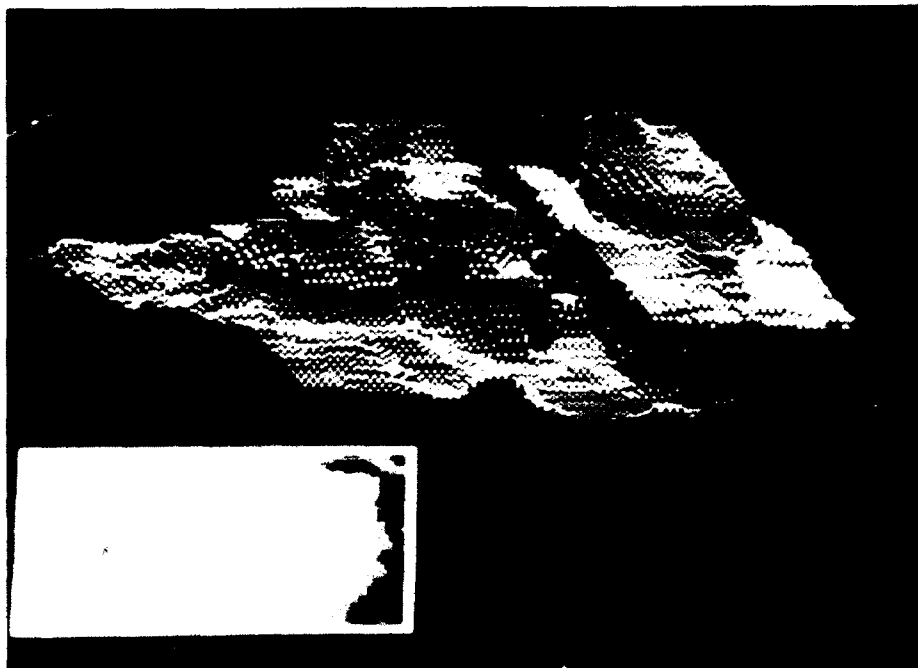


Figure 35. Schwartz Electro-Optics Multi-Channel three-dimensional image of a tank next to a bush (Schwartz Electro-Optics Incorporated, 1991c).

Selected Specifications:

Maximum range	1500 feet
Minimum range	50 feet (10-percent diffuse Lambertian target)
Static accuracy	± 0.5 foot at minimum range +1 to 2 foot at maximum range
Range resolution	0.4 feet
Range jitter	0.25 feet at minimum range 1 foot at maximum range
Field of regard	4 by 10 degrees
Pixel array	25 by 60
Frame rate	30 Hz
Weight	24 pounds
Dimensions	13 by 13 by 9 inches

Point of Contact:

Aaron Penkacik
Schwartz Electro-Optics, Inc.
3404 N. Orange Blossom Trail
Orlando, FL 32804-3411
(407) 298-1802

3.1.20 Optech G150 Laser Rangefinder

The Model G150 made by Optech Systems, Toronto, Canada, is a rugged, compact pulsed-laser rangefinder that measures distances out to 100 meters with an accuracy of 5 centimeters (Optech Systems Corporation, 1992). Maximum range depends on target reflectance, atmospheric attenuation, and background solar radiation. Range and accuracy values quoted are typical for diffuse targets of 20-percent Lambertian reflectance in clear weather.

Measurements can be initiated either by pressing a push-button switch on the unit, or by an external trigger from a computer or control circuit. A near-infrared laser diode generates an eyesafe (Class I) optical pulse that is reflected by the target surface; a precision counter measures the round-trip time of flight. By employing a high pulse repetition rate in conjunction with averaging to reduce random errors, a resolution of 1 centimeter is achieved. Both 0- to 5-volt and 4- to 20-milliamp analog outputs are available, as well as an RS-232 digital output.

Selected Specifications:

Ranging technique	Time of flight
Range	0.2 to > 100 meters
Resolution	1 centimeter
Size	7 by 11.5 by 17.5 centimeters
Weight	2.6 pounds
Power	12 volts DC at 0.75 amp
Update rate	2 Hz
Wavelength	890 nanometers
Beamwidth	5 milliradians

Point of Contact:

Optech Systems Corporation Code 152
701 Petrolla Road
Downsview (Toronto), Ontario
Canada M3J 2N6
(416) 661-5904

3.1.21 Laser Systems Devices MR-101 Missile Rangefinder

The MR-101 Missile Rangefinder manufactured by Laser Systems Devices, Alexandria, VA, is a MIL-qualified eyesafe device that is capable of ranging out to 350 meters (Laser Systems Devices, 1992). Designed specifically to fit inside a missile head, the MR-101 weighs less than 250 grams, occupies a volume of approximately 100 cubic centimeters, and consumes less than half a watt. An RS-232 serial output is provided.

Selected Specifications:

Range	350 meters
Resolution	60 centimeters
Size	100-cubic centimeters (modular)
Weight	250 grams
Update rate	100 Hz
Wavelength	904 nanometers

Point of Contact:

V. J. Corcoran
Laser Systems Devices
5645R General Washington Drive
Alexandria, VA 22312-2403
(703) 642-5758

3.1.22 IBEO Pulsar Survey Series Rangefinders

The PS 2 and PS 10 systems manufactured by IBEO, Hamburg, Germany, are high-resolution pulsed near-infrared laser ranging sensors designed for the short range of 3 and 15 meters, respectively (Hoskin Scientific Limited, 1992b). Both sensors are eyesafe (Class I), and can be optionally equipped with an integrated HeNe red-laser marker to visually indicate the target point.

The PS 50 and PS 100 are intended for ranges up to 50 and 100 meters, respectively, and incorporate a built-in 7 X 20 telescope (Hoskin Scientific Limited, 1992c). An optional red-laser marker can be ordered, which replaces the telescope. Maximum range is increased to over 15 kilometers with the use of cooperative targets (retroreflectors). The PS 50 and PS 100 are precision eyesafe sensors designed to withstand operation in rugged field and industrial environments.

The reflection from diffuse surfaces of short laser-light pulses emitted by the internal laser diode is detected, and round trip time of flight converted to distance. A programmable number of single-pulse measurements are then averaged to eliminate faulty returns for improved accuracy. The elapsed time between transmission and detection of the reflected energy is measured in pico-

seconds, which provides millimeter accuracies. Output is via an LCD dot-matrix display and configurable RS-232 interface.

The LADAR series (Hoskin Scientific Limited, 1992a) of scanning rangefinders developed by IBEO locates surrounding objects with the same eyesafe laser components used in the company's PS line. LADAR instruments contain rotating mirrors that move the beam across a plane (two-dimensional scans) or through a prism angle (three-dimensional scans). The scans represent digital pictures of the surrounding environment; the range measurement information is available through an RS-232 link to an external computer for further processing and analysis.

The basic modules for the LADAR series are as follows:

- IBEO distance sensor of the PS series,
- Scanner for directional control of the beam,
- Control processor for measuring process and scanner,
- Evaluation processor for further analysis of data.

The LADAR 2D system employs a mechanical scanning mirror that rotates the beam at constant speed in a single horizontal plane. A new profile of the measured area, consisting of up to 4600 measurements per second, is updated every 8 seconds. The LADAR 2D LINEAR version is a high-speed scanner optimized for operation over a limited field of view (3 or 6 degrees), and can produce the same images as the LADAR 2D, but much faster. An innovative mirrorless scanning technology employed in the LADAR 2D LINEAR makes possible scan speeds of up to 100 scans per second, with 30-range measurements per scan.

The LADAR 3D is a scanning laser rangefinder that produces three-dimensional images based on distance and angle coordinates relative to the sensor. The measuring beam is mechanically deflected in azimuth and elevation by a pair of rotating mirrors. Every point thus measured is precisely located in a three-dimensional coordinate system. As with the other LADAR systems, the LADAR 3D sensor can be configured to various distances and scanning angles. Horizontal profiles of the measured surfaces are built up onto one another until the desired image is created.

Selected Specifications (PS Series only):

Ranging technique	Time of flight	
Range	PS2	0.3 to 3.5 meters
	PS 10	0.6 to 15 meters
	PS 50	50 meters
	PS 100	100 meters
Resolution	1 millimeter	
Accuracy	3 to 20 millimeters	
Size	234 by 115 by 98 millimeters	
Weight	1.7 kilograms	
Power	5 volts DC at 1.3 amps	
Update rate	PS 2	100 Hz
	PS 10	100 Hz
	PS 50	120 Hz

3.1.24 Banner Near-Infrared Proximity Sensors

Banner Engineering, Minneapolis, MN, offers a full line of modular near-infrared proximity sensors of the break-beam, reflective, and diffuse type (see section 2.1.1). Effective ranges vary from a few inches out to 6 or 7 feet; robotic applications include floor sensing and collision avoidance (Everett, 1985a, 1985b). Full details and application notes are provided in their catalog (Banner Engineering Corporation, 1993a) and applications guide (Banner Engineering Corporation, 1993b).

Point of Contact:

Floyd Schneider
Banner Engineering Corporation
9714 10th Ave N.
Minneapolis, MN 55441-5019
(612) 544-3164

3.1.25 TRC LABMATE Proximity Sensor Subsystem

Originally introduced in 1987, and updated in 1988, Transitions Research Corporation, Danbury, CT, offers a Proximity Subsystem using Polaroid ultrasonic rangefinders and Banner near-infrared diffuse-type proximity sensors (Transitions Research Company, undated). The basic system consists of a central processing unit (CPU) and interface card, each capable of handling eight ultrasonic and eight infrared sensors. The CPU can control up to three interface cards. Typical ultrasonic ranges are from 9 inches to 35 feet, with an accuracy of approximately 0.36 inch/yard under ideal conditions. The near-infrared proximity sensors yield Lambertian-surface detections up to 30 inches away, although for specular and retroreflective surfaces, detections can occur at ranges up to 20 feet. Sensor groups and firing priorities can be set with a software protocol similar to LABMATE.

Selected Specifications:

Ranging technique	Ultrasonic time of flight
Range	6 inches to 36 feet
Resolution	1 percent
Size	<ul style="list-style-type: none">• One proximity board, one proximity I/O controller: 4.5 by 6.5 by 2.6 inches• With up to three proximity boards: 4.5 by 6.5 by 5.0 inches• Three proximity boards with TRCNET: 4.5 by 6.5 by 7.25 inches
Weight	0.75 to 2.5 pounds
Power	+5 and +12 volts at 250 milliamps for one board (5 volts @ 50 milliamps and 12 volts @ 250 milliamps for each additional board.)
Update rate	Programmable, depending on maximum range

Point of Contact:

Stuart Lob
Transitions Research Corporation
15 Great Pasture Rd
Danbury, CT 06610-8153
(203) 798-8988

3.1.26 TRC Strobed Light Triangulation System

Transitions Research Corporation, Danbury, CT, developed a structured light system to detect and measure the position of objects lying within or adjacent to the forward path of their HELPMATE mobile platform (Evans, King & Weiman, 1990; King, 1990). The system (figure 36) is comprised of a CCD camera having a rectangular field of view, and two near-infrared strobes operating on a low-duty cycle (3 Hz each). To enhance the received signal-to-noise ratio, TRC employs a bandpass filter at the camera end, thereby minimizing noise contributions from outside the near-infrared spectrum. By performing a pixel-by-pixel subtraction of a nonflashed image from a flashed image, that portion of the scene resulting from reflected radiation is emphasized. The reflected-light planes are viewed across the horizontal pixel lines of the camera. An object approaching the mobile platform first appears at the top of the field of view and then appears to move down the image plane as the distance closes. In this way, each pixel in the image plane corresponds to a predetermined range and bearing derived through simple triangulation.

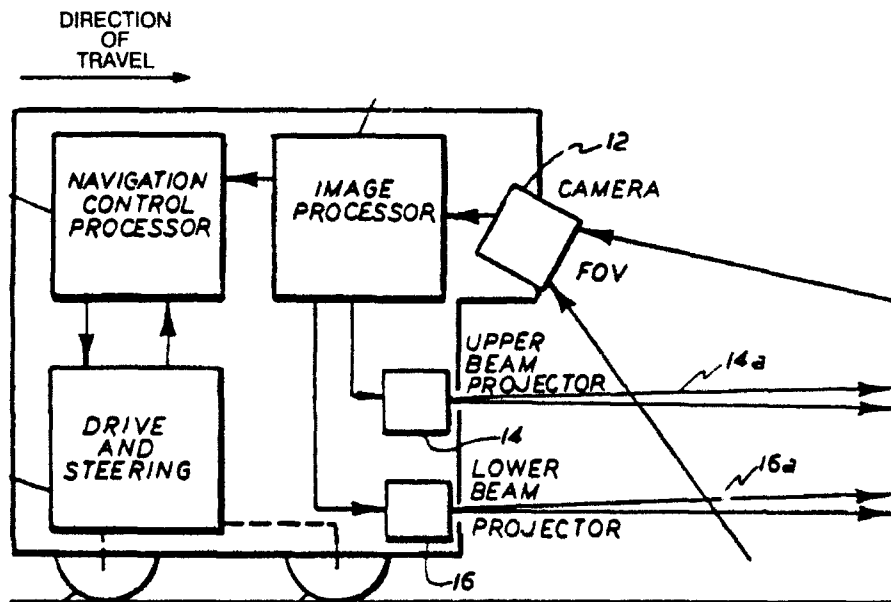


Figure 36. A block diagram of Transitions Research Company's Strobed Light Triangulation System mounted on the HELPMATE mobile platform (Courtesy Transitions Research Corporation).

To ensure realtime computation, TRC has implemented a thresholded algorithm that uses every sixth pixel in an image of 512 x 480 pixels. Once the image is processed, the range and bearing information must be associated with the surrounding environment to facilitate an intelligent avoidance maneuver. Using a predefined two-dimensional occupancy grid, range and bearing information of a potential obstacle is associated with a measure-of-confidence value for each grid cell in the floor map. The level of confidence increases as successive observations continue to detect a presence at that same grid location. Once the presence of an obstacle is established, the platform must navigate around it and continue to its original destination.

Selected Specifications:

Ranging technique Active triangulation

Range 2 meters

Resolution Range: 1 to 3 inches

Bearing: 2 degrees

Size AT Computer, Frame Grabber, Camera, and 2 Strobes

Weight 10 pounds

Power 5 volts at 3 amps
12 volts at 0.25 amp
-12 volts at 0.25 amp
24 volts at 0.8 amp

Update rate 300 milliseconds

Wavelength (frequency) >700 nanometers

Beamwidth 25 mm high, 60 degree sweep

Point of Contact:

Steven J. King
Transitions Research Corporation
Shelter Rock Lane
Danbury, CT 06810
(203) 798-8988

3.1.27 TRC Light Direction and Ranging System, LIDAR

Transitions Research Corporation, Danbury, CT, has developed a low-cost light direction and ranging system (LIDAR) for use on mobile robot platforms. The sensors are useful for detecting obstacles in the vicinity of the robot and for estimating the robot's position from local landmarks or from beacons in the environment. The LIDAR sensor uses an eye-safe LED to project a beam of near-infrared light, which is intensity modulated at 2 or 5 MHz. A large area lens gathers the light returned from an object, then sensitive circuitry compares the phase of the 2 or 5 MHz modulation of the returned light with that of the transmitted light. The result is a measure of the round-trip distance to the illuminated object. Two voltages, one representing range and the other representing signal strength, are fed to a controlling microprocessor (in this case a 68HC11) to be converted into actual range units. The system is based on a prototype device developed first by AT&T. Significant improvements have been made in signal strength, signal-to-noise-ratio, and increased range linearity with a lower phase-shift AGC stage. Additionally, both one-dimensional and two-dimensional scanning capabilities have been added.

Two versions of the sensor have been completed. The first version, useful for large area navigation, scans the environment for retroflective beacons at a modulation frequency of 2 MHz. TRC reports that retroflective targets can be detected at a range of 25 meters with a range resolution of 120 mm and an angular resolution of 0.125 degree. The system employs a gold front-surfaced mirror mounted at 45 degrees on a scanning platform. The platform scan rate is variable from 0 to 4 Hz. The system can sense multiple retroflective targets in the scene that can be used to determine the robot's position and route. Multiple targets increase the accuracy of the system; 4 beacons can increase the positional accuracy to 50 mm.

The second version of the sensor is used for close range detection, and uses a 5-MHz modulation. It can detect white objects at 10 meters and darker objects at 7 meters. The range resolution is typically 75 mm. This system employs a 2-D scanning mechanism. A mirror is mounted so that it rotates and nods simultaneously under the power of a single motor. The scanner rotates 360 degrees around at 10 Hz. It nods from 0 down to 45 degrees, then back up to 0 degree at 1 Hz. The effect is to create a protective spiral of detection around the robot. The angular resolution is approximately 0.5 degree.

Selected Specifications:

	2 MHz CW Phase-shift	5 MHz CW Phase-shift
Ranging technique	25 meters	10 meters
Range	120 mm	75 mm
Range Resolution	360 degrees horizontal	360 degrees horizontal 45 degrees vertical
Field of view	0.125 degree	0.5 degree
Angular Resolution	4 by 4 by 4 inches	5 by 5 by 7 inches
Scan Unit Size	6 by 6 by 6 inches	6 by 6 by 6 inches
Electronics Size	5 pounds	5 pounds
Weight	5 volts at 0.1 amp	5 volts at 0.1 amp
Power	12 volts at 0.5 amp	12 volts at 0.5 amp
Wavelength	850 nanometers	850 nanometers

Point of Contact:

Steven J. King
 Transitions Research Corporation
 Shelter Rock Lane
 Danbury, CT 06810
 (203) 798-8988

3.1.28 NOMADIC Sensus 300 Infrared Proximity System

The Sensus 300 by NOMADIC Technologies, Inc., Palo Alto, CA, is a 16-channel near-infrared ranging system capable of generating range information out to 36 inches (Nomadic Technologies Incorporated, 1991a). Each of the 16 sensor units that make up the Sensus 300 contains an LED emitter and photodiode detector; full 360-degree coverage is possible when configured as shown in figure 37.

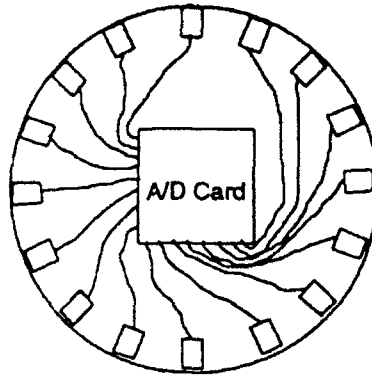


Figure 37. The Sensus 300 configured for 360-degree coverage (Courtesy NOMADIC Technologies Incorporated).

Range is estimated from the intensity of reflected energy as sensed by the detector. A voltage-controlled oscillator (VCO) generates a square-wave output with frequency proportional to the input voltage; the greater the intensity of light at the detector, the higher the output frequency of the VCO. A *calibrate* line is used to control the on/off state of the emitter, a feature useful in quantifying ambient noise.

The Sensus 300 is featured onboard the Nomadic Technologies NOMAD 100 series mobile robot (Nomadic Technologies Incorporated, 1991b).

Selected Specifications:

Ranging technique	Return signal intensity
Maximum range	36 inches
Accuracy	varies with surface topography
Power	12 volts DC at 500 milliamperes

Point of Contact:

Jim Slater
 Nomadic Technologies, inc.
 858 La Para Ave
 Palo Alto, CA 94306-2647
 (415) 493-7700

3.1.29 NOMADIC Sensus 500 Vision System

The Sensus 500 Vision System uses a near-infrared structured light source and a 510- by 490-pixel CCD camera for image generation in determining target range through triangulation. The collimated output of a 10-milliwatt 780-nanometer laser is passed through a cylindrical lens to form a horizontal plane of light. The camera, as illustrated in figure 38, is situated above and at an angle to the emitted light plane. Any target intersecting the horizontal light plane is seen by the camera as a light stripe segment, and its displaced scan-line position provides range information.

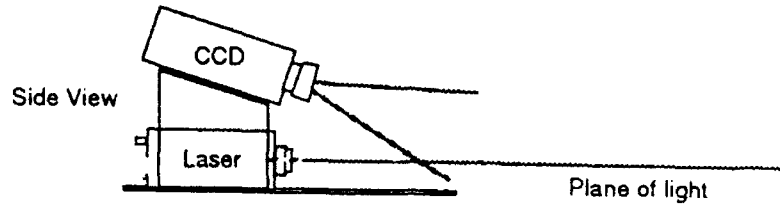


Figure 38. The Sensus 500 light vision system
(Courtesy NOMADIC Technologies Incorporated).

This vision system advertises a 5-inch range resolution at a maximum range of 120 inches. The resolution improves nonlinearly as range approaches the minimum measurable value of 18 inches. The CCD camera operates at 480 scan lines per frame and 30 frames per second. Data are written directly to dual-ported RAM output at 57.6 kbytes per second. A video post-processing unit has been incorporated to reduce each scan line of data to four bytes:

1. Pixel location having the most incident light energy.
2. Gray-scale illumination magnitude.
3. First pixel to rise above a user defined threshold.
4. Last pixel to fall below this same threshold.

The Sensus 500 is available in both ISA (PC) and VME bus-compatible versions (Nomadic Technologies Incorporated, 1991c).

Selected Specifications:

Ranging technique	Active triangulation
Maximum range	120 inches
Minimum range	18 inches minimum
Resolution	5 inches at maximum range
Power	12 volts DC at 1 amp
Light source	780-nanometer laser diode
Scan rate	480 scan lines per frame 30 frames per second

Point of Contact:

Jim Slater
NOMADIC Technologies, Inc.
858 La Para Ave
Palo Alto, CA 94306
(415) 493-7700

3.1.30 VRSS Automotive Collision Avoidance Radar

One of the first practical short-range collision avoidance radar systems for use on ground vehicles was developed by Vehicle Radar Safety Systems (VRSS) of Mt. Clemens, MI (Vehicle Radar Safety Systems, Incorporated, 1983). This specially modified Doppler radar unit is

intended to alert automobile drivers to potentially dangerous situations. A grill-mounted miniaturized microwave radar antenna sends out a unique narrow-beam signal that detects only those objects directly in the path of the vehicle, ignoring objects (such as road signs and parked cars) on either side. When the radar signal is reflected from a slower moving or stationary target, it is detected by the antenna and passed to an under-the-hood electronic signal processor.

The signal processor continuously computes the host vehicle speed and acceleration, distance to the target, its relative velocity and its acceleration. If these parameters collectively require the driver to take any corrective or precautionary action, a warning buzzer and signal light are activated on a special dashboard monitor. An *alert* signal lights up when an object or slower moving vehicle is detected in the path of the host vehicle. If the target range continues to decrease, and the system determines that a collision is possible, a *warning* light and buzzer signal the driver to respond accordingly. If range continues to decrease with no reduction in relative velocity, then a *danger* light illuminates indicating the need for immediate action.

A sophisticated filter in the signal processor provides for an optimum operating range for the system, based on the relative velocity between the vehicle and the perceived object. The response *window* corresponds to a calculated difference in speed of between 0.1 and 30 miles per hour (Vehicle Radar Safety Systems, Incorporated, 1983). If the speed differential exceeds 30 miles per hour, the filter circuit delays signals to the dashboard monitor. This helps to filter out false signals and signals that might otherwise be caused by approaching vehicles when passing another vehicle on a two-lane highway.

The VRSS collision warning system has been tested over a million miles of driving conditions in fog, rain, snow, and ice with good results. The present model was perfected in 1983 after 36 years of research, and approved by the FCC in 1985. Although aimed at the bus and trucking industries, the low-cost unit offers convincing proof that small, low-power radar systems offer a practical alternative to ultrasonic rangefinders for the collision avoidance needs of a mobile robot, particularly in outdoor scenarios.

Selected Specifications:

Unable to obtain from company.

Point of contact:

Charles Rashid
Vehicle Radar Safety Systems, Inc.
10 South Gratiot, Suite 303
Mt. Clemens, MI 48043-7903
(313) 463-7883

3.1.31 AM Sensors Microwave Range Sensors

AM Sensors, Incorporated, offers a variety of proximity, direction of motion, displacement, level and velocity sensors which cover numerous industrial applications. Their products include the MSM10500 series of microwave range sensors which provide noncontact position detection of metallic and non-metallic moving objects.

The MSM10500 range sensor provides continuous distance information, range-gated position indication and direction of motion. These range gates can be adjusted to any fraction of the

50-foot maximum detection area. The MSM10502 is either preset to sense objects moving toward or away from the sensor, and indicates distance as it passes through three range gates.

The microwave portion of the unit uses a Gunn diode transmitter, two microwave mixer diode receivers, and a varactor diode to vary the transmitted microwave frequency. The output of the oscillator is focused by a horn antenna into a beam and any object moving through this beam is detected.

The signal conditioning circuitry contains the power supply, amplifiers, comparator, and microcontroller to drive the oscillator and convert the detected outputs into useful control signals. The amount of averaging applied to each reading is adjustable so the user may choose between maximum noise immunity and minimum output response time. The power supply allows the module to operate with a wide range of input voltages, such as in automotive systems, and provide high electrical noise rejection.

The three range gates operate by determining the distance from a moving target to the sensor. When this target is moving inside a given range window, the corresponding output will turn on and remain on as long as the target is within this range, specified in normal environments to be accurate within 6 inches. This accuracy can be degraded if there are multiple targets moving in the range or if the target has low reflectivity. The point where a range gate will turn on for a given target is repeatable within 1 inch; worst case 2 inches.

The microwave based sensors manufactured by AM Sensors, Inc., do not constitute a safety or health hazard to operating personnel. Emissions from the sensors are below the 10 mW/cm² level specified in OSHA 1910.97, and the sensors meet the requirements of Massachusetts regulatory document 105 CMR for public safety. No additional shielding or protection is required to assure the safety of operating personnel.

Selected Specifications:

Ranging technique	FMCW
Range	50 feet
Resolution	6 inches (Depends on averaging)
Size	<ul style="list-style-type: none">• MSM10500: 6.5 by 6.5 by 4.25 inches• MSM10502: 4.25 by 4.25 by 3.5 inches
Weight	1 pound
Power	<ul style="list-style-type: none">• MSM10500: 10 to 16 volts DC at 150mA• MSM10502: 10 to 28 volts DC at 50mA
Range gates	<ul style="list-style-type: none">• MSM10500: Adjustable• MSM10502: Preset at 3, 5, and 10 feet
Wavelength (frequency)	10.525 GHz \pm 25MHz
Beamwidth	<ul style="list-style-type: none">• MSM10500: Wide or narrow beam option• MSM10502: Wide beam

Point of Contact

Chris Anne Wheeler
AM Sensors, Inc.
26 Keewaydin Drive
Salem, NH 03079-9857
(800) 289-2611 (603) 898-1543
Fax: (603) 898-1638

3.1.32 VORAD Vehicle Detection and Driver Alert System

VORAD Saftey Systems, Incorporated, a subsidiary of IVHS Technologies in San Diego, CA, has developed a high frequency radar system designed for use onboard a motor vehicle (Rose, 1992; Douglass, 1991). The 5- by 5-inch antenna, when mounted on the front grill of a vehicle, monitors speed and distance to other vehicles on the road. Located inside the vehicle is a control panel which uses a series of caution lights and audible beeps to alert the driver of potentially hazardous driving situations. As an optional feature, the Vehicular Onboard Radar (VORAD) Vehicle Detection and Driver Alert system offers blind-spot detection along the right-hand side of the vehicle. A standard recording feature stores 15 minutes of most recent historical data, to include steering, braking, and idle time.

Selected Specifications:

Maximum range	350 feet
Minimum range	1 foot
Size	8.1 by 6.7 by 5.1 inches
Weight	3.5 lbs
Power	12/24 volts, 20 watts nominal
Frequency	24.125 GHz

Point of Contact:

Don Murphy
VORAD Safety Systems, Inc.
10802 Willow Court
San Diego, CA 92127-2408
(619) 674-1450

3.1.33 Nissan Diesel Motor Company's Traffic Eye

Nissan Diesel Motor Company, an affiliate of Nissan Motor Company, is now marketing in Japan the Traffic Eye, a vehicular anticollision laser ranging system (McCosh, 1992). The Traffic Eye alerts the driver of a motor vehicle when it is approaching the vehicle ahead too quickly. The system consists of three components connected by fiber-optic cable: a near-infrared laser radar head fitted onto the front of the vehicle, a speed sensor connected to the transmission, and a display unit inside the cab.

Selected Specifications:

Unable to obtain specifications or a point of contact.

3.1.34 National Semiconductor's LM1812 Ultrasonic Transceiver

The LM1812 is a general purpose ultrasonic transceiver designed for use in a variety of ranging, sensing, and communications applications. The chip contains a pulse-modulated class C

transmitter, a high-gain receiver, a pulse modulation detector, and noise rejection circuitry. The chip's specifications (National Semiconductor Corporation, 1988) list the following features:

- One or two transducer operation
- Transducers interchangeable without realignment
- No external transistors
- Impulse noise rejection
- No heat sinking
- Detector output drives 1A peak load
- 12 watts peak transmit power

Two different types of ultrasonic transducers, electrostatic and piezoceramic, are commonly used with the LM1812 (Everett, 1982; Pletta et al., 1992). Electrostatic transducers transmit an outgoing signal and act as an electrostatic microphone to receive the reflected signal. Piezoceramic transducers are electrically similar to quartz crystals. Piezoceramic transducers are resonant at only two frequencies, the resonant and antiresonant frequencies. Transmission is most efficient at the resonant frequency while optimum receiving sensitivity occurs at the antiresonant frequency. In two transducer systems, the frequency of the transmit transducer is matched to the antiresonant frequency of the receiver. Most systems use a single transducer which the maximum echo sensitivity occurs at a frequency close to resonance.

Selected Specifications:

Ranging technique	Time of flight
Range	100 feet in water, 20 feet in air
Maximum frequency	325 KHz (typical)
Power	18 volts at 50 milliamps

Point of Contact:

National Semiconductor Corporation
2900 Semiconductor Drive
P.O. Box 58090
Santa Clara, CA 95052-8090
(408) 721-5000

3.2 UNDER DEVELOPMENT

3.2.1 FMC Ultrasonic Imaging Sensor

The Ultrasonic Imaging Sensor is an obstacle detection and collision avoidance system designed by the FMC Corporation, Santa Clara, CA, for their research involving autonomous vehicles. The device is a phased-array sonar system with four piezoelectric transmitters, and a linear array of 16 microphones (figure 39). The system functions as a direct-measure time-of-flight ranging device, where sound pulses are sent out and returning echoes detected from objects between 2 and 50 feet away. Most of the major sensing components are commercially available and the absence of moving parts makes the instrument highly rugged.

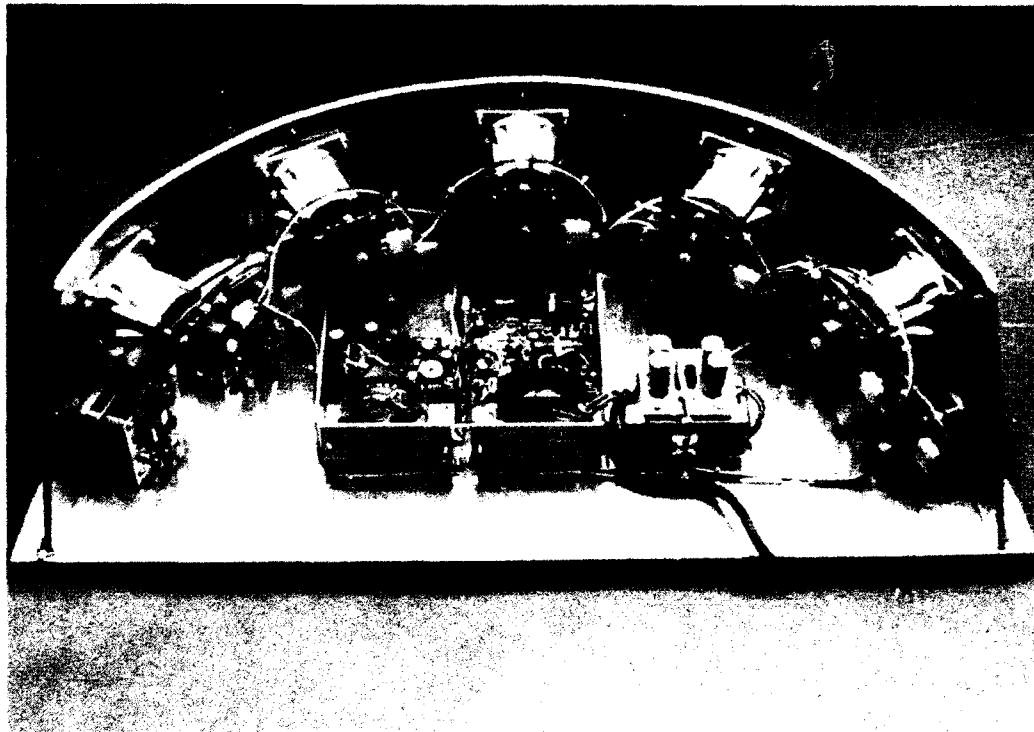


Figure 39. FMC Corporation's Ultrasonic Imaging Sensor
(Courtesy FMC Corporation).

The phased-array circuitry electronically scans the transmission across a 180-degree field of view, and creates a new terrain image consisting of 280 pixels every 200 milliseconds. The minimum object size seen by the sensor is 0.5 meter on a side. Angular resolution for the system is on the order of ± 11.25 degrees, while range resolution is ± 0.75 feet. Figure 40 shows the device mounted on an Army M113 armored personnel carrier used by FMC as their autonomous mobile testbed.

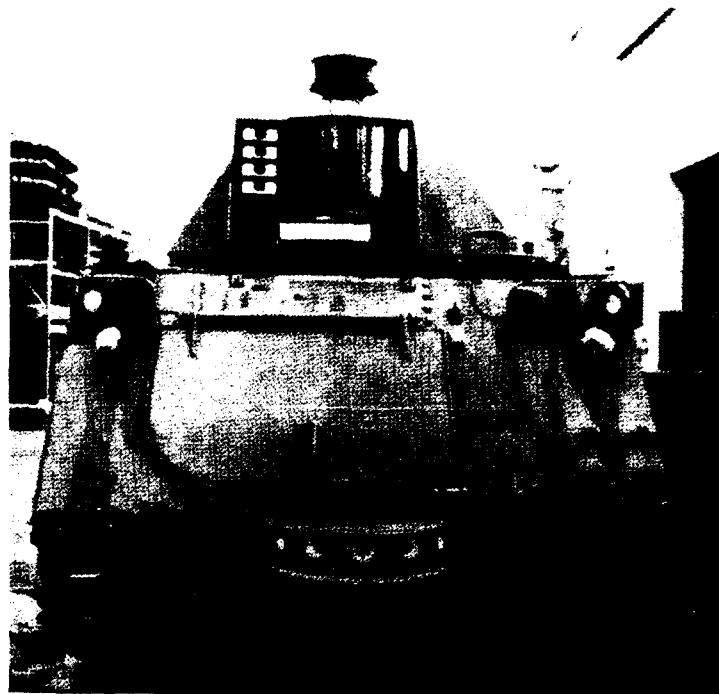


Figure 40. The imaging sensor mounted on an Army M113 armored personnel carrier used by FMC as an autonomous mobile testbed (Courtesy FMC Corporation).

The resultant terrain image data from the sensor are input into the autonomous navigation controller of the platform and used to help the vehicle avoid obstacles. The system has been effectively demonstrated at a speed of 5 miles per hour on the M-113. An eventual goal of 15 miles per hour is considered to be the operational limit because of excessive vehicle noise at higher velocities, which saturates the signal-processing electronics.

This device is an experimental unit only, and currently on loan to Carnegie-Mellon University for use onboard their NAVLAB robotic vehicle.

Selected Specifications:

Ranging techniques	Time of flight
Field of view	180 degrees
Maximum range	50 feet
Minimum range	2 feet
Range accuracy	± 0.75 feet
Angular resolution	± 11.25 degrees
Scan rate	280 pixels/200 milliseconds

Point of Contact:

Louis S. McTamanev
FMC Corporation
Corporate Technology Center
1205 Coleman Avenue, Box 580
Santa Clara, CA 95052-4368
(408) 289-3577

3.2.2 Honeywell Displaced Sensor Ranging Unit

Honeywell Visitronic has developed a prototype returned-signal-intensity (section 2.1.7) ranging system using a near-infrared LED source and displaced silicon detectors. Range measurements are possible from 0.5 to 2 meters, with a resolution of 6 millimeters at a distance of 1 meter. System response is less than 5 milliseconds. This prototype is packaged in an enclosure 51 by 51 by 150 millimeters with a weight of 0.65 kilograms.

The basic approach is to project a momentary pulse of near-infrared radiation onto the surface to be measured, and detect the reflected flux with two sensors that are displaced along the measurement axis. The signal from each sensor may be represented by the following:

$$S_1 \propto \frac{FR}{D^2}$$
$$S_2 \propto \frac{FR}{(D + d)^2}$$

where S_1 and S_2 are the detected signals
 F = projected spot flux
 R = surface reflectivity
 D = distance to target
 d = displacement seen by S_2

The detected signal intensities thus determine range independent of the surface reflectivity. The use of twin displaced detectors as opposed to two displaced emitters offers the advantage of matched stable response and excellent linearity. LED emitters are temperature sensitive and their performance changes with age, thus making it difficult to maintain identical output.

Computation of range can be achieved in a variety of ways to provide an output that is linear with range. The current prototype provides a pulse-repetition frequency that is proportional to range, and gives linear output and enhanced performance at maximum distances.

One characteristic of active systems is that when a specular surface (mirror-like reflection) is viewed along a normal to the surface, anomalous range information results. This condition does not occur frequently and is avoided if the sensor is inclined a few degrees or more from the surface normal.

Selected Specifications:

Ranging technique	Return signal intensity
Maximum range	2 meters
Minimum range	0.5 meter
Resolution	0.5 to 34 millimeters

Sensitivity	10 to 90 percent reflectivity at 5 meters
Output	0 to 5 volts DC
Field of view	7 degrees
Ambient illumination	100,000 lux sunlight 5,000 lux tungsten
Target characteristics	> 30% nonspecular reflectivity

Point of Contact:

Norman L. Stauffer
Honeywell Visitronics
P.O. Box 5077
Englewood, CO 80155
(303) 850-5050

3.2.3 Quantic Wide Angle Optical Ranging System

A relatively simple and inexpensive near-infrared ranging system was developed for the Navy by Quantic Industries, Inc. under the Small Business Innovative Research (SBIR) Program (Moser & Everett, 1989). The system will be employed as a collision avoidance ranging module on the modular robot depicted in figure 41.

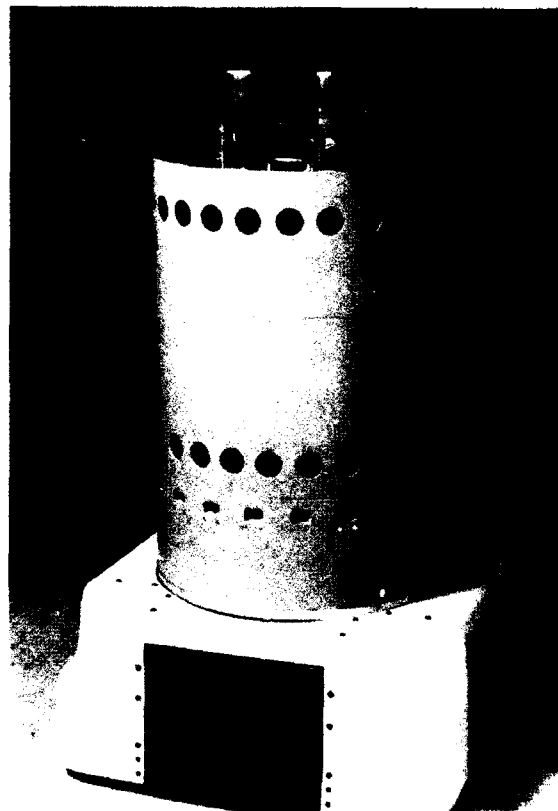


Figure 41. Quantic's Wide Angle Optical Ranging System will be employed on this modular robot developed by NCCOSC.

The prototype unit was designed around the following general guidelines:

- Coverage of 100-degrees azimuth, 30-degrees elevation
- Realtime range measurements out to 7 meters
- 10-Hz update rate
- Small size and weight
- Low cost
- Minimal power consumption
- Rugged and maintainable, with no moving parts

Active triangulation ranging is employed with about 5-degree spatial resolution over a nominal field-of-regard of 100-degrees azimuth and 30-degrees elevation. Under typical indoor conditions, fairly accurate target detection and range measurements are obtained to about 8 meters in the dark and about 5 meters under daylight conditions. No mechanical scanning is employed, and the entire field-of-regard can be scanned in 0.1 to 1 second (depending upon the required accuracy) allowing range measurements to be taken in realtime while the robot is in motion.

The transmitter consists of 164 high-power, gallium-aluminum-arsenide LEDs mounted in an array behind a spherical lens so as to produce a corresponding number of narrow, evenly spaced beams that interrogate the volume of interest. The LEDs in the array are sequentially activated at a particular repetition rate, and a synchronous receiver detects reflected energy from targets within its field of view. Figure 42 shows a portrayal of the structure and the projected light beams.

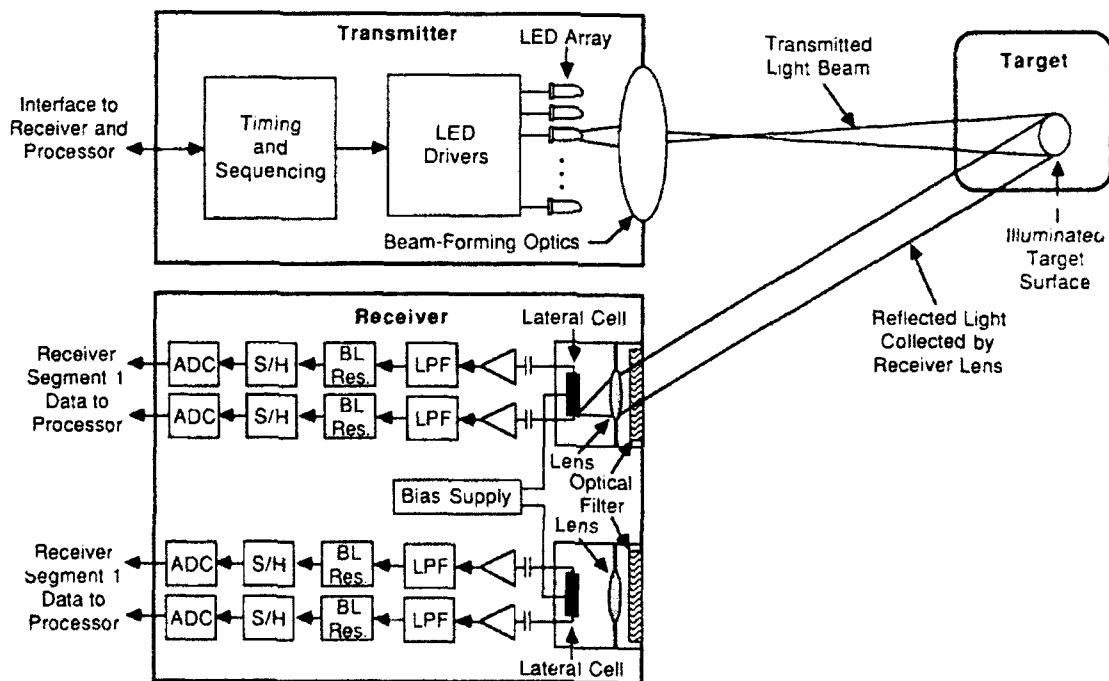


Figure 42. A block diagram of the transmitter and receiver subsystems of Quantic's sequentially scanned active triangulation system. (Courtesy Quantic Industries Incorporated).

The LEDs are self-lensed to yield relatively narrow beams, so most of their power is projected within the critical angle of the sphere lens for high power transfer efficiency. Figure 43 shows the pattern of the beams and their positioning behind the lens for the desired 5-degree spatial sampling.

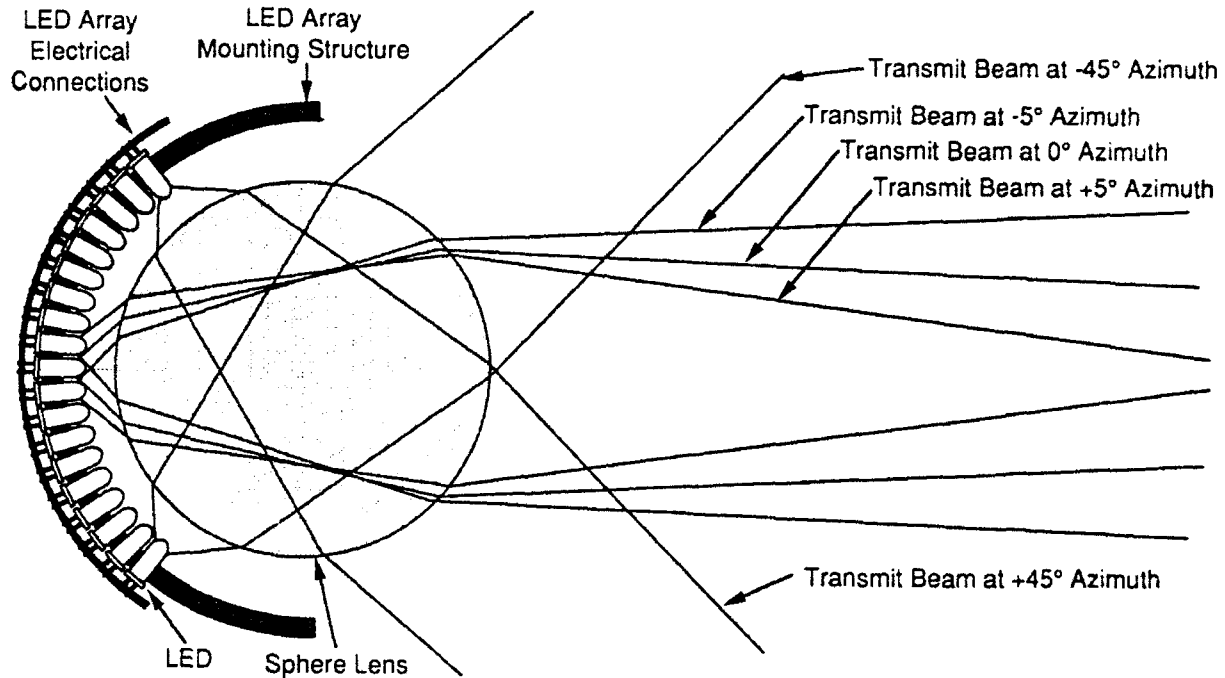


Figure 43. The pattern of the LED beams and their positioning behind the lens (Courtesy Quantic Industries Incorporated).

The optical receiver consists of two identical units, each covering a field of view of about 50 by 50 degrees. Both units contain a Fresnel lens, an optical bandpass filter, a position-sensitive detector, and the associated electronics to process and digitize the analog signals. The receiver uses a silicon lateral-effect position-sensing photodetector to measure the location (in the image plane) of transmitted light reflected (scattered) from a target surface. The transmitter and receiver are vertically separated by a 10-inch baseline.

The location of the centroid of reflected energy focused on the position-sensing detector is a function of the particular beam that is active and the range to the target being illuminated by that beam. The position signals from the detector (resulting from the sequential activation of LEDs in the transmitter) are collectively processed by a dedicated microcomputer to determine the ranges to valid targets throughout the sensor's field of view. Target azimuth and elevation are a function of the position of the LED (in the transmitter array) active at the time of detection. A look-up table derived from calibration data is used to perform the position-to-range conversions and to compensate for receiver nonuniformities.

Selected Specifications:

Ranging technique	Active triangulation
Range	5 meters
Size	14 by 5 by 4 inches
Weight	10 pounds
Update rate	1 to 10 Hertz depending on resolution
Wavelength	880 nanometers
Beamwidth	30 degrees elevation
100 degrees azimuth	

Point of Contact:

Shabtai Evan
Quantic Industries, Inc.
990 Commercial Street
San Carlos, CA 94070-4017
(408) 867-4074

3.2.4 SEO Helicopter Obstacle Proximity Sensor System

Schwartz Electro-Optics, Orlando, FL, is developing the Helicopter Obstacle Avoidance Proximity Sensor System for the U.S. Army (Schwartz Electro-Optics Incorporated, 1991e) as an onboard pilot-alert to the presence and location of obstacles. The sensor system is located on the main-rotor drive shaft, providing continuous distance and azimuth measurements in the horizontal plane of the helicopter (figure 44).

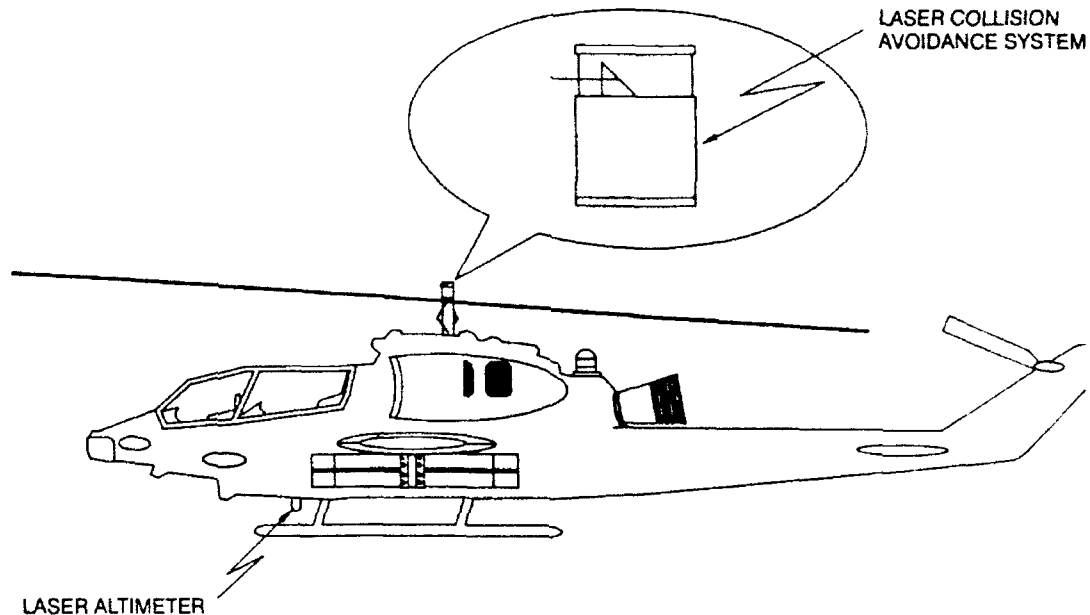


Figure 44. Planned placement for the Helicopter Optical Proximity Sensor System in a U.S. Army Helicopter (Schwartz Electro-Optics Incorporated, 1991d).

A high-pulse-repetition-frequency GaAs laser diode transmitter shares a common aperture with a sensitive avalanche photodiode receiver; the transmit and return beams are reflected from a motor-driven prism rotating at 300 rpm. Range measurements are taken at 1.5-milliradian intervals and correlated with the azimuth angle using an optical encoder. Obstacles detected are displayed in a format similar to a radar plan position indicator.

To achieve broader three-dimensional sensor coverage, a concept employing two counter rotating wedge-prisms is under investigation (Schwartz Electro-Optics Incorporated, 1991e). By directing the laser output through the rotating prisms, the beam can be steered such that an angular scan amplitude of $2\theta_d$ is traced out in one plane. The scan amplitude, $2\theta_d$, is proportional to the angle at the apex of the prism wedge. The laser beam, which is rotating at some rate (ω) about the vertical axis, can then be reflected from a surface (figure 45). Figure 46 shows the resulting beam pattern when the prism rotation rate (β) is much greater than the angular velocity of the reflecting surface (ω), and the angle of inclination of the reflecting surface (ϕ) is 45-degrees. As the reflective surface spins about the vertical axis, the rotating prisms direct the beam in a sinusoidal trace, as if projected onto a cylinder. The beam pattern can be modified by changing ϕ . For example, let $0 < \phi < 45$ -degrees, the resulting beam pattern would be inclined, as if it were projected onto the ground rather than a cylinder.

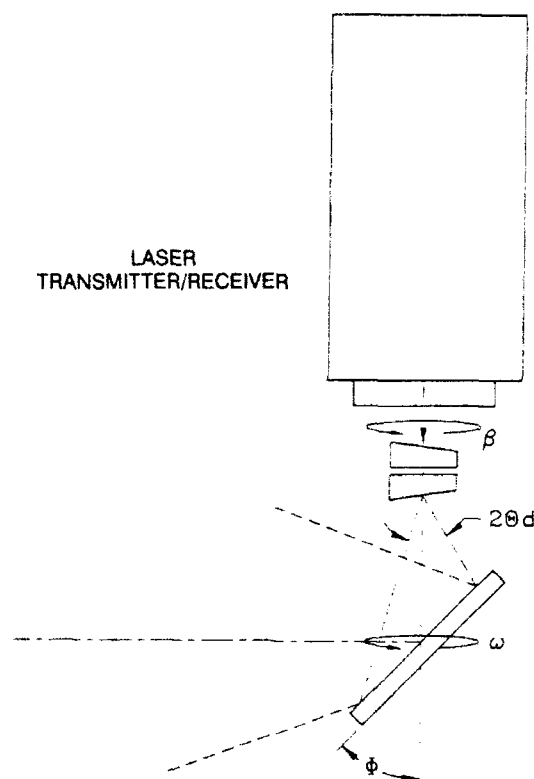


Figure 45. The laser beam is reflected from a surface that is rotating about the vertical axis with angular velocity ω (Schwartz Electro-Optics Incorporated, 1991e).

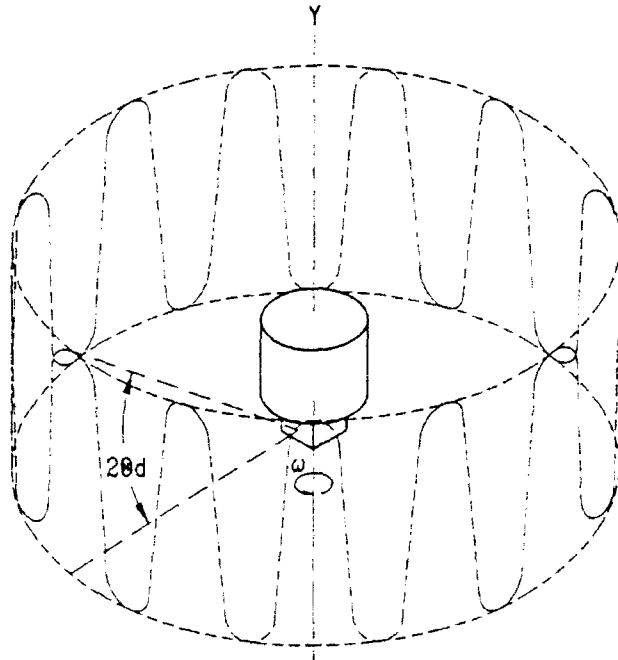


Figure 46. The beam pattern if the prism rotation rate, β , is greater than the angular velocity, ω , of the reflecting surface (Schwartz Electro-Optics Incorporated, 1991e).

Selected Specifications:

Range	8 to 400 feet
Accuracy	± 2 feet
Scan angle	360 degrees
Scan rate	5 Hz
Sample rate	20 KHz
Samples per scan	4096
Size	7-inch diameter, 11.75 inch length
Power	18 to 36 volts DC

Point of Contact:

Aaron Penkacik
 Schwartz Electro-Optics, Inc.
 3404 N. Orange Blossom Trail
 Orlando, FL 32804
 (407) 298-1802

3.2.5 RVS SI Ship Surface Scanner

The Ship Surface Scanner was developed by Robotic Vision Systems, Inc., Hauppauge, NY, under contract to the Navy, and intended for automated surveying of the interior spaces of ships. The sensor is designed to support ship overhaul and repair functions by reducing the time required for measurement, documentation, and planning. The tripod-supported,

three-dimensional scanner employs a GaAlAs laser diode which projects an eighth-inch diameter footprint of illumination at 12 feet.

Distance is measured by active triangulation as illustrated in figure 47; a two-dimensional solid-state camera is mounted 35 inches away from the laser source. The stepper-motor-driven scanner pans a horizontal field of view ± 35 degrees in elevation. The azimuth scan rate for the system is 10 degrees/second, with just 1 second required to stop to the next elevation line. The system has an effective depth of field of 8 feet between the distances of 4 and 12 feet, with accuracies varying from 0.05 inch at 4 feet to 0.225 inch at 12 feet. To accurately survey entire interior spaces, several scanners can be placed in a circular arrangement so their collective fields of view traverse 360 degrees. Alternatively, a single sensor can be relocated to multiple positions.

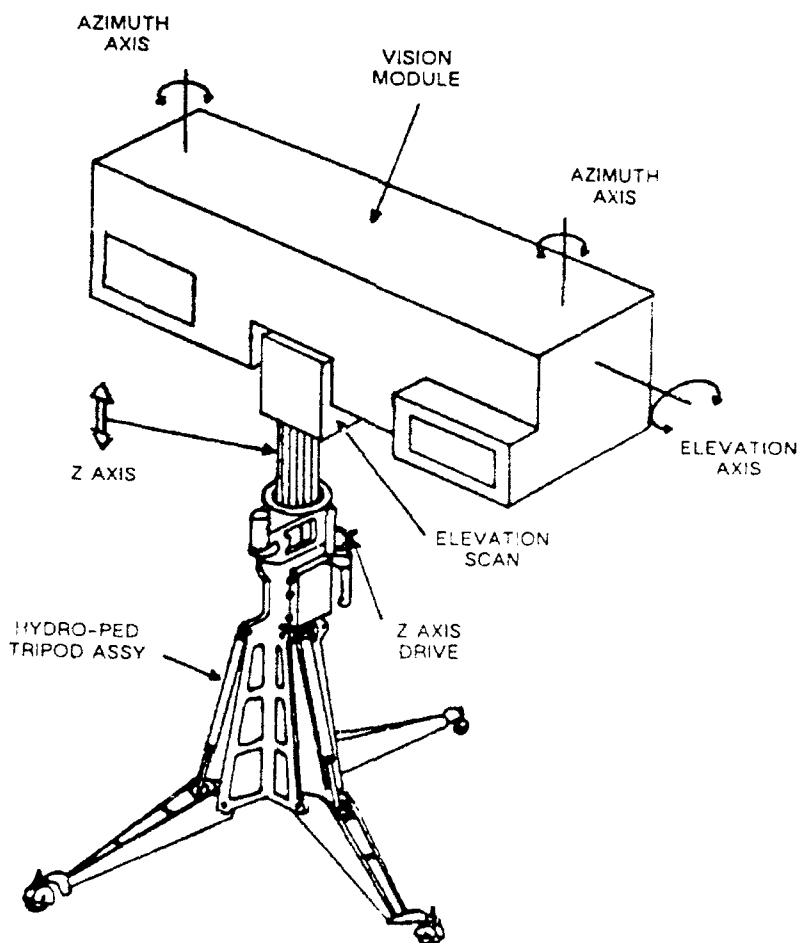


Figure 47. RVSI Ship Surface Scanner was designed to digitize the interior of ship spaces for overhaul planning (Courtesy Robotic Vision Systems Incorporated).

Selected Specifications:

Ranging technique	Active triangulation
Field of view	± 35 degrees azimuth, + 35 degrees elevation
Range resolution	0.050 inch at 4 feet, 0.225 inch at 12 feet
Minimum range	4 feet
Maximum range	12 feet
Laser source	GaAlAs laser diode
Wavelength	850 nanometers
Power requirements	115 volts AC at 20 amps
Enclosure	37 by 5.75 by 7.75 inches
Weight	32 pounds

Point of Contact:

Robert Metzger
Robotic Vision Systems, Inc.
425 Rabro Drive East
Hauppauge, NY 11788
(516) 273-9700

3.2.6 Multispectral ALV Sensors

An advanced ALV ranging device known as the Multispectral ALV (MS-ALV) Sensor, intended to provide the same navigation and collision avoidance capabilities of the earlier devices used in the ASV and ALV programs, was developed by the Environmental Research Institute of Michigan (ERIM). The operational environment, however, will be rugged cross-country terrain as opposed to the relatively uniform road surfaces seen in the initial tests of the autonomous land vehicle concept. The variations in terrain, surface cover, and vegetation encountered in off-road scenarios require an effective means to distinguish between earth, rocks, grass, trees, water, and other natural features.

During preliminary investigation, ERIM conducted an in-depth analysis of these features to determine their optimum detection bandwidth frequencies. Wavelengths between 0.52 to 0.55 micrometer were found to be useful in observing the green reflectance peak of the general terrain, analyzing the soil composition, and determining water depth. On the other hand, wavelengths of between 2.0 to 2.35 micrometers are well suited for determining the types of vegetation present and the moisture content of the soil. Evaluation of the findings determined that a sensor which could transmit and receive a multispectral signal composed of six different wavelengths should satisfy the requirements for cross-country navigation. The selected wavelengths are 0.53, 0.63, 0.82, 1.06, 1.53 and 2.29 micrometers.

Following the terrain analysis, work began to design and develop actual hardware capable of emitting and detecting at these wavelengths. The resulting transmitter consists of two laser sources and a series of bandwidth-separating, collimating, and beam-splitting optics. The principle lasing device is a Nd:YAG laser which produces a primary signal at 1.06 micrometers. By

frequency doubling this source the wavelength is effectively halved, creating the 0.53 micrometer signal.

Passing both of these transmissions through Raman capillary tube fibers produces wavelengths of 0.63, 1.53, and 2.29 micrometers. Raman fibers are optical conduits that scatter a portion of the photon energy from the incident laser light resulting in a frequency reduction (i.e., wavelength increase) for the dispersed energy. The scattering is the result of collisions between the incoming laser photons and the molecules that make up the fiber.

The final sensing band, 0.82 micrometer, is supplied by the second lasing source, a gallium-aluminum-arsenide (GaAlAs) laser diode. All of the signals are combined by dichroic mirrors and other optics to form a single continuous transmission waveform composed of six time-synchronous wavelengths. Once emitted, the multispectral beam is passed through beam-expansion optics to produce the desired rectangular footprint, and then sent to the scanning mechanism.

The scanner for the MS-ALV is essentially identical to the scanners developed for the earlier ASV and ALV sensors. The only significant difference is the substitution of a hexagonal rotating mirror instead of a square mirror for panning the beam in azimuth. This configuration causes the transmitted and returned signals to impinge on separate mirrored surfaces, resulting in reduced crosstalk and simplified sensor alignment (figure 48). The nodding mirror, which tilts the beam in elevation, remains largely unchanged.

The receiver for the MS-ALV sensor presents a special problem because it must detect the presence of all six transmitted wavelengths in the return signal. To accomplish this, ERIM designed a receiver with six separate photodetectors, each matched to one of the corresponding sources. The reflected energy from the terrain is directed through the scanning optics to the receiver. This rectangular beam encounters a dichroic beam-splitting mirror that separates the 2.29-micrometer band from the signal. This portion of the waveform passes through a narrow band-pass filter matched to the wavelength, then continues through a condenser that forms the beam into a point source for the photodetector. In the case of the 2.29-micrometer wavelength, the receiver requires liquid nitrogen cooling because the low-transmission intensity of this infrared wavelength results in minimal return radiation. (The extremely cold detector produces a high-contrast surface for the relatively warm beam to strike.)

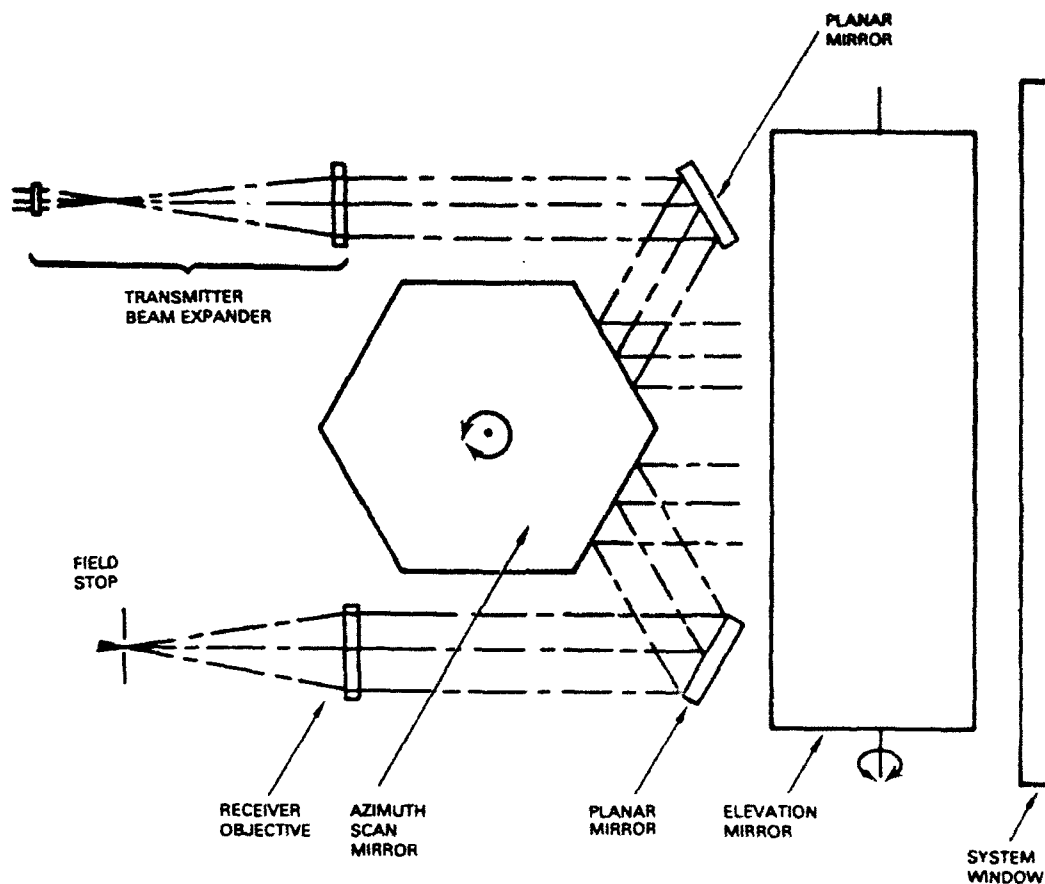


Figure 48. Hexagonal rotating mirror used in the multispectral scanner reduces crosstalk and simplifies mirror alignment (Courtesy Environmental Research Institute of Michigan).

The remaining energy, which does not pass the first dichroic mirror, is deflected in a cascading fashion to other detectors of similar design. At each receiver the specific wavelength is separated out, condensed, and sent to the respective sensing surface. Figure 49 shows how this process continues until the final band, 0.53 micrometer, is detected.

Ranging is performed by measuring the phase shift that occurs between the returning continuous wave and a reference beam. The ambiguity interval of the MS-AIV (the distance over which the phase difference remains less than 360 degrees) is 75 feet, which dictates the maximum effective range of the sensor. (Beyond this point the phase pattern repeats, causing uncertainty in the distance measurement.)

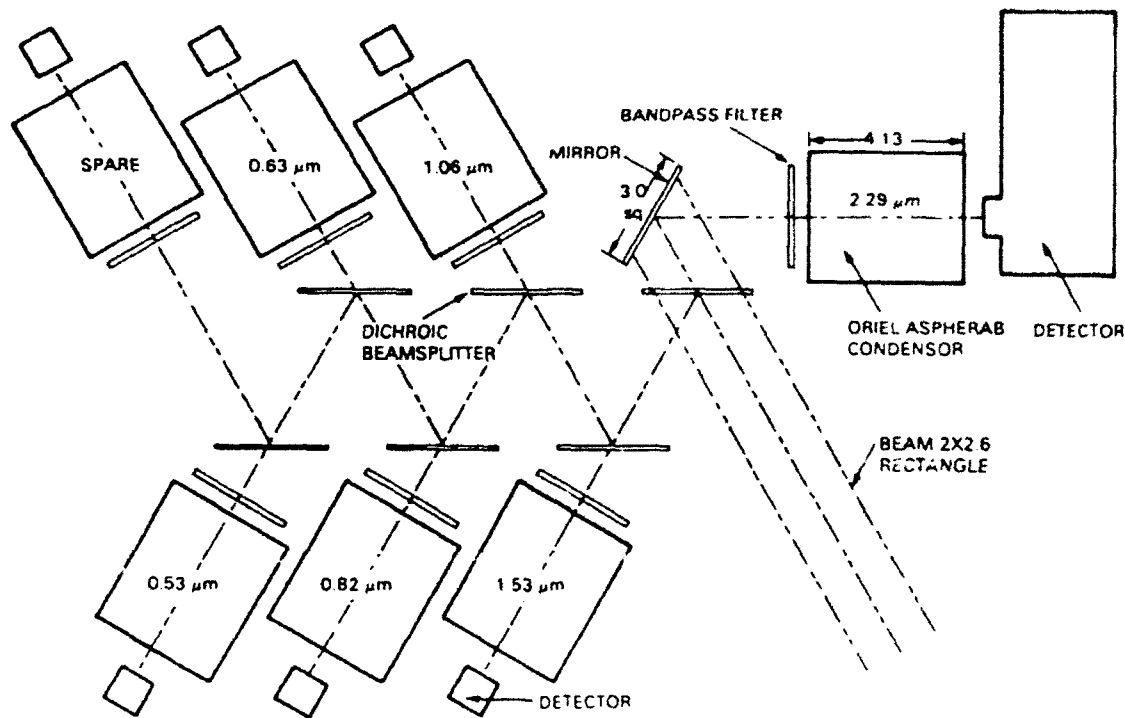


Figure 49. Block diagram of the multispectral ALV scanner (Courtesy Environmental Research Institute of Michigan).

The raw data produced are presented as output according to an *angle-angle-attribute* format. The angles correspond to the position and orientation of the scanning mirrors, and locate the point being observed within the field of view. The attribute field is a 13-bit word containing a single range value for the site, and six reflectance values representing the intensity of each of the laser wavelengths present in the composite beam reflected from that location. The range figure is based on the 1.06-micrometer source because of the strength of its transmission.

The multiple frequency sources, corresponding detectors, detector cooling system, and scanner result in significant power consumption (15 kilowatts). The mass of the scanning mirrors and mechanism plus the plurality of lasers, optics, and detectors make the multispectral sensor heavy, increasing the complexity of the control and analysis required to produce results. As a result, initial prototypes will have application only on the largest of mobile robotic platforms capable of supporting the size, weight, energy, and computational overhead.

Selected Specifications:

Ranging technique	Phase-shift measurement
Field of view	60 degrees (horizontal) 60 degrees (vertical)
Beamwidth	0.23 degree
Frame rate	2 frames/second
Scan rate	640 lines/second
Ambiguity range	75 meters
Light source	Nd:YAG laser

Laser wavelengths	0.53, 0.63, 0.83, 1.06, 1.53, 2.29 micrometers
Power requirements	15 kilowatts
Enclosure	12 by 3 by 2 feet
Weight	600 pounds

Point of Contact:

Environmental Research Institute of Michigan
 Box 8618
 Ann Arbor, Michigan 48107
 (313) 994-1200

3.2.7 RVSI Long Optical Ranging and Detection System

From research conducted over a 10-year period, Robotic Vision Systems, Inc. has conceptually designed an innovative laser-based time-of-flight ranging system capable of acquiring three-dimensional image data for an entire scene without scanning. The Long Optical Ranging and Detection System (LORDS) is a patented concept incorporating an optical encoding technique with ordinary vidicon or solid state camera(s), resulting in precise distance measurement to multiple targets in a scene illuminated by a single laser pulse. LORDS is designed to operate over distances between 1 meter and several kilometers. Characteristics such as realtime data acquisition rates, day or night operation, low cost, compact size, and high-resolution from low-bandwidth components make LORDS potentially suited to the navigation, guidance, obstacle avoidance, and target detection functions of military and industrial robotic vehicles.

The design configuration is relatively simple, and comparable in size and weight to traditional phase-shift measurement laser rangefinders (figure 50). Major components include a single laser-energy source, one or more imaging cameras, each with an electronically implemented shuttering mechanism, and the associated control and processing electronics. In a typical configuration, the laser will emit a 25 millijoule pulse lasting 1 nanosecond, for an effective transmission of 25 megawatts. The anticipated operational wavelength will lie between 532 and 830 nanometers, due to the ready availability within this range of the required laser source and imaging arrays.

The cameras will be two-dimensional charge-coupled device (CCD) arrays spaced closely together, side by side, with parallel optical axes resulting in nearly identical, multiple views of the illuminated surface. Lenses for these cameras will be of the standard photographic varieties between 12 and 135 millimeters. The shuttering function will be performed by Microchannel Plate Image Intensifiers (MCPs) 18 or 25 millimeters in size, which will be gated in a binary encoding sequence, effectively turning the CCDs on and off during the detection phase. Control of the system will be handled by a single-board processor based on the Motorola MC-68040.

LORDS obtains three-dimensional image information in realtime by employing a novel time-of-flight technique requiring only a single laser pulse to collect all the information for an entire scene. The emitted pulse journeys a finite distance over time; hence, light traveling for 2 milliseconds will illuminate a scene a greater distance away than light traveling only 1 millisecond.

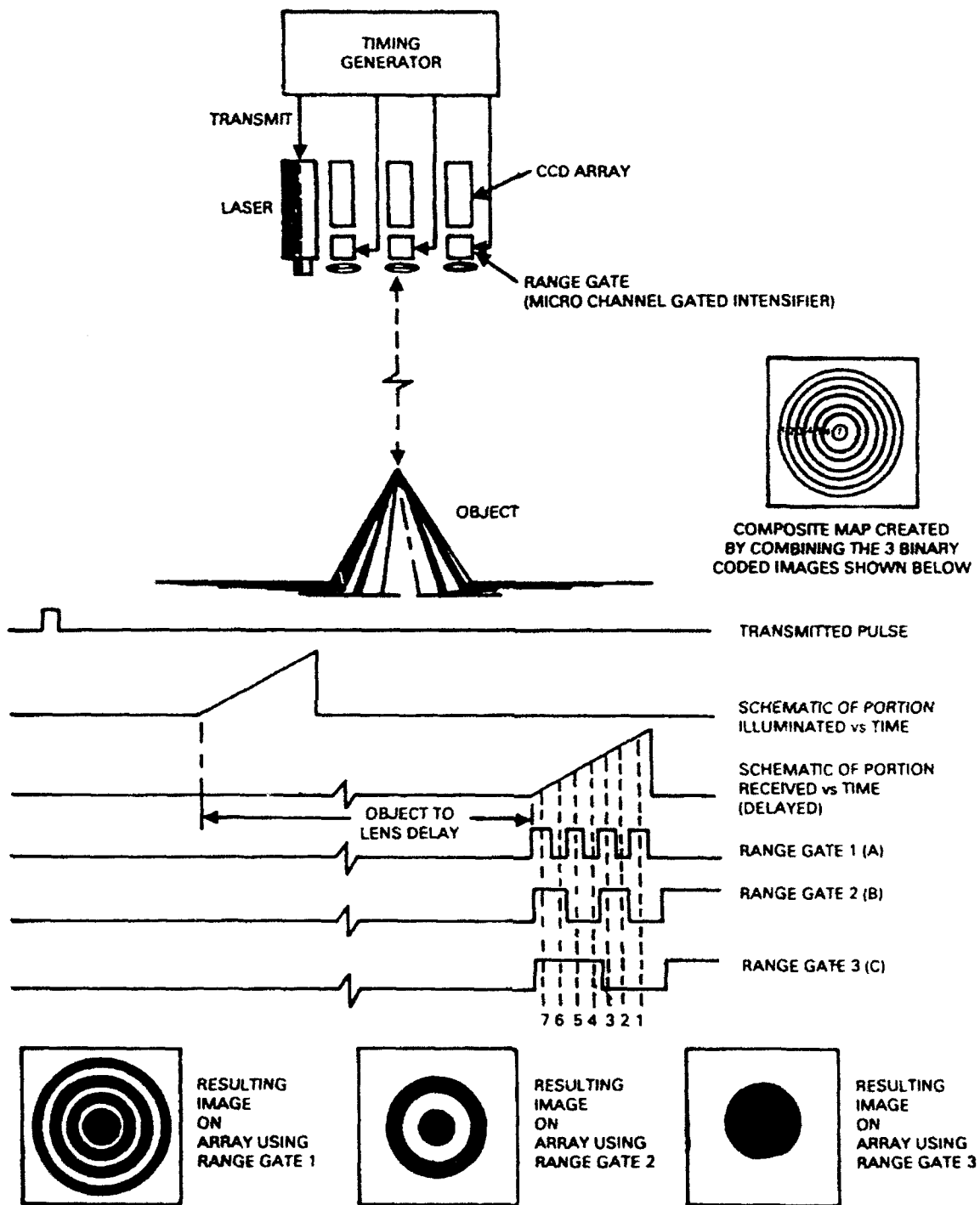


Figure 50. Block diagram of the RVS I LORDS ranging concept (Courtesy Robotic Vision Systems Incorporated).

LORDS divides its entire sensing range into discrete distance increments, each representing a distinct range plane. This is accomplished by simultaneously gating the MCPs of the observation cameras according to their own unique on-off encoding pattern over the duration of the detection phase. This binary gating alternately blocks and passes any returning reflection of the laser emission off objects within the field of view. When the gating cycles of each camera are lined up and compared, there exists a uniquely coded correspondence that can be used to calculate the range to any pixel in the scene.

For instance, in a system configured with only one camera, the gating MCP would be cycled on for half the detection duration, then off the remainder of the time. Figure 50 shows any object detected by this camera must be positioned within the first half of the sensor's overall range (half the distance the laser light could travel in the allotted detection time). However, significant distance ambiguity exists because the exact time of detection of reflected energy could have occurred anywhere within this relatively long interval.

This ambiguity can be reduced by a factor of two through the use of a second camera with its associated gating cycled at twice the rate of the first. This scheme would create two complete *on-off* sequences, one taking place while the first camera is on and the other while the first camera is off. Simple binary logic can be used to combine the camera outputs and further resolve the range. If the first camera did not detect an object but the second detector did, then by examining the instance when the first camera is off and the second is on, the range to the object can be associated with a relatively specific time frame.

Incorporating a third camera at again twice the gating frequency (2 cycles for every 1 of Camera two, and 4 cycles for every 1 of Camera one) provides even more resolution. Following the same logic as before, if the example object is also seen by the third detector, the unique occurrence of the pattern *off-on-on* for the first, second, and third cameras respectively pinpoints the range more precisely.

Notice that for a three-camera arrangement there are eight nonrepeatable detection combinations, which means the sensing range is divided into eight intervals of which seven are usable. (The eighth corresponds to no-return in any of the three cameras.) For each additional CCD array incorporated into the system, the number of distance divisions is effectively doubled, resulting in significant improvements in resolution over the specified range.

Alternatively, the same encoding effect can be achieved using a single camera when little or no relative motion exists between the sensor and the target area. In this scenario, the laser is pulsed multiple times, and the gating frequency for the single camera is sequentially changed at each new transmission. This creates the same detection intervals as before, but with an increase in the time required for data acquisition. A combination of both methods is also possible. This modularity allows for customizing to meet the needs of the specific application.

An important characteristic of LORDS is its projected ability to range over selective segments of an observed scene. This feature can be used to improve resolution; in that, the distance over which a given number of range increments is spread can be variable. The entire range of interest is initially observed, resulting in the maximum distance between increments (coarse resolution). An object detected at this stage is thus localized to a specific, abbreviated region of the total distance.

The sensor is then electronically reconfigured to cycle only over this region, which significantly shortens the distance between increments, thereby increasing resolution. A known delay is introduced between transmission and the time when the detection/gating process is initiated. The laser light thus travels to the region of interest without concern for objects positioned in the foreground.

Selected Specifications:

(Concept only)

Ranging techniques	Time of flight
Minimum range	1 meter
Wavelength (frequency)	532–830 nanometers

Point of Contact:

Howard Stern
Robotic Vision Systems, Inc.
425 Rabro Drive East
Hauppauge, NY 11788
(516) 273–9700

3.2.8 Digital Signal Laser Radar Sensor

An advanced laser-radar sensor developed by Digital Signal Corporation to precisely measure distances to as close as 0.0001 inch has potential application to three-dimensional vision for robotic platforms. The proposed system incorporates a continuous-wave, frequency-modulated injection laser diode with fiber-optic scanning for ease of system implementation (Goodwin, 1985). The device is capable of performing continuous, high-resolution (0.001 inch) ranging to machined-metal or composite surfaces at distances of several yards, at scan rates of 1000 pixels/second. Initial applications include contour mapping, noncontact gaging, and surface quality determination.

This accuracy is inherent to the extremely wide frequency tuning range of the injection laser (see section 2.1.5). The scanner is composed of a General Scanning GF-220D optical system for tilting the transmission beam in elevation, and a 24-surface Lincoln Lasers spinning-facet wheel for panning the source in azimuth.

For three-dimensional vision applications associated with mobile robotic platforms, the sensor can be configured as a high-frame-rate mapper. To achieve realtime operation, the time spent per pixel (pixel-dwell time) must be reduced to submicrosecond values. System accuracy diminishes as a consequence, but the decrease is not excessive and precision remains reasonable. Resolutions approaching 0.1 inch are possible at dwell times of approximately 5 microseconds per pixel, which translates to a scan rate of 5 megapixels/second. Range-picture frame rates for a 256 by 256 pixel field of view can reach 100 frames per second.

Selected Specifications:

Unable to obtain specifications from company.

Point of Contact:

Digital Signal Corporation
5554 Port Royal Road
Springfield, VA 22151
(703) 321-4910

3.2.9 Passive Swept-Focus Three-Dimensional Vision

The swept-focus three-dimensional vision system developed by Associates and Ferren of Wainscott, NY, is a monocular camera system (figure 51) that performs ranging and three-dimensional imaging tasks by use of the swept-focus technique discussed in section 2.1.6 (Farsaie et al., 1987; Associates & Ferren, undated). The initial application was to serve the collision avoidance needs of a mobile robotic platform. The design therefore employed special optical preprocessing techniques to minimize the onboard computational requirements for image understanding.

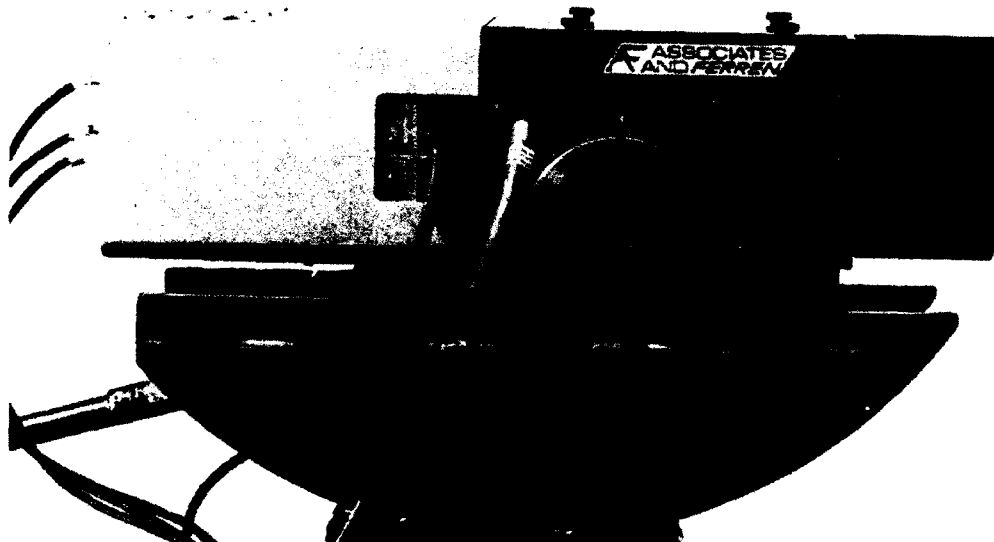


Figure 51. Swept-Focus Camera Subsystem developed for the Navy for passive three-dimensional vision applications (Courtesy Associates and Ferren).

The system consists of the swept-focus sensor, mounted on a robotic vehicle, in communication with a computer and frame grabber. To determine the range to objects in the sensor's field of view, the lens is swept through hundreds of discrete focal positions, remaining at each position for 1/60th of a second, or one video field time. During this time, the analog signal processor integrates the high frequency response in that field. This summation is a measure of the amount of edge information in the associated range slice, and representative of the relative degree of focus

(figure 52). In other words, the best-focus lens position for an object corresponds to a peak in the high-frequency response with range.

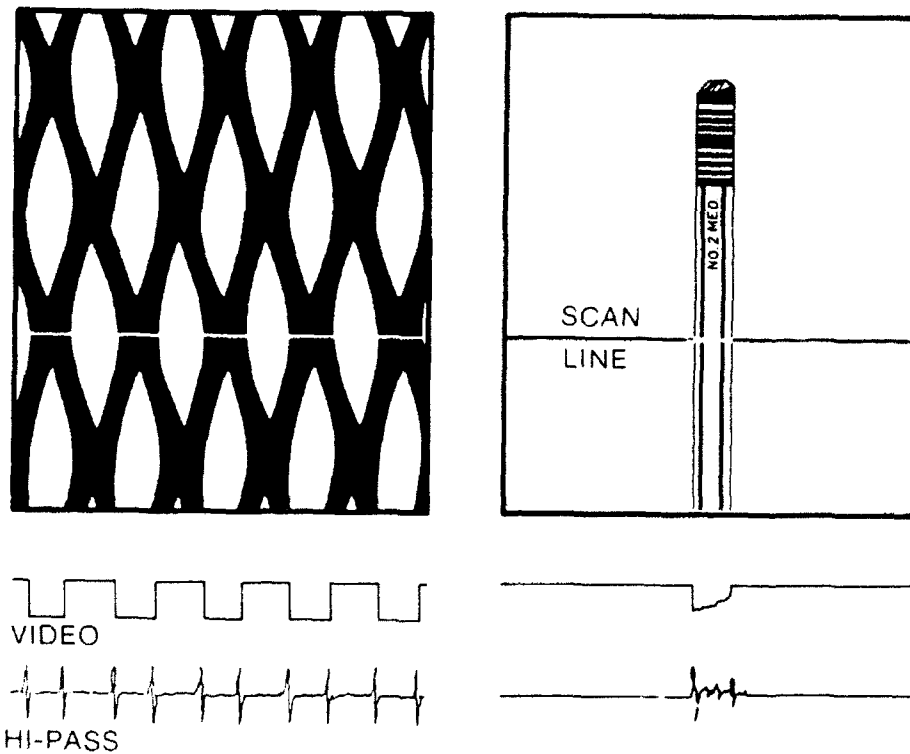


Figure 52. Video and high-pass filter output when viewing a piece of expanded metal (left) and a pencil (right).

Multiple targets at different ranges in the field of view can be accurately located by this technique. To perform the ranging function, only the high-frequency response at each lens position must be recorded. Good accuracy (about 1 inch) and repeatability are obtained with a 600-position scan over a 25-foot range interval, which takes approximately 12 seconds (50 millimeter/f1.0 lens). Accuracy and resolution vary with range, and are greatest at closer range, using the current exponential scan profile. Ranging accuracy and repeatability are dependent upon lens characteristics, specifically on the depth of field of the lens. The shorter the depth of field, the greater the ranging accuracy and resolution of closely spaced targets (section 2.1.6). In practice, the two lenses found to be most useful are a 50 millimeter/f1.0 and a 105 millimeter/f1.8, both good quality photographic lenses. The longer lens offers better ranging accuracy and resolution, but has a narrower field of view than the shorter lens.

The swept-focus vision system described has been used as the primary sensor for a mobile robot with success. The main factor limiting the speed of this technique is the standard 60-Hz video field rate. The system supplies accurate range data and generates a floor-plan map of its environment that is used in map-based path planning. For such an imaging task, a quick full-range scan could be executed to find the gross location of a target. The lens could then be scanned through the identified range space at smaller increments, saving the entire video field at each position in a large bit-mapped model. A three-dimensional representation of the edge-enhanced object could thus be generated and stored in memory.

During motion of the robotic vehicle, the vision camera can be used as a visual proximity detector by positioning the lens at a fixed focus, and monitoring the change in high-frequency content of the scene as the robot travels. A significant rise in this high-frequency information is indicative of a target coming into focus at the range that the lens is imaging. When this condition arises, the robot pauses until it can determine whether or not a collision is imminent. In this application, the 50 millimeter lens has been most useful. The accuracy of the 105 millimeter lens is superior, but its 110-degree field of view is too restrictive.

The use of optical preprocessing in the swept-focus sensor gives it some advantages over other ranging techniques. For example, ranging is accomplished at higher update rates than with some other visually based ranging systems, such as binocular vision. There is no *missing parts* problem since there is only a single lens, and daily or periodic mechanical alignment is not necessary. The preprocessing action of the short depth-of-field lens also allows for ranging that is not computationally intensive.

The system operates passively under normal ambient lighting conditions, responding well to all target objects except those which present a flat field, such as newly painted walls with no visible texture or markings. Determining the dimensions of an object along three orthogonal axes has been demonstrated, and the system has the capability to collect and store three-dimensional image information if required. For these reasons, the swept-focus vision system can be a good primary sensor for mobile robot applications, provided power consumption is not a critical problem. However, the addition of redundant sensors (such as ultrasonic) is recommended to ensure the detection of objects which are out of the camera's field of view at close range.

Selected Specifications:

Ranging techniques	Swept focus
Scan rate	12 seconds/600 positions/25 foot range interval
Frame rate	60 Hz

Point of Contact:

Bran Ferren
Associates and Ferren
Box 609 Wainscott-NW Road
Wainscott, NY 11975-9999
(516) 537-7800

3.2.10 JPL Range-From-Focus Optical System

A program to develop a semi-autonomous navigation system for use onboard a planetary rover has been underway at NASA, Jet Propulsion Laboratory (JPL) since late 1988. A testbed vehicle is now complete, using a passive vision-based navigation technique that requires a great deal of computation. To reduce the computational overhead, researchers at JPL are working an alternate approach: a range-from-focus optical system (figure 53). The goal is to minimize the necessary computation so that navigation of the rover can be practically performed onboard rather than remotely from earth (Wilcox, 1990).

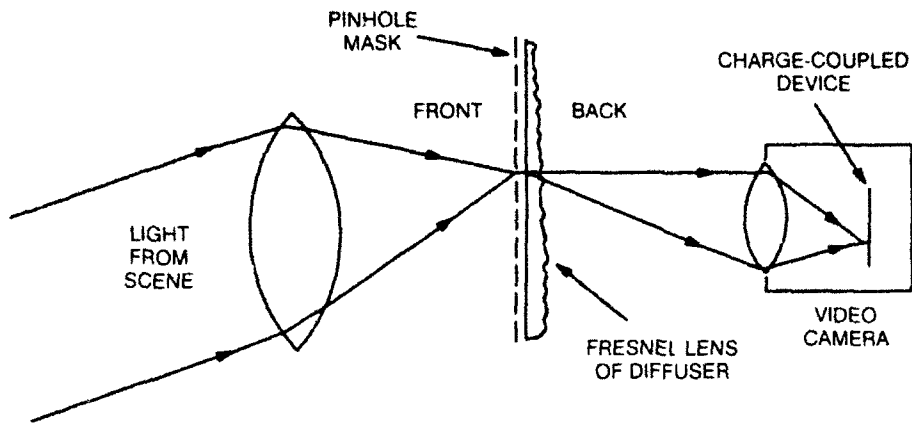


Figure 53. A focus-based optical ranging sensor (Wilcox, 1990).

This focus-based ranging system uses a large-aperture, short-focal-length lens with a pinhole mask at the prime focus. This mask is transparent only in an array of pinholes at or near the diffraction-limiting spot size of the lens. A diffuser or Fresnel lens is placed behind the mask to direct the light coming through the holes back toward a CCD camera. The camera is focused on the mask that there is a one-to-one correspondence between each pixel and pinhole. When successive frames from the CCD camera are differenced and the magnitude of that difference averaged, the only significant signal remaining will be in those parts of the image where the terrain is in focus.

The initial prototype will use a 75 millimeter, F1.9 lens. By way of example, if the lens is focused at a range of 10 meters, the corresponding focal distance is 75.567 millimeters; at 10.5 meters it is 75.540 millimeter. The difference in focal distance is 27 microns, which leads to a 14-micron circle-of-confusion for a point source at 10.5 meters. The pinhole array is focused for 10 meters, and the diffraction limiting spot is approximately 2 microns. Even a highly textured surface at 10.5 meters will not produce strong difference values between successive frames (assuming the image moves less than 14 microns across the array), whereas an object at 10 meters will produce a 100-percent contrast change with only 2 microns of image motion.

Two or three different range planes could be mixed on different video scan lines in the same sensor. To accomplish this, the pinhole array could be corrugated so that alternate scan lines represent different range distances. A practical implementation would be made from layers of photographic film, with stripes of clear film alternating with the pinhole arrays. For robotic collision avoidance purposes, it is generally not required to have a range map as dense as a standard video image (approximately 500 by 500); several pixels can be averaged horizontally, assuming they will be at approximately the same range. This approach yields two 250 by 250 range maps at two different ranges from the single sensor.

Another variation would incline the image pinhole array to match the flat-earth ground plane. Using the corrugated approach previously described, one could mix the resulting images using resistors to produce a single video image depicting elevation deviations. This method would allow obstacle detection from brightness changes in the video image alone; no postprocessing would be required.

Selected Specifications:

Unable to obtain specifications.

Point of Contact:

Brian Wilcox
NASA Jet Propulsion Laboratory
4800 Oak Grove Drive
Pasadena, CA 91109-8001
(818) 354-4321

3.2.11 JPL Stereo Vision System

NASA Jet Propulsion Laboratory (JPL), Pasadena, CA, is developing a passive stereo vision system for use onboard the NASA Planetary Rover and U.S. Army robotic land vehicle applications (Bedard et al., 1991a; 1991b; Slack, 1989). In 1990, JPL developed a vision system that computes LaPlacian image-pyramids using Datacube hardware, followed by a method of stereo matching which applies a sum-of-squared-differences operator to 8-bit greyscale images. Currently, the sum-of-squared-differences operation is performed at the 64- by 60-pixel image level of the pyramid using a 68020 processor; range and confidence images are produced in approximately 2 seconds. Performing cross correlation with Datacube hardware is expected to reduce this time to less than half a second.

An alternate version of the algorithm uses a one-dimensional penalty function to model reliability, allowing interpolation over textureless image areas. Disparity estimates are performed independent of each scanline, requiring approximately 6 seconds per 64 by 60 pixel image-pair. This system has been implemented on the Planetary Rover Navigation testbed vehicle, figure 54, and performed reliably in off-road navigation tests. Both algorithms assume that the cameras are well aligned, confining the matching search to corresponding scanlines of the two images.

Development of stereo vision technology is continuing in 1992 at JPL. The NASA Rover Program is investing in new computer hardware improving the algorithms and test evaluations. The U.S. Army Tank Automotive Command is applying this technology for obstacle detection and reflexive obstacle avoidance within the context of computer-aided remote driving using the high mobility multipurpose wheeled vehicle (HMMWV).

Selected Specifications:

Point of Contact:

NASA Jet Propulsion Laboratory
4800 Oak Grove Dive
Pasadena, CA 91109-8001
(818) 354-4321



Figure 54. NASA's Planetary Rover with stereo vision system using a one-dimensional penalty function to model smoothness (Courtesy NASA Jet Propulsion Laboratory).

3.2.12 TOSC Passive Stereo Ranging

In 1988, the Optical Sciences Company, Placentia, CA, completed development and tested a laboratory demonstration prototype imaging sensor capable of providing range data to all points in the scene being viewed. Their approach was based on a unique image-processing algorithm that allows comparable portions of two images of the same scene to be compared to determine the misregistration (image displacement) between the two images. This algorithm, the Image Displacement Estimation Algorithm (IDEA), provides displacement estimates with a precision of a few millipixels.

The prototype system, accomplished under contract for the Marine Corps, consisted of a camera, a frame grabber, and custom-designed digital processing electronics hosted by a personal computer. IDEA was used to process image data as gathered by the camera alternately viewing through the two ports of a stereo rangefinder. The system was designed with a 1-meter baseline separation, and was intended to range targets from 100 meters to 10 kilometers with an accuracy of 3 percent at full range. Actual range testing across the San Diego Bay was performed between 1.2 and 9.3 kilometers.

The device was able to meet the designed range-accuracy criteria of 3 percent of full range most of the time. System unreliability was traced to an algorithm implemented to determine the nearest whole-pixel displacement prior to processing by IDEA. This preprocessing, or course-adjustment algorithm, proved sensitive to nonideal atmospheric conditions (i.e., ambient moisture content, turbulence caused by differential heating of the air and ground) resulting in poor

contrast-to-noise ratios (Optical Sciences Company, 1987). Although IDEA performed within the expected millipixel displacement-accuracy criterion, the data passed to it by the course-adjustment algorithm was unreliable under real-world conditions.

Selected Specifications:

Ranging technique	Stereo disparity
Maximum range	10 kilometers
Minimum range	100 meters

Point of Contact:

Dr. David L. Fried
 Optical Sciences Company
 P.O. Box 1329
 Placentia, CA 92670-1329
 (714) 524-3622

3.2.13 Millitech Modular MMW Radar Sensor

Millitech Corporation, Deerfield, MA, has designed a millimeter wave FMCW sensor system aimed at satisfying the short-distance noncontact ranging needs for robotic collision avoidance (Millitech Corporation, 1989). The key to Millitech's design is the use of a computer-controlled modulated oscillator to generate the basic transmitter waveform. Their approach calls for the coherent processing of the return signal, averaged over many successive sweeps. The relatively narrow bandwidth of the sweep serves to achieve unambiguous range resolution at a cost less than that of traditional FM/CW sensors.

Using a modular design concept, Millitech developed two baseline sensors with the operational range and waveform parameters summarized in the specifications at the end of this paragraph. Sensor A is typical of a robotic application where the range to the nearest obstruction can be monitored using the 30- by 30-degree field of view. Using a bistatic antenna configuration, this is designed to function as a proximity sensor that will respond to the single strongest return from any object within some predetermined range. Sensor B is designed to scan a fan beam 360 degrees in azimuth, track multiple targets, and determine range and bearing for each. Using a single rotating antenna in a monostatic configuration, sensor B has better than 1-degree bearing resolution.

Selected Specifications:

Ranging technique		FMCW	
		<u>Sensor A</u>	<u>Sensor B</u>
Range: maximum	(cm)	10 ³	10 ⁴
minimum	(cm)	10	10
Radar cross-section	(dBsm)	-30	-40
Resolution: range	(cm)	1	10
	azimuth	~30 deg	2 deg
	elevation	~30 deg	5 deg

Center frequency	(GHz)	95	35
Sweep width	(MHz)	320	120
Sweep time	(μ s)	100	400
Blank time	(ns)	100	1000
Number of sweeps		25	
Sample time	(ms)	10	10
Range bins		1000	1000
Baseband signal	(KHz)	2 – 200	5 – 500

Point of Contact:

Richard Huguenin
 Millitech Corporation
 South Deerfield Research Park
 P.O. Box 109
 Deerfield, MA 01373-0109
 (413) 665-8551

3.2.14 Battelle Steerable-Beam Millimeter Wave Radar

Researchers at the Battelle Memorial Institute have developed a beam-steerable millimeter-wave antenna for use on an automobile collision-avoidance radar system. The new antenna provides azimuth information in addition to distance data for any objects in the car's path. Battelle is hoping to interest automotive companies in licensing the new antenna, or becoming investment partners in the development of a collision-avoidance system, projecting that costs could be driven down quickly to a few hundred dollars (Wittenburg, 1987).

The radar is a frequency-modulated continuous-wave (FM/CW) system coupled with a beam-steerable antenna. The center frequency is at or near 50 GHz (6-millimeter wavelength). This type of radar allows range, velocity, relative amplitude (size or radar cross section), and angle determination for multiple targets. The 50-GHz frequency requires a relatively small antenna. At this frequency, long-range propagation of interfering signals is reduced due to atmospheric oxygen absorption. The basic radar is capable of monitoring a range of over 3 kilometers without range ambiguities. Returns from targets at distances exceeding 100 meters will be filtered for automotive applications so as not to interfere with signals for the targets of interest.

The 50-GHz source generates a linear frequency-modulated signal with a total change in frequency of 30 MHz. (This bandwidth is required to obtain a 5-meter range resolution.) The 50-GHz signal is used as the source for the transmit/receive antenna and for the local oscillator for the two mixers. The transmitted signal is reflected from targets of interest and is received by the same transmit/receive antenna. The received signal is mixed with the local oscillator output, generating a difference or intermediate frequency (IF). The IF amplitude is proportional to the target size (range to target must be considered), while the frequency is proportional to the distance between the antenna and target.

There are two IF outputs from the RF section, which are in quadrature. These signals are required to generate the range and velocity data. Each IF signal is band limited to the frequency range of 40 to 845 KHz, which corresponds to the IF span for a target between 5 to 100 meters away. The output from this equalizing filter is then applied to a bank of 16 individual band-pass

filters (Battelle Columbus Division, 1986). The output from each filter corresponds to a signal from a given range bin as follows:

5 to 60 meters	5-meter range bins
60 to 100 meters	10-meter range bins

This results in a range resolution of 5 meters when a target is within 60 meters of the antenna, and a resolution of 10 meters when a target is within 60 to 100 meters of the antenna.

A frequency counter is used to count the number of zero crossings of the IF signal for a given range filter. The counter determines the actual frequency of the IF signal and, therefore, the range to the target. The outputs from the 16 filters for both IF channels are multiplexed and then converted to a digital format by an 8-bit A/D converter. The data from the A/D converter is passed to a computer for further processing (Battelle Columbus Division, 1986).

The system controller provides an analog control signal to the 50-GHz solid-state source. The control signal is used to generate the linear frequency-modulated sweep over the 30-MHz bandwidth. This sweep is accomplished every 24 microseconds. The controller also serves as the interface to the beam-steerable antenna, monitoring the beam position as a function of time. This interface is required to ensure that the radar knows where the antenna is pointing, since the antenna must dwell at a particular look angle for 3 milliseconds to obtain the desired velocity accuracy. During this 3-millisecond time, the source generates 128 FM sweeps.

The proposed antenna would use a Battelle "diffraction electronics" concept (Seiler & Mathena, 1984) for a mechanically steered beam that covers ± 15 -degrees azimuth range, yielding a coverage of ± 25 meters from centerline at 100 meters. The beamwidth will vary from 1 degree at the straight-ahead or 0-degree position to 4 degrees at the ± 15 -degree positions. The scan will be a sawtooth scan with a 0.006-second dwell at each of 15-beam positions.

The antenna will be implemented by patterning a rotating drum as illustrated in figure 55. The 2-inch diameter drum will rotate at a constant speed of 666 rpm. The beam will be scanned horizontally by using different periodic grating spacings around the drum circumference. The beam width will be varied during the scan by using a novel technique developed at Battelle.

A vertical beam width of 3 degrees will be obtained through use of a cylindrical reflector. The reflector will be nominally 4.5 inches high to provide a 3-degree vertical beam at 50 GHz. The scan rate can be controlled by sensing an index mark on the drum and maintaining a constant rotation rate. The entire antenna structure (including the waveguide feed, the diffraction drum, and the reflector) will be located behind the dielectric panel which functions as a protective radome.

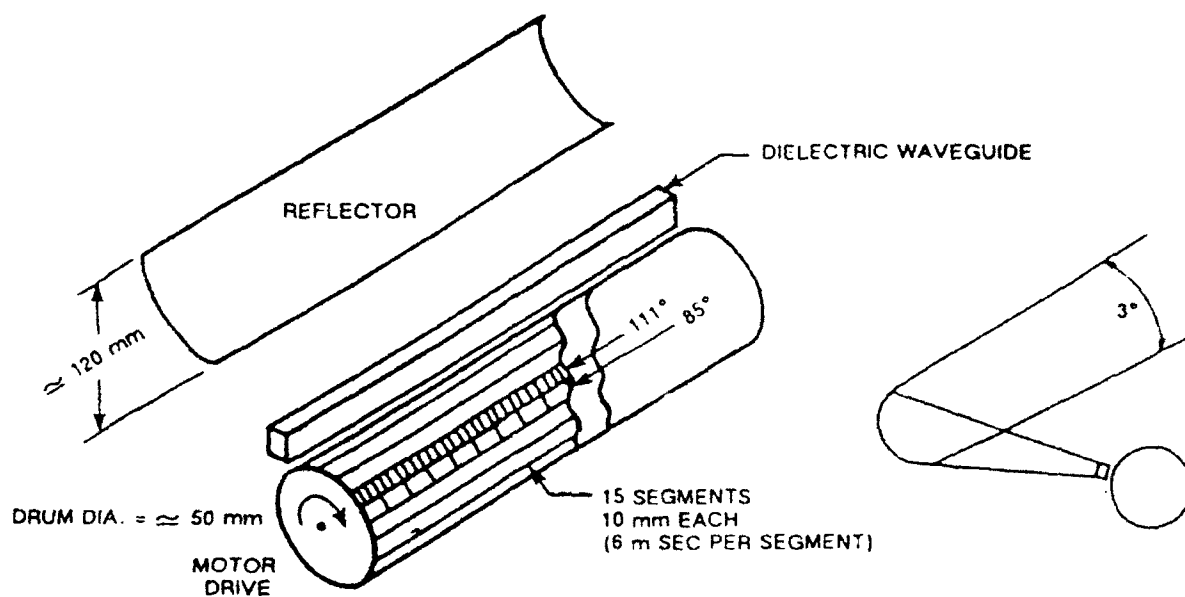


Figure 55. A rotating drum forms the heart of the Battelle diffraction antenna beam steering concept (Courtesy Battelle Columbus).

Selected Specifications:

Ranging technique	Frequency modulation
Antenna pattern	3 degrees elevation
	1- to 4-degrees azimuth
Operational frequency	50 GHz
Range resolution	5 meters from 5 to 60 meters
	10 meters from 60 to 100 meters
Maximum range	Unambiguous to 3 kilometers
Range accuracy	5 to 20 meters estimated
Velocity accuracy	1 meter/second
Update rate	0.2 second

Point of Contact:

Milt Seiler
 Battelle Columbus Division
 505 King Avenue
 Columbus, OH 43201-2681
 (614) 424-5684

3.2.15 K-MEC Low Cost Millimeter-Wave Radar

Under a Phase I Small Business Innovative Research (SBIR) contract, Kruth-Microwave Electronics Company (K-MEC), Hanover, MD, developed a radar sensor system appropriate for unmanned robotic systems for the Naval Sea Systems Command (Kruth-Microwave Electronics Company, 1989). The results of this SBIR demonstrated the feasibility of an FMCW millimeter-wave (MMW) radar system in providing accurate short-range data useful in determining range, position, and velocity of low-radar-cross-section targets. Designed specifically for use on an unmanned vehicle, primary design considerations included maximum target range, resolution, and accuracy, as well as cost, size, and weight.

The prototype system overcomes the traditional drawbacks of high-resolution MMW radar systems (moderate size and relatively high cost) through clever design and the planned use of monolithic MMW integrated circuits. Incorporating a MMW front end, a microprocessor/DSP-based signal processing unit, production systems could be packaged into a one-third cubic-foot volume. Range resolution is driven by the available processing power of available DSP ICs (i.e., the size of the Fast Fourier Transform operation.) Target velocity and associated difficulties with an FMCW radar have been overcome by employing double-sideband signal-processing techniques.

The Kruth system was designed for use in moderate rainfall of 4 millimeters per hour with a resultant attenuation of 1.2 dB/kilometer. The experimental effort featured a transmit power output of 1 milliwatt (0 dBm) along with transmit/receive antenna gains of 25 dB, and a receiver noise figure of 7 dB. By increasing transmit power consistent with available devices, increasing receiver gain, and reducing IF processor bandwidths, Kruth anticipates that useful target returns at ranges in excess of 3 kilometers are achievable.

Selected Specifications:

Range	1 kilometer
Resolution	< 1 meter
Minimum target size	≤ 0.1 meter

Point of Contact:

Jeff Kruth
Kruth-Microwave Electronics Company
2600 Cabover Dr.
Hanover, MD 21076-1704
(301) 768-6666

3.2.16 NASA Capaciflector Proximity Sensor

The capacitive reflector (capaciflector) developed by NASA Goddard Space Flight Laboratory extends the range of capacitive-proximity sensors to 1 foot and more (Vranish, McConnell & Mahalingham, 1991), and thus shows as a potential collision avoidance device. The NASA objective is to produce a proximity-sensing skin for use on a electrically grounded robot arm (figure 56).

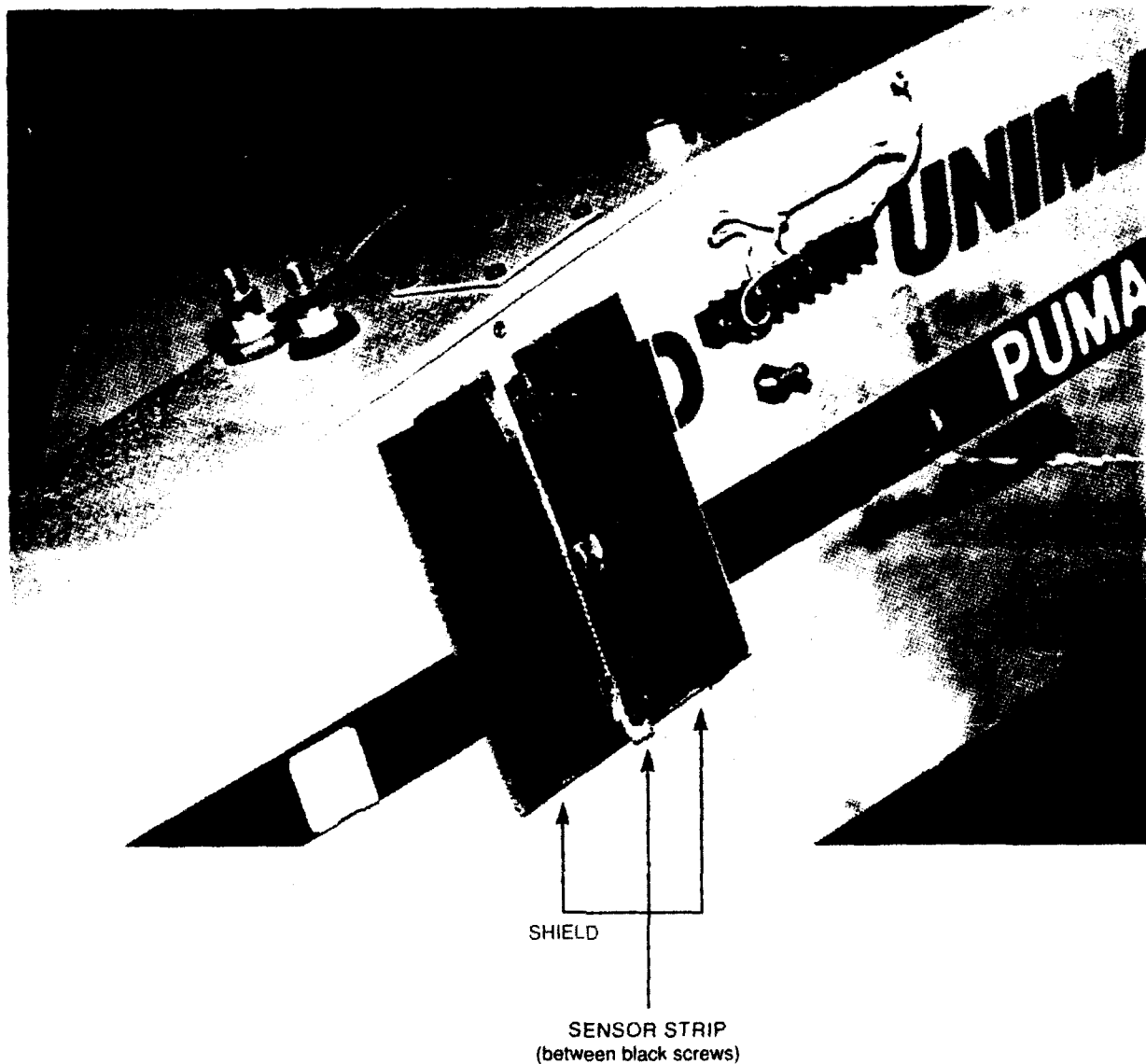


Figure 56. NASA's capaciflector mounted on the robot arm (Courtesy NASA Goddard Space Flight Laboratory).

To obtain the necessary ranges with conventional capacitive sensors would require mounting with a significant stand-off separation from the arm, adding unnecessary bulk as well as increasing cross talk between sensor elements (Vranish et al., 1991). To solve these problems, an instrumentation technique for controlling stray capacitance (Webster, 1988) was adapted to the problem of robotic collision avoidance. The resulting capaciflector is a capacitive-sensing element backed by a reflector element; both the sensor and the reflector are driven by the same voltage. Figures 57 and 58 illustrate the principles of operation in terms of electric field lines. The field lines from the sensor that would ordinarily return to ground (figure 57) are prevented from doing so by the reflector. These electric field lines are reflected back toward the obstacle (figure 58), effectively enhancing sensor-obstacle capacitive coupling.

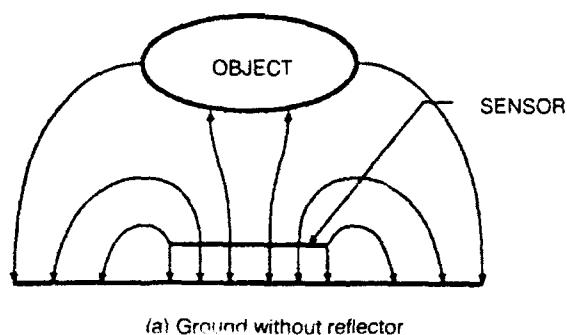


Figure 57. Illustrating the principle of the capaciflector: electric field lines without a reflector (Vranish, McConnell & Mahalingham, 1991).

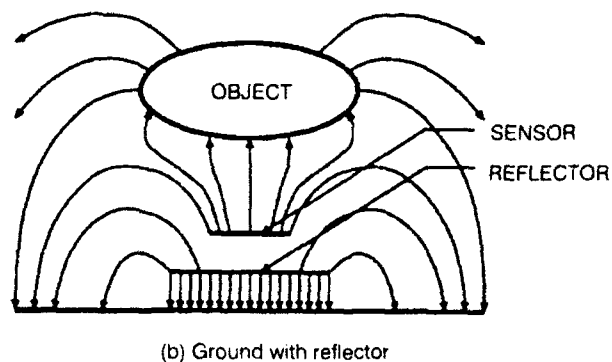


Figure 58. Electric field lines when a reflector is present (Vranish et al., 1991).

Figure 59 shows the electronic circuitry involved (Vranish et al., 1991). The total capacitive-coupling C_t (between sensor and obstacle, sensor and ground, and ground and obstacle) is the input capacitance tuning the oscillator, where V_0 is the oscillator's output frequency. As the range of the obstacle diminishes, the input capacitance increases and the oscillator frequency decreases. Used in a voltage-follower configuration, the reflector is in phase with and reflects the electric field lines emanating from the sensor. The reflector is unaffected by any changes in the sensor-obstacle coupling.

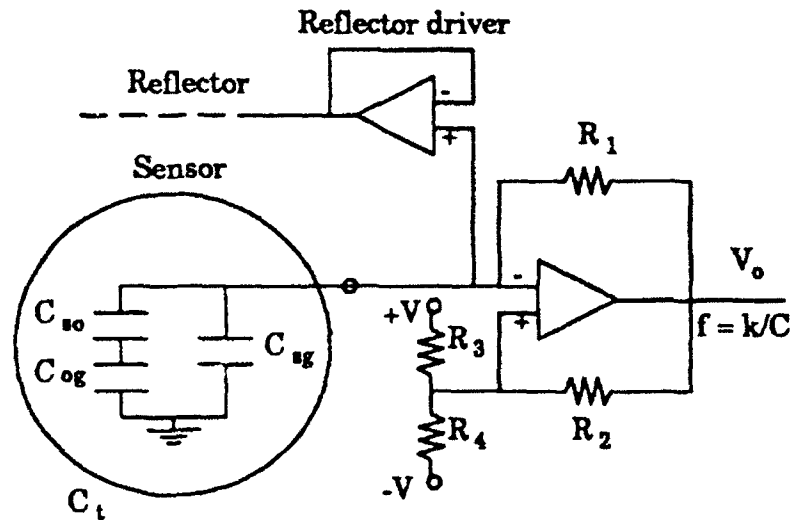


Figure 59. Schematic of the electronics of the capaciflector (Vranish, et al., 1991).

Selected Specifications:

Unable to obtain specifications.

Point of Contact:

John M. Vranish
 NASA Goddard Space Flight Laboratory
 Code 714.1
 Greenbelt, MD 20771
 (301) 286-4031

3.3 INTERESTING RESEARCH

3.3.1 Ultrasonic Scanning System

This ultrasonic ranging system, developed at Taiwan University and intended for installation on an intelligent mobile robot, employs a combination of time-of-flight and triangulation techniques for the detection and location of moving objects (Ma & Ma, 1984). The sensor consists of a square-pattern array of four ultrasonic transceivers that detect in pairs for measurement redundancy and improved reliability (figure 60). Range is determined by time-of-flight sensing for each of the active transducers, whereupon the position of the object is determined by triangulation.

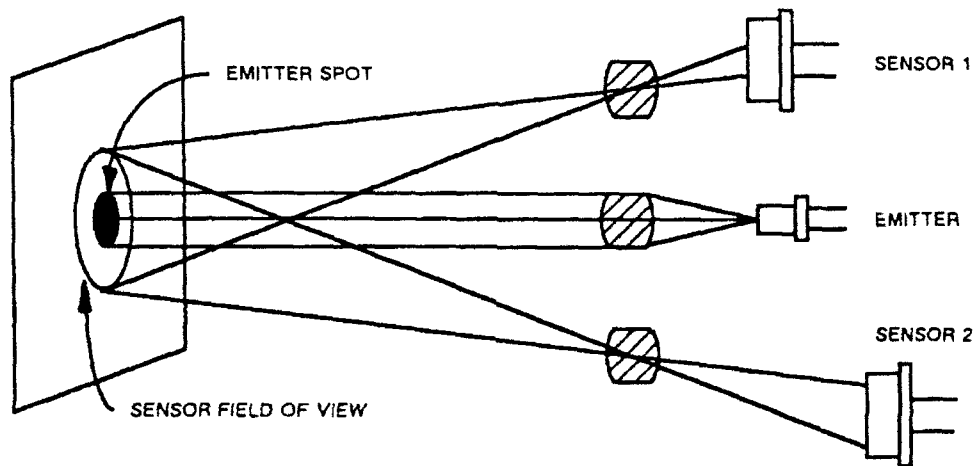


Figure 60. Block diagram of the Honeywell displaced sensor ranging system.

Detection capability is improved through the use of multifrequency transmissions obtained by selectively firing one of four transceiver drivers, each operating at a different frequency. The activation sequence is provided by a microprocessor controlled multiplexer. This capability takes advantage of the longer ranges characteristic of lower frequencies, and the directional nature and higher resolution afforded by higher frequencies. The term *scanning* refers to the dispersion of the ultrasonic energy over a wide field of view and to the added coverage afforded by multiple transducers, not to any electrical or mechanical slewing of the device.

Limitations of the present prototype include the occurrence of dead sensing spots due to the physical separation of the transducers (figure 61), and the narrow coverage area. There are problems in detecting multiple objects as well, because the control circuitry only accepts the first returned echo.

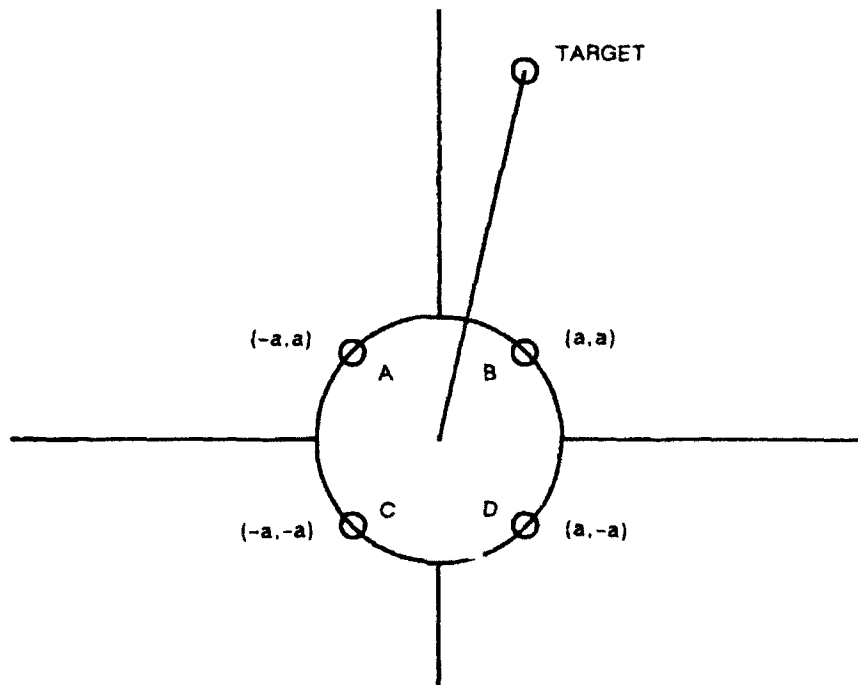


Figure 61. Target position is more precisely determined through a combination of time-of-flight ranging and triangulation using an array of four transducers (Ma & Ma, 1984).

3.3.2 HILARE

Early work performed at the Laboratoire d'Automatique et d'Analyse des Systemes, Toulouse, France involved the development of a navigation subsystem for the mobile robot HILARE based on ultrasonic rangefinders and near-infrared proximity detectors (Banzil et al., 1981). This research was part of a larger effort in the design and production of multisensor and multilevel decision systems for autonomous mobile robots.

The tracking subsystem of the HILARE robot used for determining vehicle position and orientation consists of two near-infrared emitter-detector pairs mounted 25 centimeters apart on a rotating vertical mast, used in conjunction with reflective beacons at known locations in three corners of the room. Each of the three beacons in turn is constructed of retroreflective tape applied to three vertical cylinders spaced in a recognizable configuration 25 centimeters apart (figure 62). One of the beacon configurations is inverted so as to be distinguishable from the others, for purposes of establishing an origin. The cylinders are vertically spaced so as to intersect the two planes generated by the rotating optical axes of the two sensor pairs on the robot. A detected reflection pattern (in figure 63) confirms beacon acquisition. Angular position is inferred from the stepper motor commands that drive the scanning mechanism.

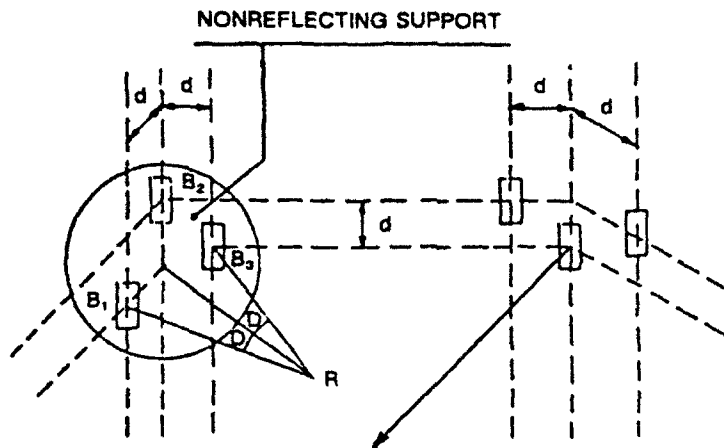


Figure 62. Vertical retroreflective cylinders used for navigation (Banzil et al., 1981).

NONREJECTED CASE

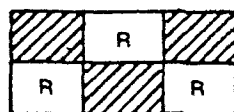


Figure 63. Detected reflection pattern confirms acquisition.

Ultrasonic transducers are employed for close-in obstacle avoidance and specialized navigation without using vision. (Specialized navigation includes traversing corridors, moving along walls, and circumventing obstacles.) The ultrasonic ranging subsystem uses 14 Philip EFR RSP 36K21 transceivers operating at 36 KHz with a 30-degree transmission dispersion. The transceivers determine range by time-of-flight methods, and can measure distances of about 2 meters with an accuracy of 0.5 centimeter.

3.3.3 Ultrasonics For Object Recognition

A high-resolution time-of-flight ultrasonic rangefinding system was developed at the Robotics Research Laboratory of the University of California, Davis, to overcome the limitations of grey-scale imaging techniques in object recognition (Dorf & Nezamfar, undated). The system consists of two ultrasonic transducers spaced close together on a platform capable of moving in three dimensions. One transducer transmits a highly directional 215-KHz narrow-beam (10 degrees) acoustic pulse, while the other transducer detects the returning echo. The update rate is 100 pulses per second with a resolution of ± 0.001 inch, but the maximum range is only 2 feet due to attenuation of the high-frequency beam in air.

Object recognition occurs in two steps. The learning phase takes the range data acquired from known objects, creates a descriptive model of the objects, and stores the models for later

use. The recognition phase involves observing objects in an unknown environment, obtaining range data points for the objects, and matching the resulting object descriptions to the stored models. Matching is region-based.

3.3.4 Ultrasonic Phased Array Rangefinder

Research at the Massachusetts Institute of Technology, Boston, MA, resulted in the design of a prototype multitransducer ultrasonic ranging sensor with improved angular resolution (Kim, 1986). The device arranges four Polaroid transducers in a linear array spaced 1-inch apart. By firing the transceivers in sequence with a uniform delay period, the additive and/or subtractive properties of the overlapping transmissions combine to form a highly directional beam with an adjustable dispersion angle. This phased-array sensor has a minimum effective range of 4.4 feet, below which the interelement phasing becomes increasingly harder to implement until the advantages of the array no longer surpass the capabilities of a single transducer.

The research discussion does not mention a specific maximum range for the sensor; however, the four transducer system is compared to a previously developed device with eight transducers which can range to 75 feet. The beam width (and angular resolution) can be electronically adjusted to suit the application requirements.

3.3.5 University of Michigan Ultrasonic and Infrared Sensor Fusion

The Navigation Group at the University of Michigan, Ann Arbor, MI, has nearly completed its research in ultrasonic and near-infrared sensor fusion as applied to realtime navigation and map building (Borestein, 1991). The objective was to improve the accuracy of sensor-generated maps, overcoming some of the shortcomings inherent with ultrasonic sensors (i.e., poor angular measurement accuracy and sensitivity to surface orientation).

To accomplish this, an assembly of 24 near-infrared range sensors was developed. The narrow-beam sensors were designed to measure 16 discrete ranges to a maximum range of 2 meters. Triangulation technology is employed to minimize sensitivities to target surface reflectivity and orientation. Upon completion of the interface electronics, the near-infrared assembly was installed aboard CARMEL, a robotic vehicle, developed by Dr. Yoram Koren (Miller, 1991). The near-infrared assembly is capable of obstacle avoidance and environmental mapping. Each near-infrared sensor in the assembly of 24 looks in the same direction as a previously-mounted ultrasonic sensor. Figures 64 and 65 illustrate the simultaneous beam patterns formed when (1) the measurements taken by the ultrasonic sensor does not agree with that taken by the infrared sensors, and (2) when the ultrasonic sensor measurements do agree.

Producing more accurate maps with this system involves a sensor-fusion algorithm based on heuristic rules. The fusion (or preprocess verification) algorithm is applied to the combined sensor data, where it evaluates the readings before updates to the histogram grid are made. When a cell in the histogram grid is updated, its associated level-of-confidence or certainty value is modified accordingly. Three versions of the preprocess verification algorithm have been implemented, differing in the complexity of comparison.

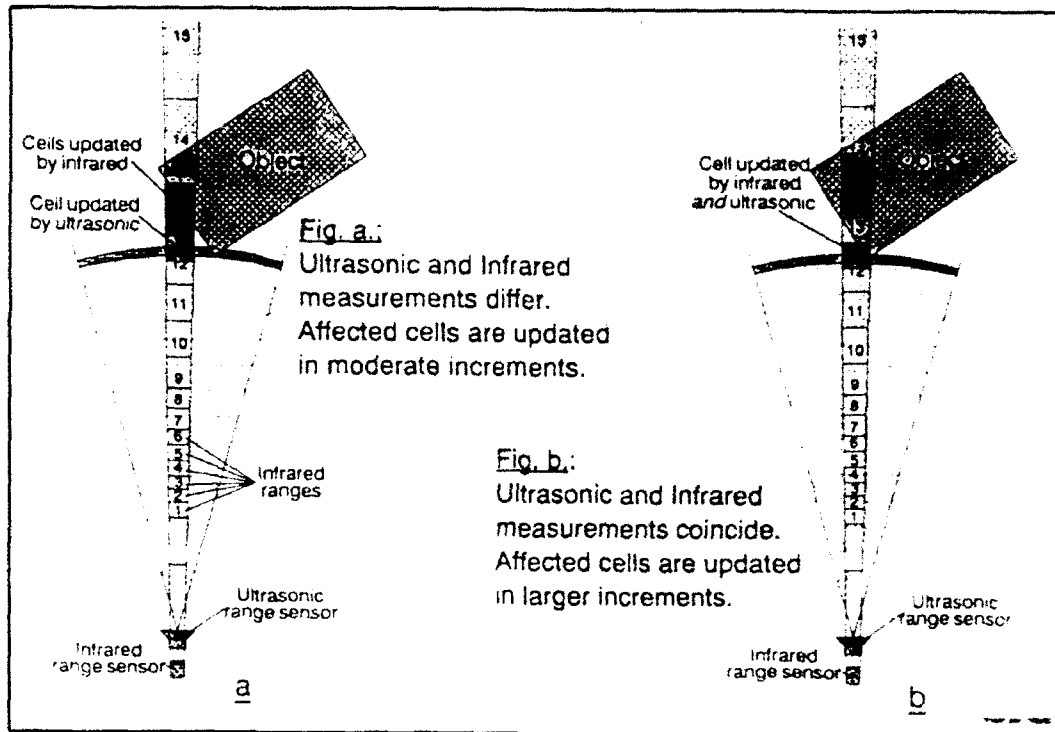


Figure 64. Simultaneous beam projections when the measurements differ (University of Michigan Mobile Robotics Laboratory, 1991a).

Figure 65. Simultaneous beam projections when the measurements coincide (University of Michigan Mobile Robotics Laboratory, 1991a).

Performance is measured in centimeters as a physical distance, which represents the weighted average distance between each filled cell in the histogram grid and the nearest actual obstacle boundary. This performance indicator serves to quantify the improvement resulting from the fusion of ultrasonic and near-infrared sensor data with respect to ultrasonic data only. A typical result gives a performance measure of 9 centimeters with the preprocessing verification algorithm active, as opposed to 14 centimeters using ultrasonic sensors only.

Qualitatively, the map generated by the fusion algorithm appears to have better definition and is generally smoother. The work remaining includes further refinement of the heuristic rules implemented in preprocess verification. Additional improvement can be likely achieved by increasing the number of discrete ranges, currently 16, seen by each near-infrared sensor (University of Michigan Mobile Robotics Laboratory, 1991b).

Point of Contact:

Dr. Yoram Koren
MEAM Mobile Robotics Laboratory
University of Michigan
2250 G. G. Brown Bldg/or 1101 Beal Avenue
Ann Arbor, MI 48109-2106
(313) 936-3596

3.3.6 University of Minnesota Ultrasonic Range Sensing Array

A reconfigurable ultrasonic range sensing array, presently configured as a ring, was designed and developed for use on a mobile robot platform. This range sensing ring provides the mobile robot with the position of surrounding objects that exist in the mobile robot's environment. A block diagram of the ultrasonic range sensor hardware components is shown in Figure 66.

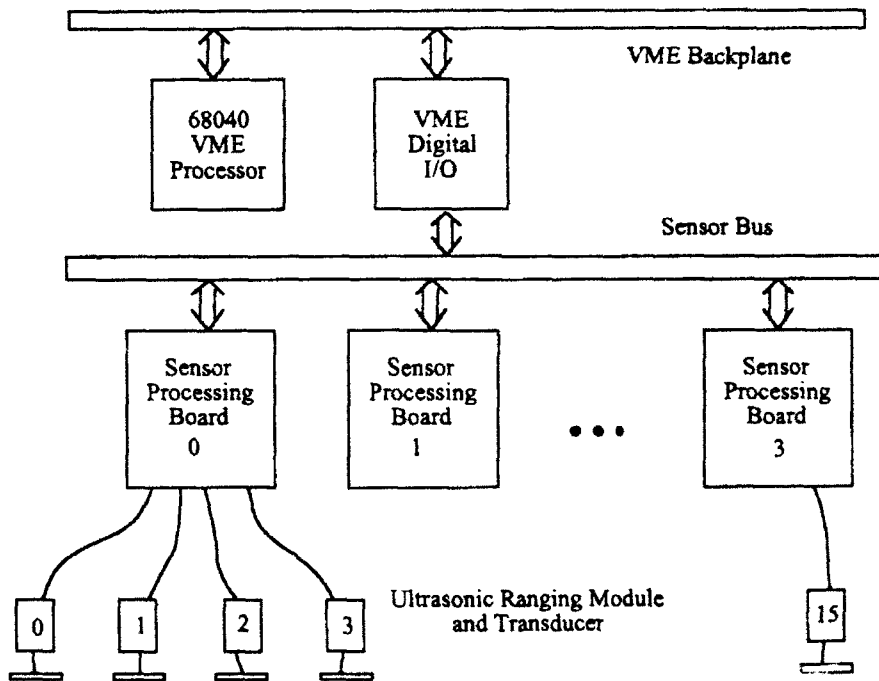


Figure 66. Ultrasonic range sensing array system design
(University of Minnesota Robotics Laboratory, 1992).

In the present configuration, four Polaroid ultrasonic sensors (based on the Model 7000 transducer and a modified version of the 6500 series sonar ranging module) are interfaced to each of four custom-designed sensor processing boards, providing the mobile robot with a total of 16 sensors in a ring. Each sensor processing board provides independent control and timing for four ultrasonic range sensors. Up to 8 of these sensor processing boards (handling a total up to 32 sensors) can be connected via a custom sensor bus to a digital parallel I/O board located in any computer bus. (A VME bus is used.) This digital I/O board is mapped to the VME short I/O address space where it is accessed by the VME processor. Software for accessing and controlling each sensor processing board can be executed on any VME based CPU. (Currently, the software

runs in the background on a Motorola 68040-based MVME167 processor.) This software was developed on a SparcStation IPC using standard Unix program development tools, and the GNU C cross-compiler. Compiler-generated object code was downloaded across Ethernet to the VME processor and dynamically linked with VxWorks, a multitasking realtime operating system. For each sensor, and application program running on the VME processor can independently address and set the near and far range limits, set the range resolution and map it to fit between the near and far range limits, fire a sensor, detect and time the returned echo, and reset the sensor.

The ultrasonic range processing boards provide all lower level processing of the raw Polaroid sensor signals and provide an interface that is readily connected to the VME processor. A layout of each processing board is shown in Figure 67.

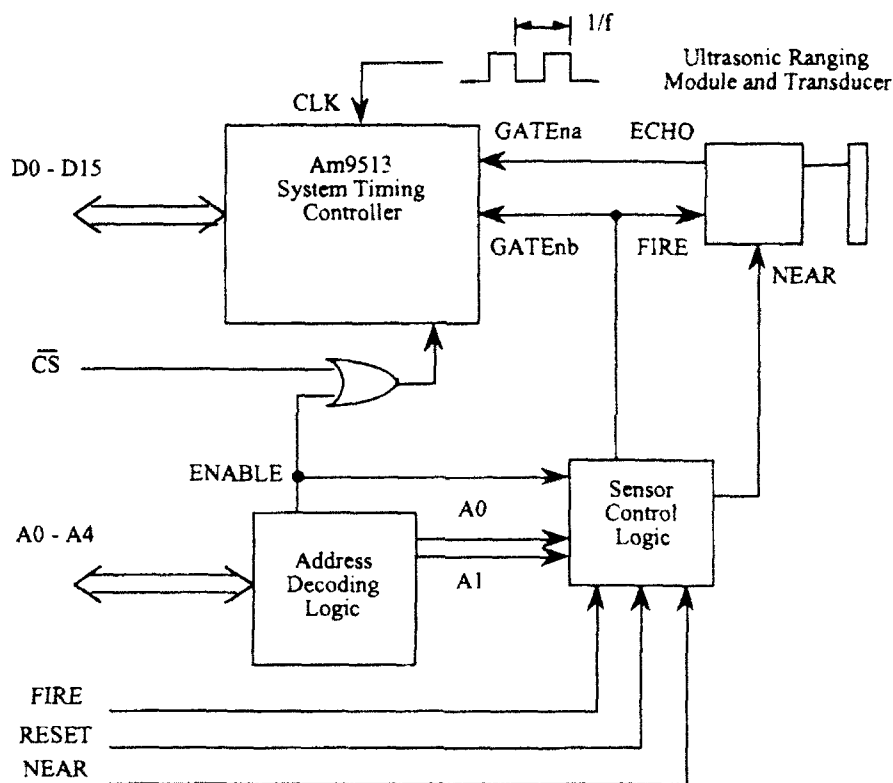
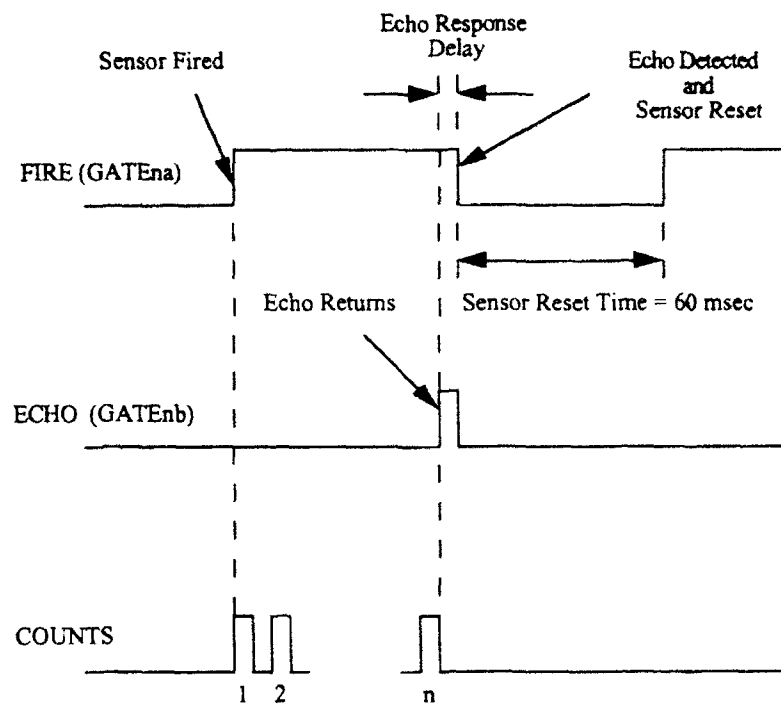


Figure 67. Schematic of ultrasonic processing board (University of Minnesota Robotics Laboratory, 1992).

The Am9513 System Timing Controller from Advanced Micro Devices, the main component on the sensor processing board, provides control and timing for each sensor. In addition to the Am9513, each board contains components that provide address decoding so that each board can be uniquely identified and independently accessed. Figure 68 shows a timing diagram that illustrates operations performed by the Am9513.



$$2 \times \text{Range} = \frac{(\text{Speed of Sound}) (n \text{ COUNTS})}{\text{Frequency}}$$

Figure 68. Ultrasonic sensor timing diagram (University of Minnesota Robotics Laboratory, 1992).

Two signals from each sensor, FIRE and ECHO, are interfaced to the Am9513. The FIRE signal is used to fire the Polaroid sensor and to initiate the Am9513 counting sequence, which counts pulses at a predetermined counting frequency. The FIRE signal is activated by the command from the VME processor. The ECHO signal indicates a returned echo from the Polaroid sensor and terminates the AM9513 counting sequence. The VME processor senses the ECHO line and resets the sensor so another firing sequence can be initiated. At the end of a counting sequence, the Am9513 holds the current count that is proportional to the time it takes for an ultrasonic pulse to leave the Polaroid sensor, hit an object, and return to the sensor. The count is retrieved by the VME processor through the VME Digital I/O board, interfaced in turn to each sensor processing board via the custom sensor interface bus.

The near and far range limits of each sensor are software adjustable with the closest near range limit of 4.5 inches and the farthest far range limit of 35 feet. The range resolution is 16 bits and can be scaled through software to fit the selected far range limit. The sampling frequency for all 16 sensors in the ring varies from 5 to 8 Hz for objects depending on the selected far range (for between 5 and 20 feet).

The current sensor design based on 16 sensors has been implemented and tested on a mobile robot at the University of Minnesota's Robotics Laboratory and on a robot located at the U.S.

Army Armament Research Development and Engineering Center (ARDEC) at Picatinny Arsenal in New Jersey. An upgrade to include a total of 32 sensors and 8 sensor processing boards is planned for the near future. The system is presently being used in a number of collision avoidance, landmark recognition and mapping research projects which follow up on work reported earlier (Anderson and Donath, 1990).

3.3.7 Error Eliminating Rapid Ultrasonic Firing

Error Eliminating Rapid Ultrasonic Firing is a method whereby the effects of noise on group of ultrasonic ranging sensors is minimized and the sensor firing rate for the group maximized. The University of Michigan Mobile Robotics Lab (Borenstein & Koren, 1992, University of Michigan Mobile Robotics Laboratory, 1991b), has defined three types of noise:

- Environmental noise resulting from the presence of other functional devices operating in the same space (a continuous disturbance)
- Cross talk or environmental noise resulting from the proximity of other sensors in the group (a discrete disturbance)
- Self noise, generated by the sensor itself.

A noise rejection measure for each of the components was developed and integrated into a single rejection algorithm, which was in turn combined with a fast sensor firing algorithm. This combination noise-rejection fast-firing algorithm has been implemented and tested onboard a mobile platform that was able to traverse an obstacle course of densely packed 8-millimeter diameter poles at a maximum velocity of 1 meter/second.

Point of Contact:

Dr. Johann Borenstein
Yoram Koren
MEAM Mobile Robotics Lab
University of Michigan
1101 Beal Avenue
Ann Arbor, MI 48109-2110
(313) 763-1560

3.3.8 Potential Field Obstacle Avoidance for Large Mobile Robots

The University of Michigan Mobile Robotics Laboratory, Ann Arbor, MI, has developed a method for realtime obstacle avoidance specifically designed for mobile robots carrying an overhanging payload (Borenstein & Raschke, 1991). By combining two obstacle avoidance methods previously developed at the lab, a large oddly shaped platform can safely and reliably navigate in close proximity to obstacles in a confined space, while using data acquired by relatively inaccurate detection sensors.

This technique is referred to as the combined vector field method, and incorporates the vector field histogram approach (which determines the principal steering direction) and the virtual force field approach, (which applies virtual forces as corrective measures) taking into account the vehicle's dimensions.

The virtual force field method is specifically designed to accommodate and compensate for inaccurate reading from ultrasonic and other ranging sensors. To represent the world as seen by

the vehicle, a two-dimensional cartesian histogram grid is employed. Range data are represented in cells of the histogram grid as certainty values, or measures of confidence relating to the perceived presence of an obstacle, each cell representing a 10- by 10-centimeter square. As the vehicle moves, a subset of the complete histogram grid is highlighted by an overlying window, 30 by 30 cells (figure 69).

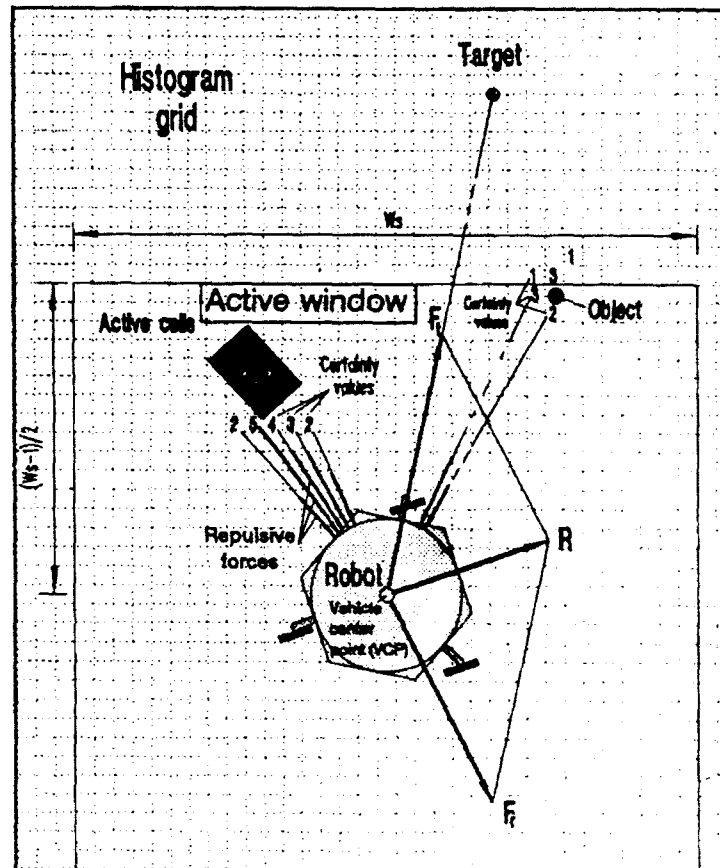


Figure 69. Schematic of the Virtual Force Field concept (University of Michigan Mobile Robotics Laboratory, 1991b).

The active cells within the windowed region exert repulsive forces upon the vehicle. The magnitudes of these forces are proportional to the individual certainty values, and inversely proportional to the squared distance between the respective cells and the center of the vehicle. The vector sum of all repulsive forces yields the resultant force, F_r .

Simultaneously, an attractive force of constant magnitude, F_t , is acting on the vehicle, effectively pulling it towards the destination target. Summing the vectors F_r and F_t yields the resultant vector R , which provides the steering direction reference for the robot.

The virtual force-field approach possess certain inherent problems:

- Trap situations due to local minima
- No passage between closely spaced obstacles
- Oscillations in the presence of obstacles
- Oscillations in narrow passages

These problems were overcome in the vector-field histogram algorithm.

The vector-field histogram algorithm builds a histogram in the same way as the virtual force-field method, but introduces an intermediate data representation called the polar histogram. This approach reduces the amount of data that must be handled. The polar histogram maps the Cartesian histogram grid into 72 discrete 5-degree radial sectors representing instantaneous obstacle density. After generating the polar histogram, the vector-field histogram algorithm computes the required steering direction for the vehicle.

Figures 70 and 71 show the polar histogram has peaks and valleys corresponding to high and low certainty values found in the cartesian grid. Figure 70 shows the actual location of obstacles; figure 71 shows this same obstacle pattern as an overlay of the two mapping algorithms: the VFF cartesian grid and the VFH polar histogram. In the Cartesian grid, the size of the black blobs is indicative of certainty, the larger the blob, the greater the associated certainty value. Likewise, the length of a radial sector is indicative of obstacle density. Any sector with an instantaneous polar density less than some threshold value represents a potential direction travel.

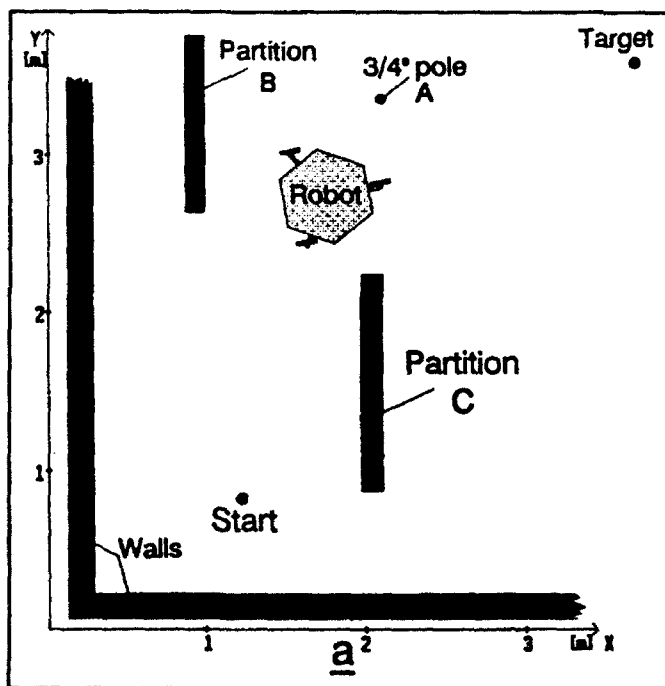


Figure 70. Schematic of the laboratory obstacle course (Borenstein & Raschke, 1991).

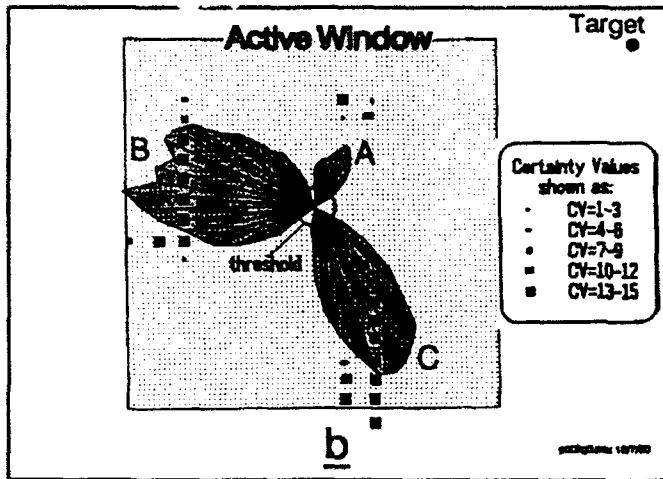


Figure 71. After interrogating the environment, a composite schematic is generated from a polar histogram overlaying the cartesian histogram grid (Borenstein & Raschke, 1991).

This research was sponsored by the Department of Energy Grant No. DE-FG02-86NE37969.

Point of Contact:

Dr. Johann Borenstein
 MEAM Mobile Robotics Lab
 University of Michigan
 1101 Beal Avenue
 Ann Arbor, MI, 48109-2106
 (313) 763-1560

3.3.9 Ground Vehicle Automatic Guidance System

An interesting application of laser rangefinding being pursued in Japan involves the automation of the world's highways. A prototype automatic lateral control system for automobiles is under development to handle the problem of keeping a vehicle at a predetermined position and direction within a traffic lane of a roadway. The combination time-of-flight/triangulation sensor incorporates a scanning laser system attached to the vehicle as an active sensing source, and corner-cube prisms distributed along the roadside as a passive reference system (Tsumura et al., 1984).

The scanner, which produces a fan-shaped laser plane, pans the plane back and forth while tilting the elevation of the plane in search of the corner-cube reference points. When the laser energy encounters a cube, the beam is reflected back to a photodetector for time-of-flight processing. Once the reflected light is detected, the pan and tilt angles are measured.

By measuring to two established reference points, the lateral position and direction of a vehicle relative to a desired path can be calculated (figure 72). The panning motion provides a forward-looking capability important to negotiating curves and other changes in the roadway. The scanner uses a 5-milliwatt HeNe laser with a 20-degree dispersion angle. The scanning frequency is 30 Hz, with an angular resolution of 0.15 degree. Position and direction are determined every half cycle of the plane scan.

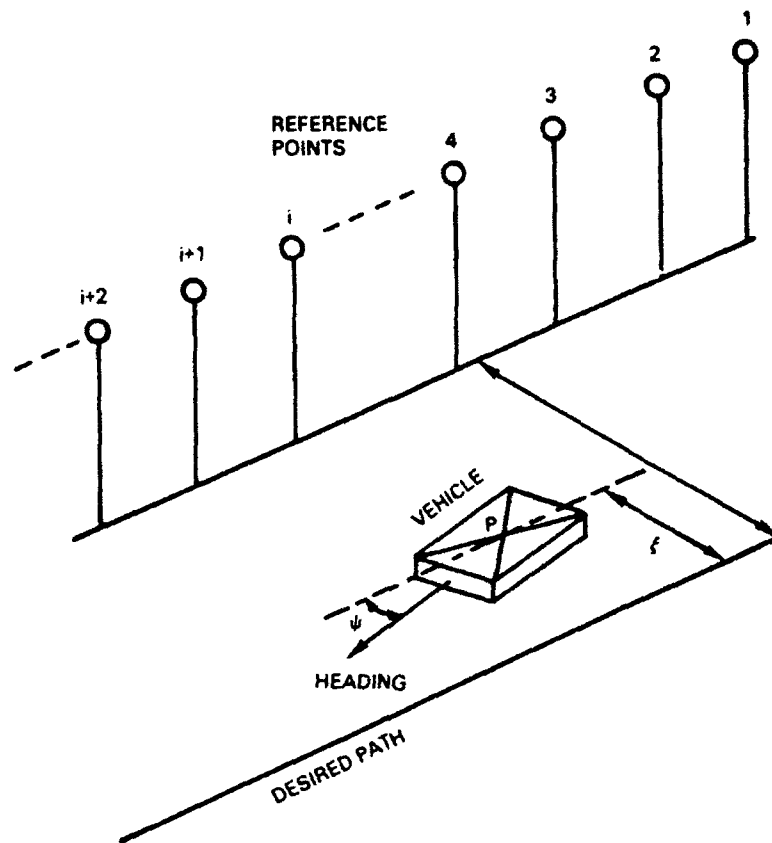


Figure 72. Retroreflectors placed alongside a roadway are used as reference in a proposed automatic lateral positioning scheme (Tsumura et al., 1984).

3.3.10 Vehicle Location By Laser Ranging

A development out of the Institut National des Sciences Appliquees, Codex, France, uses an active triangulation scanning laser rangefinder to determine the position and orientation of a mobile robot operating in a known environment. Location is determined by detecting edges of cylindrical polyhedral obstacles, then matching their perceived positions with a known model of the environment.

The first step in this process involves the creation of a visibility map for the specific surroundings. The general location of the vehicle is calculated by counting the number of edges seen by the robot from its current position in the map. This scheme is based on the assumption that from any given position in a known world, only a portion of the total points or object vertices can be viewed. Once the rough location of the robot is determined in this fashion, the absolute position is calculated from direct measurement to the observed vertices by the rangefinder. Ranging is accomplished through simple triangulation, using a 10-milliwatt HeNe laser mounted on a scanning platform. Detection of the reflected beam is performed by a 1024-element linear CCD-array Reticon camera.

3.3.11 Australian National University Laser Ranger

Early work performed at the Australian National University produced a near-infrared laser range scanner using time-of-flight methods for three-dimensional scene analysis of a robotic environment. The system consists of a 2.5-watt Hamamatsu pulsed laser that emits near-infrared pulses at a cycle rate of 10 KHz. The corresponding detector is an RCS type C31034 photomultiplier with high sensitivity and excellent response in the near-infrared range. This arrangement proved to be relatively economical in comparison with phase modulation type laser ranging systems (Jarvis, 1983b). The sensor was designed for use at ranges up to 4 meters and achieved an accuracy of ± 0.25 centimeter over that range when 100 samples per point were obtained.

The system also was given a scanning capability implemented through use of high-speed galvanometer-driven mirror components. A 64- by 64-element range picture could be obtained within 4 seconds when only 10 samples per point were obtained, with some sacrifice in accuracy. A low-power CW laser emitting in the visible red spectrum was incorporated into the sensor system for use in associating range data with image data for scene analysis.

3.3.12 Case Western Reserve University Scanning Rangefinder

Researchers at Case Western Reserve University have developed a compact scanning laser rangefinder that measures distance by triangulation (Nimrod et al., 1982). Intended specifically for use in robotic applications, the sensor incorporates a solid-state CW laser with a position-sensitive photodetector. The scanning action is generated by the sweep of a mirror that directs the beam in a horizontal plane. The reflected energy is collected by a synchronized receiving mirror offset from the transmitting mirror and then relayed to the photodetector through a focusing lens. Range is determined by inserting the known or measured values into the equation:

$$R = \frac{1}{2} B \tan \theta$$

where R = range to the target,

B = baseline distance between mirrors,

θ = angle of incidence of the laser source.

3.3.13 Rutgers Wide Field Of View Rangefinder

An experimental scanning laser rangefinder developed at Rutgers University uses active triangulation to create a robotic sensor capable of wide-field viewing. The sensor consists of a HeNe laser transmitting at a wavelength of 632.8 nanometers and an RCA 4840 photomultiplier single-element detector with an optical bandpass filter to minimize ambient lighting effects (Pipitone & Marshall, 1983). The laser and detector are housed in individual scanning mechanisms separated by a known distance along one of the axes of rotation, and mechanically synchronized to move in unison.

Scanning takes place in two dimensions and is based on spherical coordinates. Besides calculating the range for individual points, the system also generates a pseudocolor display of the overall range picture, where different colors represent relative range values. The sensor is capable of observing a maximum of 500 pixels per second, and can range out to approximately 300 inches.

3.3.14 Obstacle Avoidance For Mobile Robots

Work performed at Rensselaer Polytechnical Institute for the Defense Advanced Research Projects Agency (DARPA) resulted in a prototype scanning laser-triangulation system for obstacle detection and avoidance. The sensor was originally designed for the Mars Rover project but shifted to DARPA's Adaptive Suspension Vehicle effort at Ohio State University, Columbus, OH.

The system consists of a solid-state pulsed laser mounted on a continuously rotating mast. The laser is scanned across the ground from 1 to 3 meters in front of a robotic vehicle through the incremental rotation of the mast in azimuth, and in elevation through the step-wise rotation of an eight-sided directional mirror. Reflections from the scanned beam are detected by a linear array of 20 photodiodes also mounted on the revolving mast (Gisser, 1983).

3.3.15 Laser-Based Hazard Detection Sensor

A prototype obstacle detection and avoidance sensor is being developed by Cambridge Robotic Systems for application to the Army's Autonomous Countermine Vehicle Program. The sensor scans a near-infrared laser beam in azimuth by using a galvanometric mirror arrangement that causes the energy to strike the ground 30 meters in front of the vehicle. The scan produces a horizontal straight-line trace on the image of the scene, which is detected by a charge-coupled device (CCD) camera. The laser and camera are colocated with a synchronized scan rate of 30 frames per second.

As the vehicle approaches an object, the sensor trace will initially strike the object at its base, which is in contact with the ground. As the vehicle advances, the portion of the line not falling across the object will illuminate the ground behind it, while the line segment in contact with the target will move up the object's surface. This phenomenon will appear in the image of the scene as a break in the line.

The width of the observed discontinuity and its vertical displacement from the original trace are proportional to the width and height of the detected body. If the discontinuity surpasses a threshold value, the object is classified as an obstacle, and the vehicle reacts to avoid it. Height accuracy of the system is about 15 centimeters, while width accuracy is approximately 10 centimeters.

3.3.16 Active Two-Dimensional Stereoscopic Ranging System

ROBART II is a battery-powered autonomous sentry robot being used by the Naval Command Control and Ocean Surveillance Center, RDT&E Division, San Diego, CA, as a research testbed. An architecture of 13 distributed microprocessors makes possible advanced control strategies and realtime data acquisition. Numerous sensors are incorporated into the system to yield appropriate information for use in collision avoidance, navigational planning, environmental awareness, assessing terrain traversability, and performing security-related functions. ROBART II is a continuation of previous work begun at the Naval Postgraduate School, Monterey (Everett, 1982).

An array of nine Polaroid ultrasonic transducers is installed on the front of the body trunk to provide distance information to objects in the path of the robot (Everett et al., 1990). The

sequentially fired array is controlled by a dedicated microprocessor, which performs all time-to-distance conversions and then passes the range information up the control hierarchy. An additional Polaroid sensor is located on the rotating head assembly, allowing for range measurements to be made in various directions as required.

A stereoscopic vision system provides for additional high-resolution data acquisition, and is the robot's primary means of locating and tracking a homing beacon on the recharging station (figure 73). The system does not represent a true three-dimensional capability; each of the cameras consists of a horizontal linear (as opposed to two-dimensional) CCD array (Everett & Bianchini, 1987).



Figure 73. Active Stereoscopic Ranging System used on ROBERT II.

The cameras in effect provide no vertical resolution, but furnish range and bearing information on interest points detected in the horizontal plane coincident with their respective optical axes, 110 centimeters above the floor. This limitation is consistent with the two-dimensional simplified world model employed by the robot; objects are represented by their projection on the X-Y plane, and height information is not taken into account.

A structured-light source is employed in conjunction with these stereo cameras for ranging purposes. A 6-volt incandescent lamp is pulsed at about a 10-Hz rate, and projects a sharply defined V-shaped pattern across the intersection of the camera plane with the target surface. This active illumination greatly improves system performance when viewing scenes with limited contrast. The incandescent source was chosen over a laser-diode emitter because of simplicity, the response characteristics of the CCD arrays, and the limited range requirements for an indoor system (Everett, 1985d).

3.3.17 Programmable Near-Infrared Proximity Sensor

A special programmable near-infrared proximity sensor was developed specifically for use on the prototype sentry robot Robart II (Everett & Flynn, 1986), to gather high-resolution geometric information for purposes of navigation and collision avoidance. The primary purpose was to provide precise angular location of prominent vertical edges, such as door openings. A Polaroid ultrasonic ranging sensor was used in conjunction with the system to provide range data (figure 74).

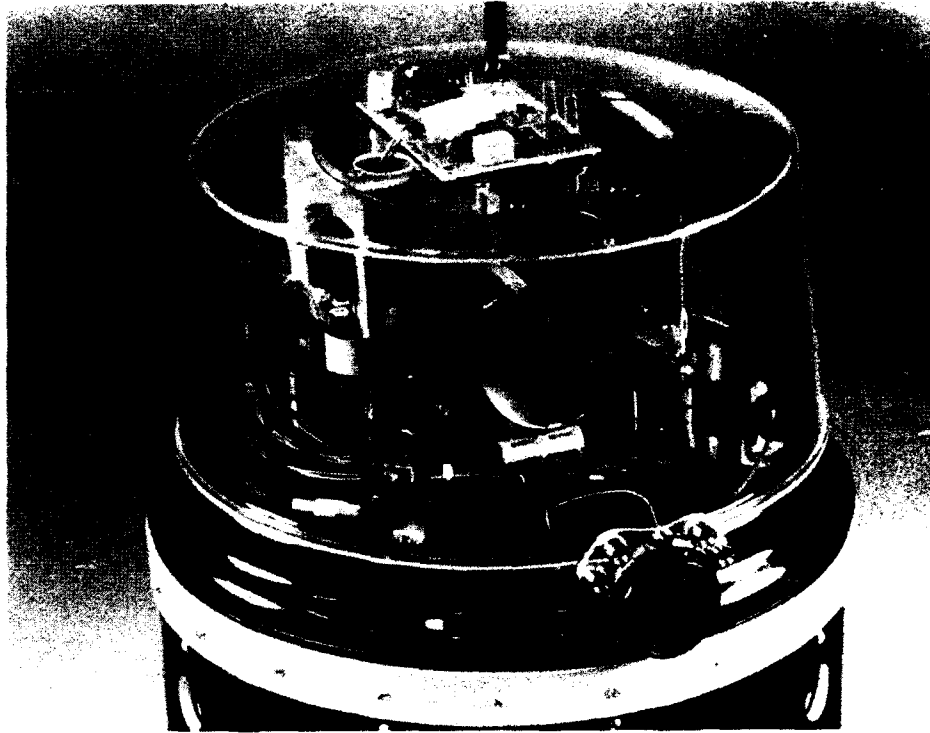


Figure 74. Programmable Near-Infrared Proximity Sensor used on ROBERT II.

An astable multivibrator produces a square-wave train of 15 microsecond pulses with a repetition period of 1.7 milliseconds, driving high-power XC-880-A gallium aluminum arsenide LEDs, which emit energy in the near-infrared spectrum. The system uses an array of adjacent LEDs for increased range and sensitivity, with reflected energy focused on the lens of a TIL413 photodiode by a parabolic reflector.

The output of this photodiode is passed through an L/C differentiator network, amplified, and then fed to four separate follow-on threshold detector stages. The receiver sensitivity is broken into four discrete levels by these individually adjustable threshold comparators. A strong return causes all four channels to go low, whereas with a weak return only the most sensitive channel indicates detection. No range information is made available, other than that inferred from the strength of the returned energy.

Unfortunately, the varying reflectivities of different surfaces preclude signal strength from being a reliable indicator of distance. This limitation turns out to be more a function of surface

topography than of surface color; varying surface characteristics create uncertainties that inhibit the establishment of a practical correlation between signal strength and target distance.

Effective range is controlled by limiting the total light intensity emitted from the LEDs; LEDs are activated singularly or in groups. Each LED emits a regulated amount of energy, and increased range is obtained by illuminating the scene with more LEDs. The maximum range of the sensor is 6 feet with one LED active, 10 feet with two LEDs active, 13 feet with three, and 15 feet with four LEDs. The number of enabled LEDs in the array at any given time is specified by a microprocessor, providing programmable control over the amount of emitted energy.

The data protocol employed for communicating the information to the robot is of the form of a single byte in which the upper nibble represents the number of LEDs that were fired before a reflection was observed, and the lower nibble represents the number of comparators in the receiver threshold detection stage that responded to the returned energy.

3.3.18 Return Signal Intensity Rangefinder

A monocular ranging technique developed at the Australian National University determines range from the return signal intensity of a pair of light sources (Jarvis, 1984). The two sources are arranged with a camera detector along a common optical axis that is focused on an object surface. The displacement between the sources will result in differing quantities of returned energy that are related to distance by the inverse-square law.

The experimental system developed for evaluation of the technique used slide projectors as the light sources. Sensitivity improved as the distance between the sources was increased. Although the prototype was capable of measuring range over uniform textured or colored surfaces, it encountered difficulty when observing multicolor nonplanar targets.

3.3.19 MIT Near-Infrared Ranging System

An experimental near-infrared ranging sensor based on the concept of return signal intensity was developed by Jon Connell at the Massachusetts Institute of Technology, Boston, MA. The sensor system consists of two near-infrared LEDs mounted a known distance apart, with a single phototransistor detector. The LEDs are fired in sequence at a target of interest, and the reflected energy from each one is detected by the phototransistor and measured by an analog-to-digital converter. By the inverse square law, the recorded intensity is inversely proportional to the square of the roundtrip distance traveled.

Furthermore, the difference in the resulting intensities caused by the offset in the distance between the LED emitters can be used to solve for the range value:

$$r = \frac{d}{\sqrt{\left(\frac{B_1}{B_2}\right) - 1}}$$

where r = the range to the target
 d = the distance between emitters
 B_1 = intensity of return for LED 1
 B_2 = intensity of return for LED 2

The basic assumptions made in the design are that all surfaces are Lambertian in nature and that the observed objects are wider than the field of view of the LEDs. Ambient light interference is

reduced by blinking the LED's and synchronizing the detector to look for this on and off sequence of energy returning from the observed scene.

3.3.20 Passive Ranging and Collision Avoidance Using Optical Flow

Optical flow may be represented in the form of an image, where each pixel has associated with it an instantaneous velocity vector representing the image motion at that point. The method of flow extraction employed by the National Institute for Standards and Technology (NIST), Gaithersburg, MD, assumes that the camera is moving in a stationary world and that the camera motion is known (Herman & Hong, 1991). These assumptions lead to two conclusions: (1) the optical-flow field in the image (i.e., the flow direction at every point) can be predicted, and (2) once the optical flow has been extracted, the flow vectors can be easily converted to range values. These conclusions are true for arbitrary camera motion, including pure translation, pure rotation, and a combination of translation and rotation.

By assuming that the flow field can be predicted, one will know the true flow-vector directions. To extract optical flow, only the magnitudes of the flow vectors need to be computed, minimizing computation. Knowledge of the flow field allows one to use local image operators (for extracting information) that can run in parallel at all points in the image, further minimizing computation time. This method proves to be highly accurate, as the vector directions are accurately known in advance. NIST has implemented three optical extraction techniques:

- Spatial and temporal derivatives
- Spatio-temporal imagery
- Temporal cross-correlation

Point of Contact:

Marty Herman
National Institute for Standards and Technology
Building 200, Room B124
Gaithersburg, MD 20899

3.3.21 Recovering 3D Scene Structure from Visual Data

Researchers at David Sarnoff Research Center have developed algorithms for recovering scene geometry from passively acquired binocular and motion imagery. These algorithms can recover the range, 3D orientation, and shape of viewed objects.

Distance measurements are derived from intensity derivatives of two or more images of the same scene. The approach combines a local brightness constancy constraint with a global camera motion constraint to relate local 3D range with a global camera model and local image intensity derivatives. Beginning with initial estimates of the camera motion and local range, the range is refined using the global camera motion model as a constraint. The global camera motion model is then refined using local range estimates as constraints. This estimation procedure is iterated several times until convergence. The entire procedure is performed within a (spatially) coarse-to-fine algorithmic framework. Currently, implementation of this technology has made use of a commercial CCD camera and frame grabber for image capture coupled with a workstation to perform the actual range recovery in nonrealtime.

Figure 75 shows a representative result. The left panel shows one image from a pair. The right panel shows the recovered range map, with brighter regions closer to the camera. The recovered range is plausible almost everywhere except at the image border and near the focus of expansion, near the image center. Limitations of this approach are two-fold. First, the basic formulation assumes that camera motion is small between captured images and that the image intensity of the same point between images is constant (brightness constancy); violation of either of these constraints can lead to erroneous results. Second, current estimates for a realtime implementation in commercially available hardware suggest that power requirements will be approximately 60 watts. Additional technical details on this technology can be found in Hanna (1991).

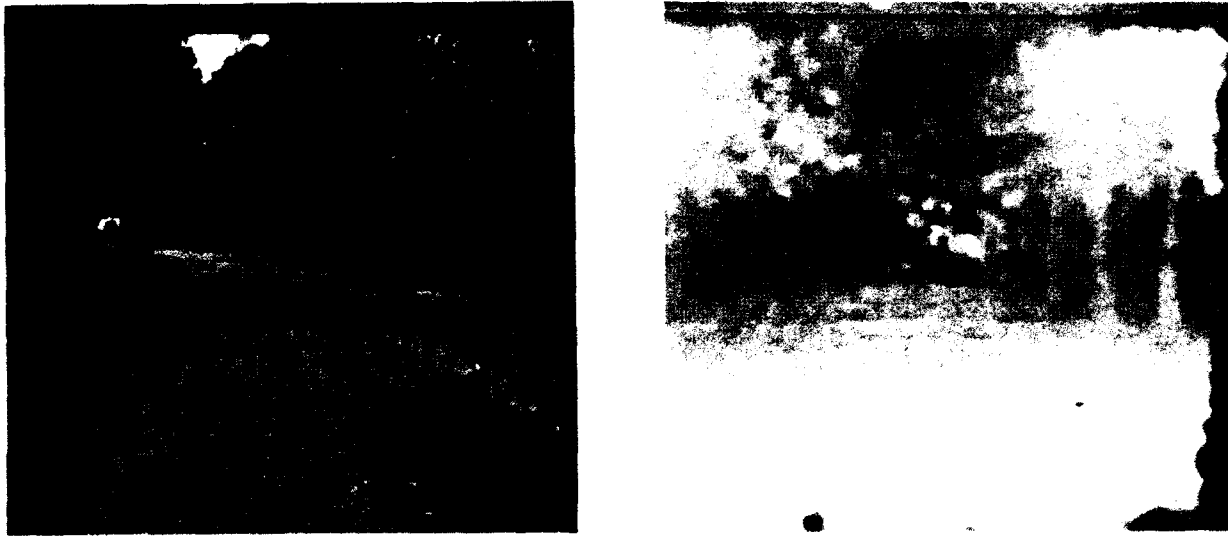


Figure 75. Recovery of 3D Range from Binocular Imagery (Wildes, 1991).

The recovery of 3D attitude (orientation) and surface curvature (shape) can be recovered from binocular images without ever explicitly recovering range information. The underlying approach relies on exploiting the relationship between the differential orientation of matched image features and the 3D orientation of the corresponding scene structure. In particular, the differential orientation of matched image features allows for recovering 3D attitude and curvature via simple least squares algorithms. Further, extensive error analysis shows that these relationships are highly accurate and robust. Algorithmically, a binocular image pair is captured with a calibrated stereo rig. From these images, oriented features (e.g. edges) are extracted. Corresponding features are then matched. Finally, depending on the need for attitude or curvature information, one of two linear least-squares estimation procedures is invoked to yield the desired parameters. Currently, implementation of these technologies has made use of a commercial CCD camera and frame grabber for image capture coupled with a workstation to perform the actual attitude and curvature recovery in nonrealtime.

Figure 76 shows a representative result for the recovery of 3D attitude. The top left and right images comprise a binocular image of a tilted surface. The lower left panel shows the recovered gradient direction superimposed on the original image. The lower right panel shows the amount of slant along the gradient direction. Figure 77 shows a representative result for the recovery of 3D surface curvature. The left and middle images comprise a binocular image of a curved

surface. The left image shows the recovered maximal and minimal curvature compared to ground truth. The first and third arcs depict the true curvatures; the second and fourth arcs depict the corresponding recovered curvatures.

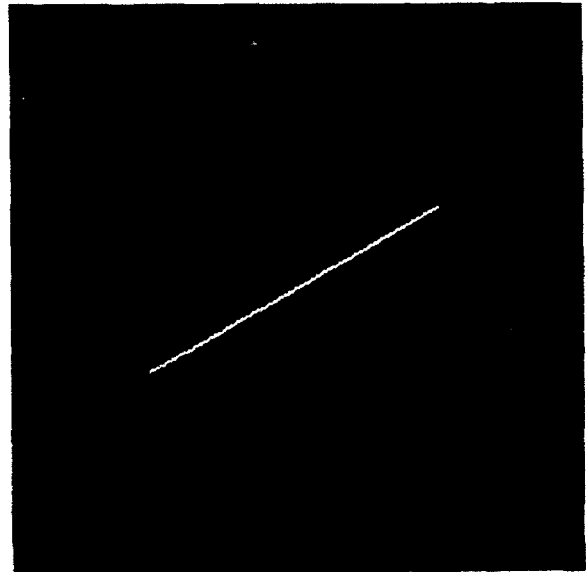
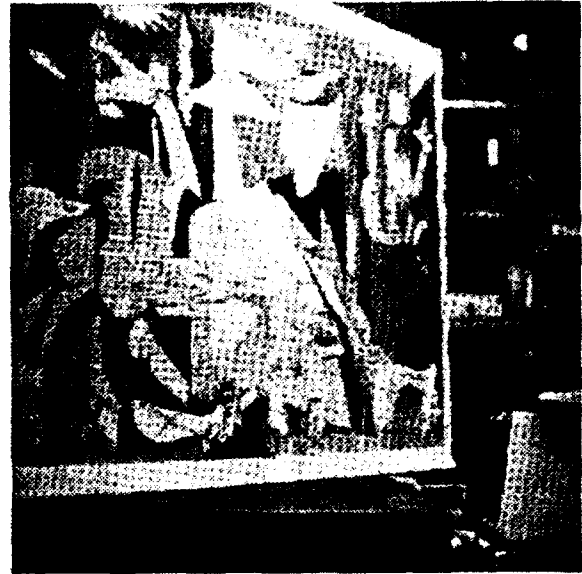


Figure 76. Recovery of 3D Attitude from Binocular Imagery (Wildes, 1990a).



Figure 77. Recovery of 3D Surface Curvature from Binocular Imagery (Wildes, 1990b).

The accuracy is high, but the limitations of these approaches are two-fold. First, images under consideration must contain oriented structures since the algorithms exploit the images' differential orientation. Second, current estimates for realtime implementations in commercially available hardware suggest that power requirements will be approximately 50 watts. Additional details can be found in Wildes (1990a, b) and Wildes (1991).

Point of Contact:

Rick Wildes
David Sarnoff Research Center
Princeton, NJ 08543-5300

3.3.22 Edge Detection by Active Defocusing

Using a combination of optical techniques and digital processing, researchers at the University of Nebraska, Omaha, NE, and Oakland University, Rochester, MI, have implemented a novel edge-extraction technique based on an approximation of a Laplacian-of-Gaussian operation (Zhu et al., 1991). The system consists of a video camera with an adjustable-focus lens, a frame grabber with software to perform realtime image extraction, and supporting computer programs to calculate edge index and control the lens focus adjustments (figure 78).

The focused image is initially stored in a frame buffer. A subsequent, slightly defocused image is passed to the subtraction processor, where realtime image subtraction is performed. The resulting residual (focused image minus defocused image) is displayed or stored as necessary. The edge index is computed simultaneously with the image subtraction operation. Performing a difference operation on two successive indices provides control information regarding the focus adjustment of the camera lens. When a predetermined edge index is achieved, the process terminates, and a final residual image is used as edge information for further processing.

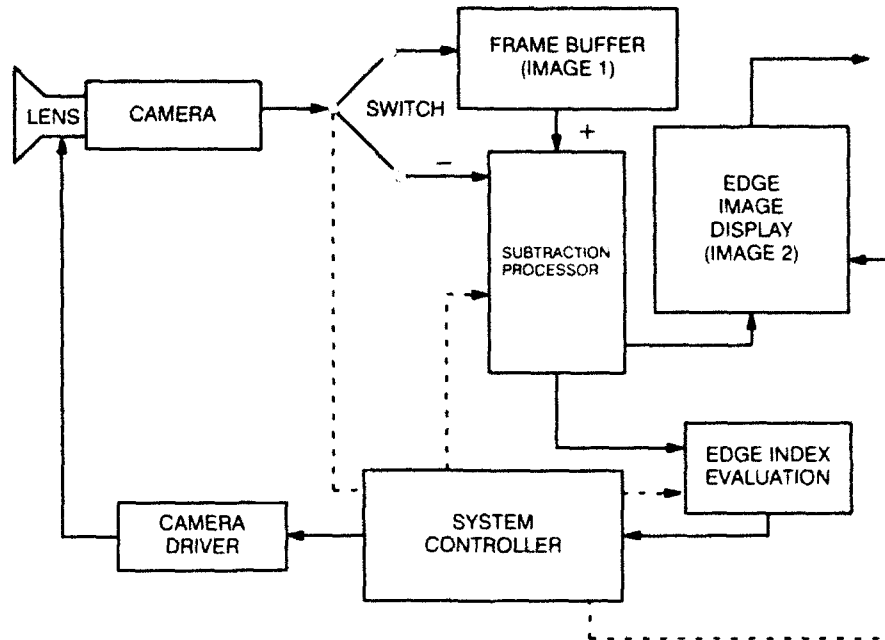


Figure 78. Block diagram of the active defocussing edge extraction system (Zhu et al., 1991).

Point of Contact:

Mr. Q. M. Zhu

University of Nebraska

Department of Mathematics and Computer Science

Omaha, NE 68182

3.3.23 MnSCAN: 3D Multipoint and Multibody Motion Tracking System

MnSCAN, developed at the University of Minnesota, is a system for tracking the three dimensional motion of multiple bodies (Sorensen et al., 1989). The data acquisition rate is a function of the laser scan rotation speed and is currently 480 Hz. The basic principle behind MnSCAN's functionality is that the intersection of three planes defines a point. Three planes of light rotate through the measurement field at a constant angular velocity (generated by a 60 Hz reluctance synchronous motor driving an 8-faceted polygon mirror at 480 scans per second, see figure 79). By measuring the elapsed time for rotation from fixed locations at the boundaries of the field to moving sensors, one can derive the swept angles and consequently the (X, Y, Z) coordinates of each sensor point.

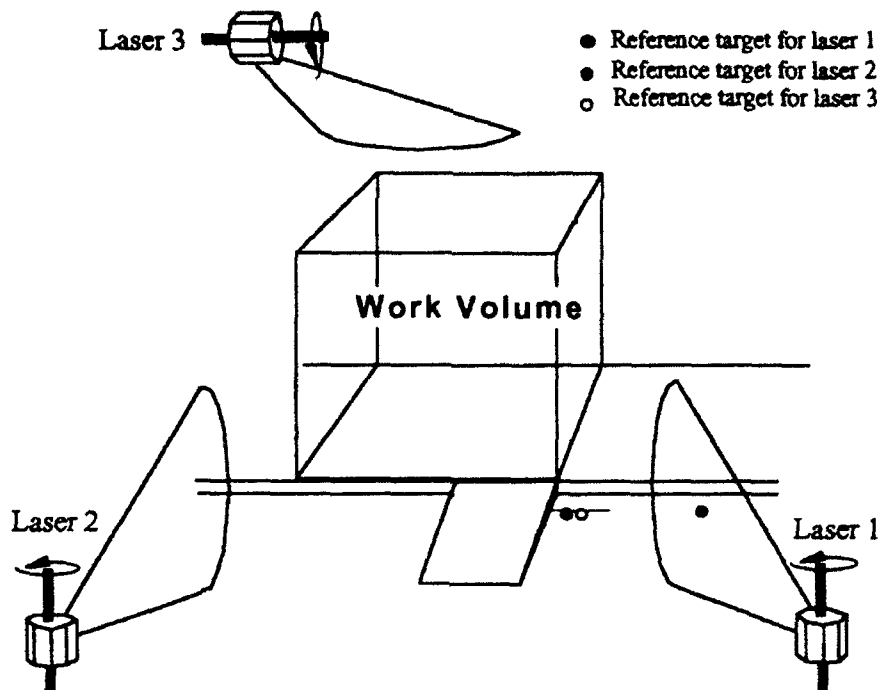


Figure 79. MnScan: 3D Multi-Point and Multi-Body Motion Tracking System Configuration (Sorensen et al., 1989).

The MnSCAN system is designed in a pipeline configuration such that each sensed point's coordinates are immediately available in registers (1 register per laser per sensor), and memory mapped into the data acquisition CPU. Sensors can be photodetectors, the receiving end of optical fibers, or retroreflectors. Each sensor has its own path into the CPU thus facilitating the accurate computation of (1) the 6 degrees of freedom of any number of bodies each carrying at least four sensors, and (2) the relative motion about the instantaneous axis of rotation between bodies. This configuration allows a large number of sensors with no effect on data acquisition bandwidth. Since the number of sensors does not affect system bandwidth, many bodies with several sensors attached can be tracked simultaneously. The accuracy in measuring the body's position and orientation improves as the number of attached sensors is increased. Since the system's limiting resolution and accuracy is not constrained by the size of the measurement volume, it can be used to track motion over large spaces.

Given the system's capabilities to track three dimensional motion of bodies, a modification of the various design parameters allows the system to be used for a variety of applications. These include

- 3D digitizing wands (incorporating a contact or noncontact range probe) that would replace massive coordinate measurement machines
- Measurement of motion in structures, drives and transmissions (including measurement of compliant effects, vibrations, and inertial effects at high speeds)
- The direct tracking of a dummy's 3D limb segment in crash tests
- Feedback sensing for robot and machine control (control of multidegree-of-freedom vehicle simulators and machine tools)

- Inertially tracking vehicles or other objects in open spaces (e.g. open pit mines) or for correcting dead reckoning sensors on vehicles
- Tracking of human limb and joint motion for ergonomic analyses, for diagnosis and rehabilitation of disability; and for the development of virtual reality based applications. The later is useful for training operators to perform difficult tasks (including sport activities), for entertainment and for telerobotic control.

3.3.24 Active Triangulation Rangefinder for a Planetary Rover

A team of 12 MIT students at the Charles Stark Draper Laboratory is designing and building a small (5 kilogram) autonomous microrover for exploration of the Martian surface. In the process, a need for a compact, short-range, and inexpensive rangefinder has emerged. Due to the limited energy and computational resources aboard the rover, potential candidates need to operate on a low power budget, and provide an output signal supporting simple range extraction.

Simplicity in the electronics was also desired, since the rover will have to endure the harsh environments found in space. It was decided that an 180-degree azimuthal scan was required in the direction of forward travel, but that an elevation scan was not necessary. A 5-percent range error was deemed acceptable in light of the inherent navigational errors associated with dead reckoning.

From these requirements, an active triangulation rangefinder was developed using a near-infrared laser source and a one-dimensional PSD as the detector element. The initial prototype (figure 80) was constructed slightly larger than necessary to simplify mounting and machining, but the diameter of the receiving lens was intentionally kept small (15 mm) to demonstrate an ability to collect returned energy with sufficient signal-to-noise ratio.

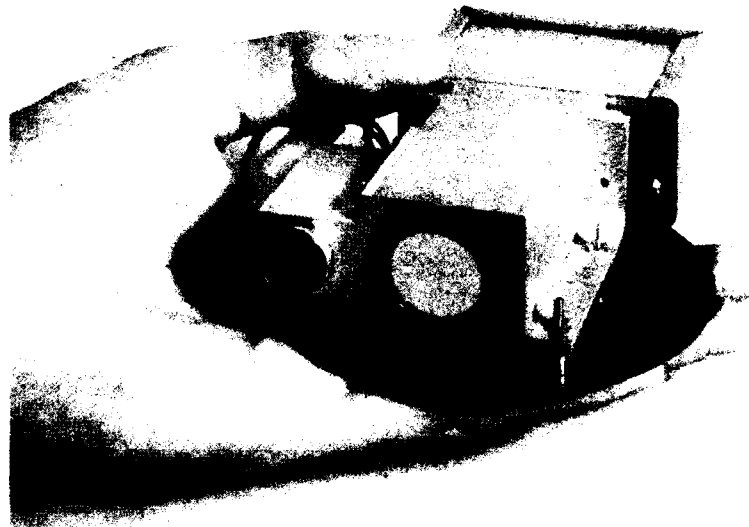


Figure 80. Photo of Draper Lab active laser rangefinding system.

Due to developmental time constraints, the electronics employed on the prototype are typical of that routinely suggested for DC operation of a standard PSD circuit. Hence, this rangefinder is very similar in concept to the Hamamatsu system described in section 3.1.4. Signal currents from the PSD are read immediately before and during the firing of the active source, a common method for subtracting off ambient background noise. Due to the slow vehicle speed, there is no need for an extremely fast ranging system, and about a 25-Hz sampling rate should suffice.

The large amounts of electronic noise associated with the rest of the rover combined with the small-diameter receiving lens made weak-signal detection difficult. Hence, the illumination source needed to be relatively high power (>250 milliwatts), at least during the short 1-millisecond pulsing interval. The source also needed to be well collimated, since triangulation systems work best when the footprint of illumination is small. To achieve these requirements, a quasi-CW laser diode was used, with a beam divergence of under 15 milliradians. The laser provides an optical power output of about 500 milliwatts for 1-millisecond intervals. This power level is not eye-safe, of course, but that is of little concern on Mars.

With a matched interference filter, the rangefinder is able to operate under sunlight conditions. Initial test results show a ranging accuracy that is about 5 percent at the maximum range of 3 meters. As with any triangulation system, this normalized accuracy improves as the range is decreased. Azimuthal scanning on the rover is currently accomplished by servoing the entire rangefinder unit through 180-degree sweeps.

Future work will focus on improved detection circuitry, so that the power of the laser can be reduced. In addition, the overall size will be reduced considerably with the use of a smaller PSD. If the size of each rangefinding unit (optics, laser, and detector) can be made small enough, it is hoped that multiple units can be positioned on the rover so scanning can be accomplished through multiplexing, in conjunction with the rover's own forward motion.

Selected Specifications:

Ranging Technique:	Active triangulation
Field-of-view:	180-degrees azimuth
Ranging Accuracy:	5 percent of range
Minimum Range:	0.5 feet
Maximum Range:	10 feet
Laser Source:	Quasi-CW laser diode
Wavelength:	920 nanometers
Power Requirements:	± 12 volts DC at less than 200 mA
Enclosure:	4 x 2 x 1.5 inches

Point of Contact:

Bill Kaliardos
The Charles Stark Draper Laboratory, Inc.
MS 27
555 Technology Square
Cambridge, MA 02139
(617) 258-1989

4.0 REFERENCES

- Anderson, D. L., 1989. "Framework for Autonomous Navigation of a Continuous Mining Machine: FACE Navigation," Report No. IC 9214. U. S. Bureau of Mines, U.S. Department of the Interior.
- Anderson, T., and M. Donath. 1990. "Animal Behavior as a Paradigm for Developing Robot Autonomy," *Robotics and Autonomous Systems*, vol. 6, pp. 145-168.
- Associates and Ferren. Undated. "3-D Computer Vision for Robots," Final Report for Phase II, NSWC Contract No. N60921-85-D-0064. Wainscott, New York.
- Azimuth Corporation. 1990a. "PRAM IV LRG-90 Laser Distance Measurement System," Product Description SMD-8063-4 (May). Westford, MA.
- Azimuth Corporation. 1990b. "PRAM 5000 Laser Distance Measurement Controller," Product Description SMD-90042-0 (April). Westford, MA.
- Banner Engineering Corporation. 1993a. Product Catalog. Minneapolis, MN.
- Banner Engineering Corporation. 1993b. "Handbook of Photoelectric Sensing." (1993b). Minneapolis, MN.
- Banzil G. et al. 1981. "Navigation Sub-system Using Ultrasonic Sensors for the Mobile Robot Hilare," *Proceedings of 1st Conference on Robot Vision and Sensory Control*, pp. 47-58. April 13, Stratford/Avon U.K.
- Battelle Columbus Division. 1986. Prospectus, "An Automotive Collision Avoidance and Obstacle Detection Radar," May 1. Columbus OH.
- Bedard, R. J. et al. 1991a. "Navigation of Military and Space Unmanned Ground Vehicles in Unstructured Terrains," *3rd Military Robotic Vehicle Conference*, September 9-12. Medicine Hat, Canada.
- Bedard, R. J. et al. 1991b. "The 1991 NASA Planetary Rover Program," presented at The 42nd International Astronautical Federation. October 6-9, Montreal, Canada.
- Beesley, M. J. 1971. *Lasers and Their Applications*, pp. 137-147. Taylor and Francis, LTD., London.
- Biber, C. et al. 1987. "The Polaroid Ultrasonic Ranging System," Audio Engineering Society, 67th Convention. October 31-November 3, New York, NY.
- Blake, L. 1990. "Prediction of Radar Range." In *The Radar Handbook*, ch. 2. Merrill Skolnik, Ed. 2d ed. McGraw Hill, New York, NY.
- Borestein, J., and Y. Koren. 1992. "Error Eliminating Rapid Ultrasonic Firing for Mobile Robot Obstacle Avoidance." Presented at IEEE Conference on Robotics and Automation. May 1992, Nice, France.
- Borestein, J., and U. Raschke. 1991. "Real-time Obstacle Avoidance for Non-Point Mobile Robots." Presented at the 4th World Conference on Robotics Research. 17-19 September 1991, Pittsburgh, PA.

- Borestein, J. 1991. "Fusing Data from Ultrasonic and Infrared Sensors." Progress Report for Department of Energy Grant No. DE-FG02-86NE37969.
- Brown, L. B. 1985. "A Random-Path Laser Interferometer System." *Proceedings of the Laser Institute of America's International Congress of Applications of Lasers and Electro-Optics*. 11-14 November 1985, San Francisco, CA.
- Brown, L. B., J. B. Merry, and D. N. Wells. 1987. "Tracking Laser Interferometer." U.S. Patent No. 4,790,651, 30 September. Lanham, MD.
- Brown, M. K. 1985. "Locating Object Surfaces with an Ultrasonic Range Sensor." *Proceedings of IEEE Conference on Robotics and Automation*, pp. 110-115. 25-28 March, St. Louis, MO.
- Chesapeake Laser Systems Incorporated. Undated. Product Brochure. Lanham, MD.
- Chesapeake Laser Systems Incorporated. 1991a. Product Literature (December). Lanham, MD.
- Chesapeake Laser Systems Incorporated. 1991b. "The CMS-2000 Laser Coordinate Measuring System." Product Literature (December). Lanham, MD.
- Chesapeake Laser Systems Incorporated. Undated. U. S. Patent No. 4, 621, 926. Lanham, MD.
- Cleveland, B. A. 1986. "An Intelligent Robotic Inspection System (IRIS)." TR, 31 March. MTS Systems Corporation, Minneapolis, MN.
- Cybermotion. 1991. "Ultrasonic Collision Avoidance System." Cybermotion Product Literature. Roanoke, VA.
- Depkovich, T., and W. Wolfe. 1984. "Definition of Requirements and Components for a Robotic Locating System." Final report no. MCR-83-669, February. Martin Marietta Denver Aerospace, Denver, CO.
- DeWitt, T. 1987. "Range Finding by Diffraction." U.S. Patent no. 4,678,324, 7 July.
- DeWitt, T. 1988. "Diffraction Range Finding for Machine Vision." *Proceedings Robots 12/Vision 88*, pp. 5-139-5-150.
- DeWitt, T. 1989. "Rangefinding by the Diffraction Method." *Lasers and Optronics*, 7 April. pp. 118-124.
- DeWitt, T. 1991. "Obtaining Range by the Diffraction Grating Method." Technical Description (4 October). Ancramdale, NY.
- Dokras, S. 1987. "Active Components in Fiber-Optic Sensors," *Sensors*, April, pp. 20-23.
- Dorf, R. C. and A. Nezamfar. Undated. "A Robot Ultrasonic Sensor for Object Recognition," pp. 21.4-21.5.
- Douglass, E. 1991. "Firms Success No Accident, Anti-Collision System Aims to Reduce Driver Toll." *The San Diego Union-Tribune* (week of 19 August).
- Dunlap, G. D., and H.H. Shufeldt. 1969. *Dutton's Navigation and Piloting*, p. 1013. Naval Institute Press.
- Duric, Z. and Y. Aloimonos, 1991. "Passive Navigation: An Active and Purposive Solution," TR CAR-TR-560. Center for Automation Research, University of Maryland, College Park, MD.

- ESP Technologies, Incorporated. 1992. "ORS-1 Optical Ranging System," Product Literature (23 March). Lawrenceville, NJ 08648.
- Evans, J. M. Jr., S. J. King, and C.F.R. Weiman. 1990. "Visual Navigation and Obstacle Avoidance Structured Light Systems," U.S. Patent No. 4,954,962, 4 September. Danbury, CT.
- Everett, H. R. 1982. "A Microprocessor Controlled Autonomous Sentry Robot." U. S. Naval Postgraduate School, Monterey, CA.
- Everett, H. R. 1985a. "A Second Generation Autonomous Sentry Robot," *Robotics Age*, April.
- Everett, H. R. 1985b. "A Multielement Ultrasonic Ranging Array," *Robotics Age*, July, pp. 13-20.
- Everett, H. R. 1985c. "Robotics in the Navy," *Robotics Age*, November, pp. 6-11.
- Everett, H. R. 1985d. "NAVSEA Integrated Robotics Program, Annual Report FY 85," NAVSEA Technical Report No. 450-90G-TR-0003 (December).
- Everett, H. R. 1987. "Noncontact Ranging Systems for Mobile Robots," *Sensors*, April, pp. 9-19.
- Everett H. R. and G. A. Bianchini. 1987. "Robart II: An Intelligent Security Robot." *U.S. Army Training and Doctrine Command, Artificial Intelligence and Robotics Symposium*. June, Norfolk, VA.
- Everett H. R. and A. M. Flynn. 1986. "A Programmable Near-Infrared Proximity Detector for Mobile Robot Navigation." *Proceedings of SPIE Mobile Robot Workshop*. October, Cambridge, MA.
- Everett, H. R., G. A. Gilbreath, T. Tran and J. M. Nieuwsma. 1990. Modeling the Environment of a Mobile Security Robot," NOSC TD 1835 (June). Naval Ocean Systems Center, San Diego CA.
- Farsaie, A., et al. 1987. "Intelligent Controllers for an Autonomous System." *IEEE International Symposium for Autonomous Control*.
- Fermuller, C. and Y. Aloimonos. 1991. "Estimating 3-D Motion from Image Gradients," TR CAR-TR-564. Center for Automation Research, University of Maryland, College Park, MD.
- Gisser, D. G. 1983. "Performance Data and Proposed New Design for a Vision System for Mobile Robots," Final Report, ARPA Order No. 4467 (8 March). Rensselaer Polytechnical Institute, Troy, NY.
- Goodwin, F. E. 1985. "Coherent Laser Radar 3-D Vision Sensor." *Proceedings Sensors '85*. November, Detroit, MI.
- Hall, D. J. 1984. "Robotic Sensing Devices," Carnegie-Mellon University Report No. CMU-RI-TR-84-3 (March).
- Hamamatsu Corporation. 1990. "16 Step Range-Finder IC H2476-01," Technical Data (January).
- Hamamatsu Corporation. 1991. "NB(8910) Optical Displacement Sensors H3065 Series," Technical Data (May 1991), Catalog No. KACC1003E01.

- Hanna, K. J. 1991. "Direct Multi-Resolution Estimation of Ego-Motion and Structure from Motion," *Proceedings of the IEEE Workshop on Visual Motion*, pp. 156-162.
- Heeger, D. J., and A. Jepson. 1990a. "Method and Apparatus for Image Processing to Obtain Three Dimensional Motion and Depth." U.S. Patent (25 December). MIT, Cambridge, MA.
- Heeger, D. J., and A. Jepson. 1990b. "Subspace Methods for Recovering Rigid Motion I: Algorithm and Implementation," TR RBCV-TR-90-35 (November). University of Toronto, Toronto, Ontario, Canada.
- Herman, M., and T. Hong. 1991. "Visual Navigation Using Optical Flow." *Proceedings NATO Defense Research Group Seminar on Robotics in the Battlefield*. March, Paris, France.
- Honeywell Visitrone. Undated. "Honeywell HVS-300 Three-Zone Distance Sensor." Product Literature, Publication No. A-24397 0186. Englewood, CO.
- Horn, B. K. P. 1986. *Robot Vision*. The MIT Press, Cambridge, MA.
- Horst, J. A. Undated. "An Application of Measurement Error Propagation Theory to Two Measurement Systems Used to Calculate the Position and Heading of a Vehicle of a Flat Surface." NISTIR 4434.
- Hoskin Scientific Limited. 1992a. "LADAR Series." Product Literature (February). Vancouver, B.C., Canada.
- Hoskin Scientific Limited. 1992b. "PS 2 and PS 10." Product Literature (February). Vancouver, B.C., Canada.
- Hoskin Scientific Limited. 1992c. "PS 50 and PS 100." Product Literature (January). Vancouver, B.C., Canada.
- Irwin, C. T., and D. O. Caughman. Undated. "Intelligent Robotic Integrated Ultrasonic System." Lockheed Georgia Company.
- Jarvis, R. A. 1983a. "A Perspective on Range Finding Techniques for Computer Vision." *IEEE Transactions on Pattern Analysis and Machine Intelligence*, March, vol. PAMI-1, no. 2, pp. 122-139.
- Jarvis, R. A. 1983b. "A Laser Time-of-Flight Range Scanner for Robotic Vision." *IEEE Transactions on Pattern Analysis and Machine Intelligence*, September, vol. PAMI-5, no. 5, pp. 505-512.
- Jarvis, R. A. 1984. "Range from Brightness for Robotic Vision." *Proceedings of 4th International Conference on Robot Vision and Sensory Controls*, pp. 165-172. 9-11 October, London, U.K.
- Johnston, A. R. 1973. "Infrared Laser Rangefinder." NASA New Technology Report No. NPO-13460 (August). Jet Propulsion Laboratory, Pasadena, CA.
- Kent, E. W., et al. 1985. "Real-time Cooperative Interaction Between Structured-Light and Reflectance Ranging for Robot Guidance." *Robotica*, January-March, vol. 3, pp. 7-11.
- Kim, E. J. 1986. "Design of a Phased Sonar Array for a Mobile Robot," Bachelor's Degree Thesis (May). Massachusetts Institute of Technology.

- King, S. J. 1990. "HelpMate Autonomous Mobile Robot Navigation System," *SPIE, Mobile Robots V*, vol. 1388, pp. 190-198.
- Koenigsburg, W. D. Undated. "Noncontact Distance Sensor Technology." Incomplete Reference. GTE Laboratories, Incorporated.
- Kruth-Microwave Electronics Company. 1989. "Final Report Phase I," NSSC Contract No. N00024-88-C-5115 (20 December). Hanover, MD.
- Laser Systems Devices. 1992. "MR-101 Missile Rangefinder," Product Literature (15 January). Alexandria, VA.
- Laskowski, E. L. 1988. "Range Finder Wherein Distance Between Target and Source is Determined by Measuring Scan Time Across a Retroreflective Target," U.S. Patent No. 4,788,441 (29 November). Mentor, OH.
- Lau, K., et al. 1985. "Robot End Point Sensing Using Laser Tracking System." *Proceedings of the NBS Sponsored-Navy NAV/CIM Robot Standards Workshop*, pp. 104-111. June, Detroit, MI.
- Le Moigue, J. and A. M. Waxman. 1984. "Projected Light Grids for Short Range Navigation of Autonomous Robots." *Proceedings of 7th IEEE Conference on Pattern Recognition*, pp. 203-206. 30 July-2 August, Montreal, Canada.
- Lewis, R. A., and A. R. Johnson. Undated. "A Scanning Laser Rangefinder for a Robotic Vehicle," *Proceedings Robots 3* pp. 762-768.
- Loewenstein, D. 1984. "Computer Vision and Ranging Systems for a Ping Pong Playing Robot," *Robotics Age*, August pp. 21-25.
- Ma, Y. L., and C. Ma. 1984. "An Ultrasonic Scanner System Used on an Intelligent Robot." *Proceedings of IEEE IECON '84*, pp. 745-748. 22-26 October, Tokyo, Japan.
- McCosh, D. 1992. "Automotive Newsfront," *Popular Science*, May p. 42.
- Miller, D. L. et al. 1985. "Advanced Military Robotics," Interim Report No. R84-48603-001 (26 July). Martin Marietta Denver Aerospace, Denver CO.
- Miller, G. L. and E. R. Wagner. 1987. "An Optical Rangefinder for Autonomous Robot Cart Navigation." *Proceedings of the Advances in Intelligent Robotic Systems: Mobile Robots II*.
- Miller, R. K. 1991. "Robotic Applications in Non-Industrial Environments," vol. 2. Richard K. Miller and Associates, Inc.
- Millitech Corporation. 1989. "Modular Millimeter Wave FMCW Sensor," Final Report for NSSC Contract No. N00024-88-C-5114 (June). South Deerfield, MA.
- Moser, J. and H. R. Everett. 1989. "Wide-Angle Active Optical Triangulation Ranging System." *Proceedings of the Advances in Intelligent Robotic Systems: Mobile Robots IV*, November.
- NAMCO Controls. 1989. "LNFL03-A 5M/4-90," Lasernet Product Bulletin (November). Mentor, OH.
- National Semiconductor Corporation. 1988. "LM1812 Ultrasonic Transceiver," National Semiconductor Databook 3. Santa Clara, CA.

- Nguyen, H. G. 1993. "Summary of Auto-Landing Problem Analysis and Proposal," NRaD Memorandum 943/11-93 (February).
- Nimrod, N. et al. 1982. "A Laser-Based Scanning Range Finder for Robotic Applications." *Proceedings of 2nd International Conference on Robotic Vision and Sensory Controls*, pp. 241-252. November, Stuttgart, Germany.
- Nitzan, D. et al. 1977. "The Measurement and Use of Registered Reflectance and Range Data in Scene Analysis," *Proceedings of IEEE*, February, vol. 65, no. 2, pp. 206-220.
- Nitzan, D. 1981. "Assessment of Robotic Sensors." *Proceedings of 1st International Conference on Robotic Vision and Sensory Controls*, pp. 1-11. 1-3 April.
- Nitzan, D. et al. 1986. "3-D Vision for Robot Applications." *NATO Workshop: Knowledge Engineering for Robotic Applications*. 12-16 May, Maratea, Italy.
- Nomadic Technologies, Incorporated. 1991a. "Sensus 300 Infrared Proximity System," Product Literature (25 October). Palo Alto, CA.
- Nomadic Technologies, Incorporated. 1991b. "NOMAD 100," Product Literature (25 October). Palo Alto, CA.
- Nomadic Technologies, Incorporated. 1991c. "Sensus 500 Structured Light System," Product Literature (25 October). Palo Alto, CA.
- Nowogrodzki, M. Undated. "Microwave CW Radars in Industrial Applications." RCA Laboratories, Princeton, NJ.
- Optical Sciences Company. 1987. "Final Report NOSC Contract No. N66001-87-R-0236," TOSC Final Report No. DR-461. Placentia, CA.
- Optech Systems Corporation. 1992. "Model G150 Laser Rangefinder", Product Literature (February). Toronto, Ontario, Canada.
- Pipitone, F. J. and T. G. Marshall. 1983. "A Wide-field Scanning Triangulation Rangefinder for Machine Vision." *The International Journal of Robotics Research*, vol. 2, no. 1, pp. 39-49.
- Pletta, J. B., et al. 1992. "The Remote Security Station (RSS) Final Report," Sandia Report SAND92-1947 for DOE under Contract DE-AC04-76DP00789 (October). Sandia National Laboratories, Albuquerque, NM.
- Poggio, T. 1984. "Vision by Man and Machine," *Scientific America*, April, vol. 250, no. 4, pp. 106-116.
- Polaroid Corporation. 1981. "Polaroid Ultrasonic Ranging System User's Manual," Publication No. P1834B (December).
- Polaroid Corporation. 1990. "6500 Series Sonar Ranging Module," Product Specifications PID 615077 (11 October).
- Ridenour, L. N. 1947. *Radar Systems Engineering*, pp. 143-147. MIT Radiation Laboratory Series. McGraw Hill.
- Robot Defense Systems, Incorporated. Undated. "OWL-3D Laser Imaging," Sales Literature. Denver, CO.

- Rose, C. D. 1992. "Four Emerging Technologies That Will Change Your Life," *The San Diego Union-Tribune*, 21 June.
- Schwartz Electro-Optics Incorporated. 1991a. "Scanning Laser Rangefinder," Product Literature (October). Orlando FL.
- Schwartz Electro-Optics Incorporated. 1991b. "LRF-X Laser Rangefinder Series," Product Literature (October). Orlando FL.
- Schwartz Electro-Optics Incorporated. 1991c. "Multi-Channel Laser Imaging System," Product Literature (October). Orlando FL.
- Schwartz Electro-Optics Incorporated. 1991d. "Helicopter Optical Proximity Sensor System," Product Literature (October). Orlando FL.
- Schwartz Electro-Optics Incorporated. 1991e. Process Report for U. S. Army Contract No. DAAJ02-91-C-0026 (December). Orlando FL.
- Schwartz, J. T. Undated. "Structured Light Sensors for 3-D Robot Vision," TR No. 65. Courant Institute of Mathematical Sciences, New York University.
- Seiler, M.R., and B.M. Mathena. 1984. *IEEE Transactions Antennas and Propagation*, (September), vol. AP 32, no. 9, p. 987.
- Sentizky, B., and A. A. Oliner. 1970. "Submillimeter Waves," *Submillimeter Wave Applications* (pp. xxvii-xxx). 31 March-2 April 1970, Microwave Research Institute Symposia.
- Simmons, J. P. Jr. 1986. "A Real-Time Three-Dimensional Vision System for Robotic Guidance," *Robotics Engineering*, January, pp. 23-25.
- Slack, M. 1989. "Generating Symbolic Maps from Grid Based Height Maps," JPL-D-6948 (7 December).
- Sorensen, B., M. Donath, R. Starr, and G.B. Yang. 1989. "The Minnesota Scanner: a Prototype Sensor for 3D Tracking of Moving Body Segments," *IEEE Journal of Robotics and Automation*, August, vol. 5, no. 4, pp. 499-509.
- Stauffer, N. and D. Wilwerding. 1982. *Electronic Focus for Cameras*, March, vol. 3, no. 1.
- Transitions Research Company. Undated. "Proximity Subsystem," Product Literature. Danbury, CT.
- Tsumura, T. et al. 1984. "An Experimental System for Automatic Guidance of the Ground Vehicle by Use of Laser and Corner Cubes." *Proceedings of IEEE IECON '84*, pp. 297-302. 22-26 October, Tokyo, Japan.
- University of Michigan Mobile Robotics Lab. 1991a. Progress Report for Department of Energy Grant. Incomplete reference. Ann Arbor, MI.
- University of Michigan Mobile Robotics Lab. 1991b. "Mobile Robotics Lab," Brochure. Ann Arbor, MI.
- Vehicle Radar Safety Systems, Incorporated. 1983. "Rashid Radar Safety Brake," Product Literature. Mount Clemens, MI.

- Vranish, J. M., R. L. McConnell and S. Mahalingham. 1991. "CAPACIFLECTOR' Collision Avoidance Sensors for Robots," Product Description (14 February). NASA GSFC, Greenbelt, MD.
- Webster, J. G. 1988. *Tactile Sensors for Robotics and Medicine*. Wiley, New York, NY.
- Wilcox, B. H. 1990. "Vision-based Planetary Rover Navigation." *SPIE International Conference on Visual Communications and Image Processing*. October, Lausanne, Switzerland.
- Wildes, R. P. 1990a. "Qualitative 3D Shape from Stereo." *Proceedings of the SPIE Intelligent Robots and Computer Vision Conference*, pp. 453-463.
- Wildes, R. P. 1990b. "Three-Dimensional Surface Curvature from Binocular Stereo Disparity." *Optical Society of America Technical Digest* vol. 25, p. 58.
- Wildes, R. P. 1991. "Direct Recovery of Three-Dimensional Scene Geometry from Binocular Stereo Disparity." *IEEE Trans. Pattern Analysis and Machine Intelligence*, August, vol. 13, no. 8, pp. 761-774.
- Wittenburg, R. C. 1987. "Automobile Collision Avoidance System Capitalizes on Beam-Steerable Antenna," *Electronic Engineering Times*, 2 February.
- Young, G. S., T. H. Hong, M. Herman, and J. C. S. Yang. 1992. "Obstacle Avoidance for a Vehicle Using Optical Flow," Technology Description (July), NIST, Gaithersburg, MD.
- Zhao, C. J. et al. Undated. "Location of a Vehicle with Laser Rangefinder." Institut National des Sciences Appliquées (INSA), Rennes Ce'dex, France.
- Zhu, O. M. et al. 1991. "Edge Extraction by Active Defocusing," *Spatial Vision*, vol. 5, no. 4, pp. 253-267.

REPORT DOCUMENTATION PAGE

Form Approved
OMB No. 0704-0188

Public reporting burden for this collection of information is estimated to average 1 hour per response, including the time for reviewing instructions, searching existing data sources, gathering and maintaining the data needed, and completing and reviewing the collection of information. Send comments regarding this burden estimate or any other aspect of this collection of information, including suggestions for reducing this burden, to Washington Headquarters Services, Directorate for Information Operations and Reports, 1215 Jefferson Davis Highway, Suite 1204, Arlington, VA 22202-4302, and to the Office of Management and Budget, Paperwork Reduction Project (0704-0188), Washington, DC 20503

1. AGENCY USE ONLY (Leave blank)	2. REPORT DATE <p style="text-align: center;">December 1992</p>	3. REPORT TYPE AND DATES COVERED <p style="text-align: center;">Final</p>	
4. TITLE AND SUBTITLE <p style="text-align: center;">Survey of Collision Avoidance and Ranging Sensors for Mobile Robots Revision 1</p>		5. FUNDING NUMBERS PR: CH01 PE: 0602624A WU: DN309216	
6. AUTHOR(S) <p style="text-align: center;">H. R. Everett, D. E. DeMuth, E. H. Stitz</p>		8. PERFORMING ORGANIZATION REPORT NUMBER TR 1194 Revision 1	
7. PERFORMING ORGANIZATION NAME(S) AND ADDRESS(ES) <p style="text-align: center;">Naval Command, Control and Ocean Surveillance Center (NCCOSC) RDT&E Division San Diego, CA 92152-5000</p>		10. SPONSORING/MONITORING AGENCY REPORT NUMBER	
9. SPONSORING/MONITORING AGENCY NAME(S) AND ADDRESS(ES) <p style="text-align: center;">U.S. Army Armament Research Development Engineering Center Dover, NJ 07801</p>		11. SUPPLEMENTARY NOTES	
12a. DISTRIBUTION/AVAILABILITY STATEMENT <p style="text-align: center;">Approved for public release; distribution is unlimited.</p>		12b. DISTRIBUTION CODE	
13. ABSTRACT (Maximum 200 words) <p>The past few years have brought about a tremendous rise in the envisioned potential of robotic systems and a significant increase in the number of proposed applications. In the nonindustrial arena, numerous programs have evolved, each intending to harness some of this promise in hopes of solving some particular application need. Many of these efforts are government sponsored, aimed at the development of systems for fighting fires, handling ammunition, transporting materials, conducting underwater search and inspection operations, and patrolling warehouses and storage areas, etc. Many of the resulting prototypes, which were initially perceived as logical extensions of the traditional industrial robotic scenarios, have met with unexpected difficulty due to an insufficient supporting technology base.</p> <p>This document provides some basic background on the various noncontact distance measurement techniques available, with related discussion of implementation in the acoustical, optical, and electromagnetic portions of the energy spectrum. An overview of candidate systems, both commercially available and under development, is provided; followed by a brief summary of research currently underway in support of the collision avoidance and noncontact ranging needs of a mobile robot.</p>			
14. SUBJECT TERMS ro' botics sensors artificial intelligence security			15. NUMBER OF PAGES <p style="text-align: center;">156</p>
17. SECURITY CLASSIFICATION OF REPORT <p style="text-align: center;">UNCLASSIFIED</p>			16. PRICE CODE
18. SECURITY CLASSIFICATION OF THIS PAGE <p style="text-align: center;">UNCLASSIFIED</p>	19. SECURITY CLASSIFICATION OF ABSTRACT <p style="text-align: center;">UNCLASSIFIED</p>	20. LIMITATION OF ABSTRACT <p style="text-align: center;">SAME AS REPORT</p>	

UNCLASSIFIED

21a. NAME OF RESPONSIBLE INDIVIDUAL	21b. TELEPHONE (include Area Code)	21c. OFFICE SYMBOL
H. R. Everett	(619) 553-3672	Code 6303